2013

The effects of sex, leg region and impact technique on leg soft tissue motion and energy dissipation following heel impacts

Evan Brydges
University of Windsor

THE EFFECTS OF SEX, LEG REGION AND IMPACT TECHNIQUE ON LEG SOFT TISSUE MOTION AND ENERGY DISSIPATION FOLLOWING HEEL IMPACTS

By

Evan Brydges

A Thesis
Submitted to the Faculty of Graduate Studies
through the Faculty of Human Kinetics
in Partial Fulfillment of the Requirements for
the Degree of Master of Human Kinetics at the
University of Windsor

Windsor, Ontario, Canada

THE EFFECTS OF SEX, LEG REGION AND IMPACT TECHNIQUE ON LEG SOFT TISSUE MOTION AND ENERGY DISSIPATION FOLLOWING HEEL IMPACTS

by

Evan Brydges

APPROVED BY:

_____

Dr. W. Altenhof
Department of Mechanical, Automotive & Materials Engineering

_____

Dr. N. Azar
Department of Kinesiology

_____

Dr. D. Andrews, Advisor
Department of Kinesiology

_____

Dr. Joel Cort, Chair of Defense
Department of Kinesiology

April 5, 2013

DECLARATION OF ORIGINALITY

I hereby certify that I am the sole author of this thesis and that no part of this thesis has been published or submitted for publication.

I certify that, to the best of my knowledge, my thesis does not infringe upon anyone's copyright nor violate any proprietary rights and that any ideas, techniques, quotations, or any other material from the work of other people included in my thesis, published or otherwise, are fully acknowledged in accordance with the standard referencing practices. Furthermore, to the extent that I have included copyrighted material that surpasses the bounds of fair dealing within the meaning of the Canada Copyright Act, I certify that I have obtained a written permission from the copyright owner(s) to include such material(s) in my thesis and have included copies of such copyright clearances to my appendix.

I declare that this is a true copy of my thesis, including any final revisions, as approved by my thesis committee and the Graduate Studies office, and that this thesis has not been submitted for a higher degree to any other University or Institution.

ABSTRACT

Controlled heel impacts were imparted to 20 participants (9 M and 11 F) in the horizontal plane using a human pendulum. Displacement and velocity of leg soft tissue were determined from automatic detection (ProAnalyst®) of manually digitized skin markers. Overall, the soft tissue moved with a mean peak displacement of 2.14 cm and velocity of 105.5 cm/s. Regions with greater amounts of soft tissue (proximal, and back of the leg) experienced greater displacement and velocity than distal regions and regions on the front of the leg, respectively. Displacement and velocity were greater in distal regions for males and in proximal regions for females, while the magnitude of tissue masses (fat mass, lean mass, bone mineral content and wobbling mass) had significantly different effects on tissue kinematics between the sexes. These results provide important information which will help us better understand how shock propagates through the body.

Keywords: lower extremity, displacement, velocity, tissue composition, sex differences

DEDICATION

To my Mom.

ACKNOWLEDGEMENTS

I would like to express my gratitude to my master's thesis advisor, Dr. Dave Andrews. Your ability to know when to step in and when to let me struggle allowed me to learn a lot about myself and has given me invaluable experience and confidence to use in my future endeavours.

Thank you to my committee, Dr. William Altenhof and Dr. Nadia Azar, for their help in the design of this study and their valuable feedback in preparation for this thesis. Thank you to the staff and faculty in the Department of Kinesiology for their support, kindness and commitment to students. Thank you Don Clarke for the contributions to all of my projects which would not have been possible without your help.

To Dr. Tim Burkhart, thank you for always being willing to take time to help no matter how small or mundane my questions seemed.

To my friends, Danielle MacIntyre and Mark Badrov for make coming into school every day an enjoyable experience. Also to Colin McAuslan for helping me push towards the finish line during my victory lap, and to Jenn Stefanczyk for all of your help with data collection. Thank you to Samantha Richardson for your continued support, friendship and guidance.

Finally, thank you to my family, including my parents as well as my older and younger brothers, for your support and encouragement throughout my life.

TABLE OF CONTENTS

LIST OF TABLES

LIST OF FIGURES

LIST OF APPENDICES

GLOSSARY

Adalat capsules: brand name for the common drug nifedipine, used to lower blood pressure. They have also been used as skin surface markers during MRI due to their low cost and highly visible MRI signal.

Anterior (displacement, velocity): describes motion of the soft tissue towards the front of the leg (tibia) following heel impacts.

AS (acceleration slope): slope of the acceleration/time response between 30% and 70% of the peak acceleration (measured in g/s).

Attenuation: the weakening or reduction in force, intensity, effect, quantity, or value that occurs as the distance from the source increases as a result of absorption, scattering, or spreading in three dimensions.

BMC (bone mineral content): the amount of bone material or mineral in a specific bone site (measured in grams).

BW (bodyweight): the measure of the force of gravity that acts on a body (measured in Newtons (N)). Impact force measurements are often normalized to an individual's bodyweight.

Compression Wave: wave consisting of a periodic disturbance or vibration that takes place in the same direction as the wave is advancing.

DEXA or DXA (dual energy x-ray absorptiometry): uses low current x-rays to perform whole body scans capable of measuring bone and soft tissue (lean and fat mass) composition.

Distal (displacement, velocity): describes motion of the soft tissue towards the feet following heel impacts.

EMG (electromyography): a technique used to evaluate and record the electrical activity produced by skeletal muscles.

Energy (mechanical): the ability a system has to do work on other systems. Represented by positive and negative work values indicating energy production and absorption, respectively (unit of measure - Joules (J)).

Energy Density: the amount of energy stored in a given system or region of space per unit volume (measured in J/m^3).

FFM (fat free mass): the total mass of all body tissue that does not contain fat (i.e. muscle, bone, water).

FM (fat mass): the total mass of the adipose tissue in the body or segment.

GRF (ground reaction force): a force applied to the body by the ground that is equal in magnitude and opposite in direction to the force that the body exerts on the ground (measured in N).

Human Pendulum: apparatus used to maximize control over impact force magnitude and velocity during lower body impact analysis.

Impact Force: describes the force produced due to the collision between two objects. Maximum forces in human locomotion occur within 50ms after the foot contacts the ground.

Kinematics: describes aspects of motion without consideration of the forces that cause the motion.

Kinetics: of or relating to the motion of bodies and the associated forces and energy.

Laplacian Filter: a type of high pass filter which is constructed from the sum of the x and y second derivatives of an image. The Laplacian filter is used for detection of edges in an image. It highlights areas in which intensity changes rapidly, producing a picture of all the edges in an image.

LM (lean mass): the total mass of all body tissue that does not contain fat (i.e. muscle, bone, water).

MRI (magnetic resonance imaging): a non-invasive diagnostic technique that produces computerized images of internal body tissues and is based on nuclear magnetic resonance of atoms within the body induced by the application of radio waves.

Non-dispersive Wave: a wave that does not change its shape as it propagates and all parts of the wave travel at the same speed.

PA (peak acceleration): largest measured acceleration magnitude (measured in m/s^2 or g).

Posterior (displacement, velocity): describes motion of the soft tissue towards the back of the leg (calf) following heel impacts.

Propagation: the transmission of a wave through a medium, such as the human body's tissues.

Proximal (displacement, velocity): describes motion of the soft tissue back towards the knee following heel impacts.

SA (shock attenuation): a reduction in impact force amplitude that occurs as the shock wave propagates through the body's tissues.

Shock: the transient condition whereby a system's equilibrium is disrupted by a suddenly applied change in force application.

Shock wave: the propagation of a stress wave through a medium, such as the body's tissues.

SNR (signal-to-noise ratio): the power ratio between the audio, video, or any signal (meaningful information) and the background noise (unwanted signal).

TPA (time to peak acceleration): time between impact and peak acceleration (measured in ms).

WM (wobbling mass): the non-rigid tissues of the body (lean and fat masses) that are attached to underlying bony structures.

CHAPTER I

INTRODUCTION

Common daily activities such as walking, running and jumping subject the lower extremities to impact forces when the feet contact the ground. These impact forces, with magnitudes as much as three times bodyweight (BW) (Cavanagh and Lafortune, 1980), result in shock waves which move proximally along the shank. Shock can lead to overuse injuries such as muscle strains in the calf and musculature surrounding the ankle joint (Chu et al., 2010), shin splints and stress fractures (Milner et al., 2006), cartilage damage (Radin et al., 1973), osteoarthritis (Radin et al., 1982) and the tearing of ligaments in the knee joint (Yu and Garrett, 2007). Therefore, it is important to better understand how shock propagates through the body, to advance our understanding of how these types of overuse injuries occur so that improved injury prevention strategies can be devised.

The movement of soft tissue masses (fat, muscle, skin) in relation to the underlying bone of the lower extremity has been shown to serve a protective role during impact events such as running (Cole et al., 1996) and drop landings (Pain and Challis, 2006; Schinkel-Ivy et al., 2012a, b) by helping to attenuate potentially injurious impact forces. The soft tissues of body segments were first termed the 'wobbling mass' (WM) by Gruber et al. (1987) and many have since incorporated WM into their models (Liu and Nigg, 2000; Pain and Challis, 2004). WM varies in composition, consisting of fat mass (FM) and lean mass (LM), but it is not understood how these individual tissues interact to affect shock attenuation and kinematic properties resulting from impact.

Previously, the biomechanical models used to predict the loads incurred during dynamic impacts consisted only of rigid segments (bone). When the outputs of these models are compared to those that are comprised of both rigid and wobbling masses, the important role of soft tissue motion in load attenuation is realized (Pain and Challis, 2006). For example, soft tissue movement can result in decreases in peak impact loads when compared to rigid segment only models (Nigg et al., 1995). More recently, soft tissue properties incorporated into biomechanical models have been shown to contribute to a reduction in peak vertical ground reaction force (GRF) of up to 8.6 times BW (Gittoes et al., 2006), and resulted in torques about the ankle, knee and hip joints that were up to 50 % lower (Pain and Challis, 2006), compared to rigid-only models. Therefore, a model of the human body using only rigid segments is not appropriate when studying impact situations (Gruber et al., 1998). The WM models that have been developed typically involve an inner segment which represents the skeleton and an outer segment that represents the WM. These WM segments have been overly simplified, usually modelled as a symmetrical shape that does not differ in shape along the proximodistal axis (Gruber et al., 1998; Pain and Challis, 2004, 2006). The kinematic properties of the soft tissue among various regions of the leg are assumed to differ based on differences in tissue mass quantities and proportions, therefore future biomechanical models should take this into consideration.

Many studies have examined the contributions of active mechanisms (i.e. muscle activation) and passive structures (soft and rigid tissue masses) on shock wave attenuation through the body following foot impacts using accelerometers placed on the tibia and head (Chu and Caldwell, 2004; Coventry et al., 2006; Dufek et al., 2009; Mercer

et al., 2003; Mercer et al., 2010; Shorten and Winslow, 1992; Zhang et al., 2005). Changes in muscle activation and initial lower body joint angles significantly affect the measured accelerations of the shank, as increases in muscle activation and initial knee angles result in greater peak tibial accelerations (Lafortune et al., 1996b; Verbitsky et al., 1998). Increases in FM, WM, and bone mineral content (BMC) respectively, have resulted in decreased acceleration responses at the tibia. It was also found that females on average experienced greater peak accelerations than males per gram of LM, FM, and BMC tissue (Schinkel-Ivy et al. 2012a). Quantifying the movement of WM may provide greater insight into the properties of the leg and how differences in the amounts of specific tissue masses between individuals affects the amount of tissue displacement that occurs.

Most of the research investigating shock wave attenuation through the body involves assessing impacts while running (Dufek et al., 2009; Mercer et al., 2003; Mercer et al., 2010; Shorten and Winslow, 1992) or following a drop landing (Coventry et al., 2006; Decker et al., 2003; Zhang et al., 2000; Zhang et al., 2005). Human pendulum methods have been utilized by many to accurately control impact consistency (Duquette and Andrews, 2010; Flynn et al., 2004; Fowler et al., 1997; Holmes and Andrews, 2006; Lafortune et al., 1996a, b). Drop landing and pendulum techniques have been compared in the past to investigate lower extremity kinematics at heel impact. Although no differences in lower extremity joint angles upon impact resulting from the two techniques were found (Fowler and Lees, 1998), it is not known if soft tissue movement and shock wave attenuation are affected differentially by the two approaches.

Soft tissue movement has been quantified previously using several different motion tracking techniques. Methods such as three-dimensional (3D) optoelectronic systems (Fuller et al., 1997; Gao and Zheng, 2008), and Magnetic Resonance Imaging (MRI) (Akbarshahi et al., 2010, Sangeux et al., 2006) involve the use of expensive equipment that may require the assistance of a trained professional to operate. Other methods such as X-ray and video fluoroscopy can subject the participant to potentially harmful radiation (Kuo et al., 2011; Sati et al., 1996; Wrbaškić and Dowling, 2007). These methods require external devices (e.g. accelerometers, skin markers) to be attached to the body, while the motion tracking system used in the current investigation eliminates the potential for a non-physiological tissue response following impact by not requiring an external device to be attached to the body. The marker system relies on a method that utilizes software with automatic feature tracking (ProAnalyst®; Xcitex, Cambridge, MA), and has been shown to be a useful tool in quantifying leg soft tissue mass motion (Brydges et al., 2012). Good to excellent reliability of accurate marker selection and resultant calculated point velocities has been shown using this method, with high intra-class correlation coefficients both between (0.86) and within (0.96) measurers for position and velocity measurements (Brydges et al., 2012).

Energy absorption during landing is affected by changes in muscle activation (Zhang et al., 2000), and initial joint angles (Yeow et al., 2011a), as well as soft tissue movement (Pain and Challis, 2002). During drop landings, it has been shown that the ankle, knee, and hip joints all play an important role in energy dissipation (Derrick et al., 1998; Devita and Skelly, 1992; Norcross et al., 2010; Yeow et al., 2011a, b; Zhang et al., 2000), however soft tissue movement can account for a large amount of the energy

dissipated following impacts (Pain and Challis, 2002). The energy carried by the soft tissue following impact has been estimated from frequency and amplitude measures of the soft tissue waveform (Pain and Challis, 2002). By tracking markers on the forearm during a hand striking task, Pain and Challis, (2002) found that the deformation of the soft tissue that occurred accounted for 70 % of the impact energy lost from the forearm during this action. However, this work was limited to the upper extremity of a single participant, and impacts were only calculated in the vertical direction. The small external markers that they used to track tissue motion may also have contributed to some tissue motion artefact, although the mass of the markers was small (0.0057 g). Therefore, examining an impact involving the lower extremity, with multiple participants, while measuring responses in both the vertical and horizontal directions, will provide a better perspective on how much of the impact energy can be dissipated by soft tissue movement. Examining the tissue composition of the lower extremity will also advance our understanding of how individual tissue masses (e.g. FM, LM, WM and BMC) affect the movement of this tissue following impact, which will improve the accuracy of kinetic outputs, and possibly estimates of injury risk, that can be obtained from biomechanical models.

Therefore the purposes of this thesis are to:

1. quantify the displacement and velocity of, and the amount of energy dissipated by, the soft tissues of the leg following impact;
2. determine if there are differences in soft tissue motion and impact energy dissipation due to sex, trial, impact method utilized (drop landing vs. pendulum) or as a function of the region of the leg measured;

3. determine the relationship between the displacement, velocity and energy absorption ability of the soft tissues of the lower extremity and the individual leg tissue masses (FM, LM, WM, BMC).

1.1 Hypotheses

It is hypothesized that:

1. it will be possible to quantify the displacement and velocity of, and energy dissipated by, the soft tissues of the leg following heel impacts by combining high speed photography and a manual digitization approach. Marker displacement waveform amplitude and frequency will be used to determine the amount of energy carried by the soft tissue wave, as per Pain and Challis (2002).

2a. males will have greater leg soft tissue displacements and velocities than females following impact. This is supported by the work of Schinkel-Ivy et al. (2012a) who found that males have significantly more WM within the leg segment.

2b. it is also hypothesized that the amount of energy dissipated will be greater for males, as Schinkel-Ivy et al. (2012a) found that females on average experienced greater peak tibial accelerations per gram of tissue for LM, FM, and BMC.

2c. furthermore, it is hypothesized that the displacement of the proximal region WM will be greater than the distal region WM, and the posterior region WM will be greater than the anterior region WM, as there are greater amounts of WM proximally and posteriorly in the leg.

2d. in addition, it is hypothesized that the total energy absorbed by the WM in the proximal regions of the leg will be greater than the more distal regions of the leg, as there are greater amounts of WM proximally.

2e. however, it is anticipated that the velocity of the soft tissues will decrease as the shock wave moves proximally through the leg as the shock wave is attenuated.

2f. lastly, it is hypothesized that, due to the influence of gravity in the vertical direction, the drop landing condition will result in greater leg soft tissue displacement, velocity and energy absorption during impact compared to the pendulum condition.

3. the energy dissipated by passive soft tissue movement will be positively correlated with the magnitude of the estimated leg tissue masses (FM, LM, WM, BMC). Magnitudes of LM, WM, FM, and/or BMC will be positively correlated with distal displacement and velocity of the soft tissue as well as with movement in the anterior and posterior directions, but will be negatively correlated with proximal displacement and velocity. This is supported by (Schinkel-Ivy et al. 2012a) who found that increases in LM, WM, and/or BMC in the lower extremity resulted in a decrease in the acceleration response at the tibia. The decrease in acceleration response is hypothesized to be a result of a corresponding increase in shock wave attenuation.

CHAPTER II

REVIEW OF LITERATURE

2.1 Tissue Properties

2.1.1 Rigid Mass (Bone)

Bone is a specialized connective tissue, important for support and protection. It is unique in that it contains organic materials that give it flexibility and resilience, as well as inorganic materials, making it hard and rigid (Nordin and Frankel, 2001). All bones are composed of compact (cortical) and trabecular (cancellous/spongy) bone (Figure 1). Compact bone is important for protection and support and is found in the external layer of all bones as well as forming the majority of the diaphyses (shaft) of long bones (Tortora, 1995). Trabecular bone is found mainly in the epiphyses (ends) of long bones and internal to compact bone in short, flat, irregular shaped bones (Tortora, 1995). Compact bone consists of many osteons, giving it a concentric ring-like structure, while trabecular bone is an irregular latticework of thin bone plates called trabeculae. The spaces between the trabeculae are filled with red bone marrow which has the ability to produce several types of blood cells (Tortora, 1995). Due to the differences in their makeup, the mechanical properties of the two types of bone are different. Compact bone is stiffer than trabecular bone, fracturing when the strain magnitude exceeds 2 %; while trabecular bone can withstand strains approaching 50 % before a fracture occurs (Nordin and Frankel, 2001). Therefore, the amount of strain that a bone can withstand is limited mostly by the compact bone, and fractures can occur in various loading modes (e.g. compression, tension, shear, torsion).

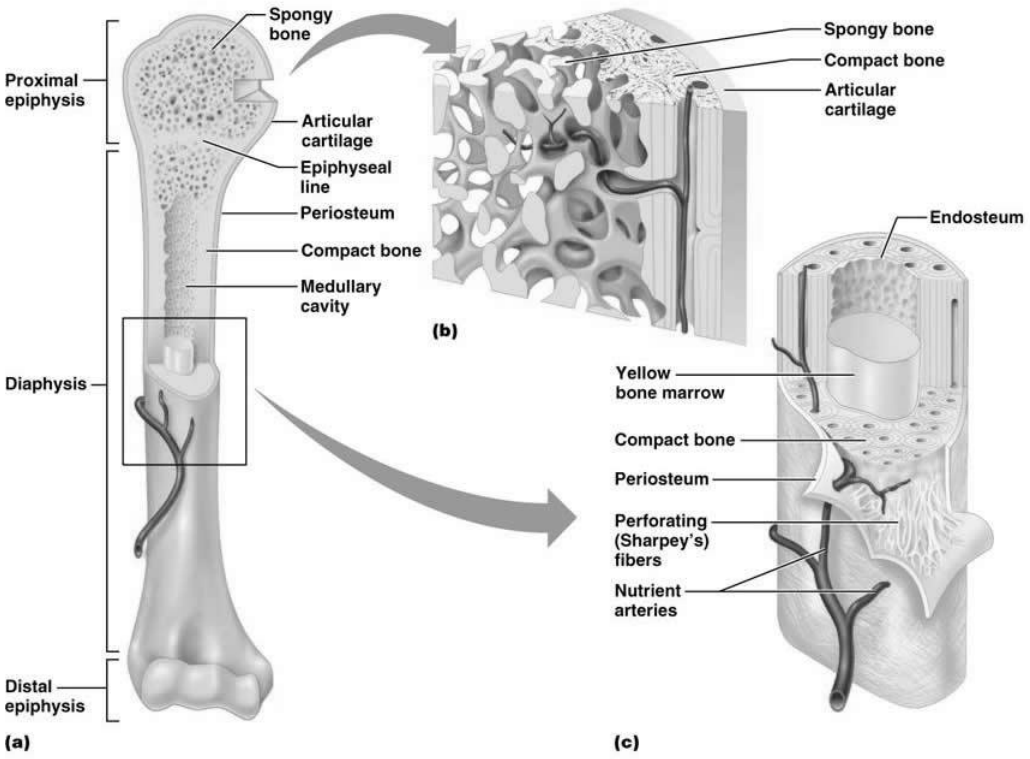

Figure 1. Femur consisting of compact and spongy bone (Modified from Aref, M., n.d.).

The stresses most commonly seen along the bones of the leg (tibia and fibula) while walking and jogging include a compressive stress during heel strike and push off, and a tensile stress during the stance phase (Carter, 1978). If tensile forces exceed the bone's tolerance, the osteons debond, resulting in a microfracture, but in compression, osteons begin to crack (Nordin and Frankel, 2001). The behavior of bone under the influence of forces is affected by the bone's mechanical properties and its geometric characteristics. Crossley et al. (1999) examined the differences in tibial bone geometry (cross-sectional area (CSA), tibial bone area), tibial bone mass and GRFs (forces that the ground exerts on the foot during impact), between those with a history of tibial stress fracture and those without. The stress fracture group had significantly smaller tibial CSA

as well as less tibial bone area. A prospective study of male infantry recruits (Giladi et al., 1987) found that narrow tibial width was a significant risk factor for developing tibial stress fractures. This emphasizes the importance of considering the loading method as well as the characteristics of the individual when determining injury mechanisms.

2.1.2 Non-Rigid Mass (Wobbling Mass)

2.1.2.1 Fat

Fat is the main form of potential energy storage in the body and a certain amount of fat is essential for life (Wood, 2006). Triglycerides are the building blocks of stored fat in adipose tissue as well as being the main form of fat found in foods (Wood, 2006). Adipose tissue can be classified according to its distribution, with subcutaneous and visceral fat accounting for the majority of total body fat; found beneath the skin and within the peritoneal cavity, respectively. Much less fat is found within the muscle tissue (interstitial) and cavities of large bones (yellow marrow) (Mattsson and Thomas, 2006). The amount of adipose tissue is affected by sex, with females having more than males at all ages, from early infancy (Malina et al., 2004) to 64 years of age (Kyle et al., 2001). The sex differences in FM continue when examining segments of the lower extremity in young healthy participants, as the mean FM for females (2744 g and 1420 g) is greater than males (906 g and 485 g) for the thigh and leg segments, respectively (Burkhart et al., 2008). Males also have lower FM in the legs (4.8 g/kg) when normalized to total body mass than females (12.1 g/kg). However, including the normalized fat masses of the foot and heel pad with the normalized fat masses of the leg resulted in greater increases in males (4.8 g/kg to 7.5 g/kg) than females (12.1 g/kg to 14.5 g/kg) (Schinkel-Ivy, 2012b).

This indicates that the magnitude of FM is greater in the feet and heel pads of males (2.7 g/kg) than females (2.4 g/kg).

During events such as running and jumping, the heel pad is often one of the first parts of the foot to strike the ground, and consists of closely packed fat cells surrounded by elastic fibrous tissue (Prichasuk, 1994). The typical heel pad ranges between 13 and 20 mm in thickness (Challis et al., 2008; Wearing et al., 2009), with men (19.4 mm) having greater heel pad thicknesses on average than women (18.1 mm) (Prichasuk, 1994). The heel pad's primary role is to absorb some of the force and attenuate some of the shock following impact (Ker at al., 1989). Men's heel pads absorb more impact energy (84.3 %) than women's (82.3 %), and typically have a greater peak displacement (Alcantara et al., 2002).

The soft tissue of the heel pad becomes stiffer with age, which may reduce the adaptability of the tissue to respond to sudden or repetitive stress. The repetitive microtraumas that occur to the heel throughout life causes a loss of collagen, a decrease in water content and elastic fibrous tissue, which leads to a decrease in the elasticity of the heel's fat pad (Ozdemir et al., 2004). Stiffer heel pads are less compressible, leading to lower levels of impact force attenuation and increases in the prevalence of plantar heel pain (Tong et al., 2003).

It is not known whether differences in heel pad thickness and energy absorption capacity are sex-related or whether increases seen in males are due to greater average body mass. The thickness of the heel pad alone cannot predict its properties, as age, sex,

and body mass affect the elasticity of the heel pad, which plays a critical role in its energy absorption capabilities.

2.1.2.2 Muscle

There are three types of muscle cells or fibres in the body: cardiac, smooth, and skeletal. Cardiac muscle is found in the heart, and smooth muscles are found in the gut, airways, urogenital tract, vasculature and some glands (Tortora, 1995). Impact analyses focus on skeletal muscles, as their major function is to move bones about joints, which is normally accomplished through voluntary control (Tortora, 1995). Each skeletal muscle fibre is composed of between 100 and 1000 myofibrils. The myofibril is the contractile unit of the muscle which consists of myofilaments organized in sarcomeres (Jennett, 1989) (Figure 2).

Forces generated within a muscle are transmitted to bone via connective tissue which surrounds the muscle, muscle fascicles and muscle fibres (Malina et al., 2004) and extends to the bones as tendons. Males have greater mean muscle fibre size, fat free mass (FFM) (Malina et al., 2004), and total muscle mass in the body than females (45 % vs. 36 %, respectively) (Komi and Karlsson, 1978). Like adipose tissue, skeletal muscle has a high degree of malleability (Malina et al., 2004) (i.e. it can deform a very significant amount), and therefore plays a significant role in energy absorption.

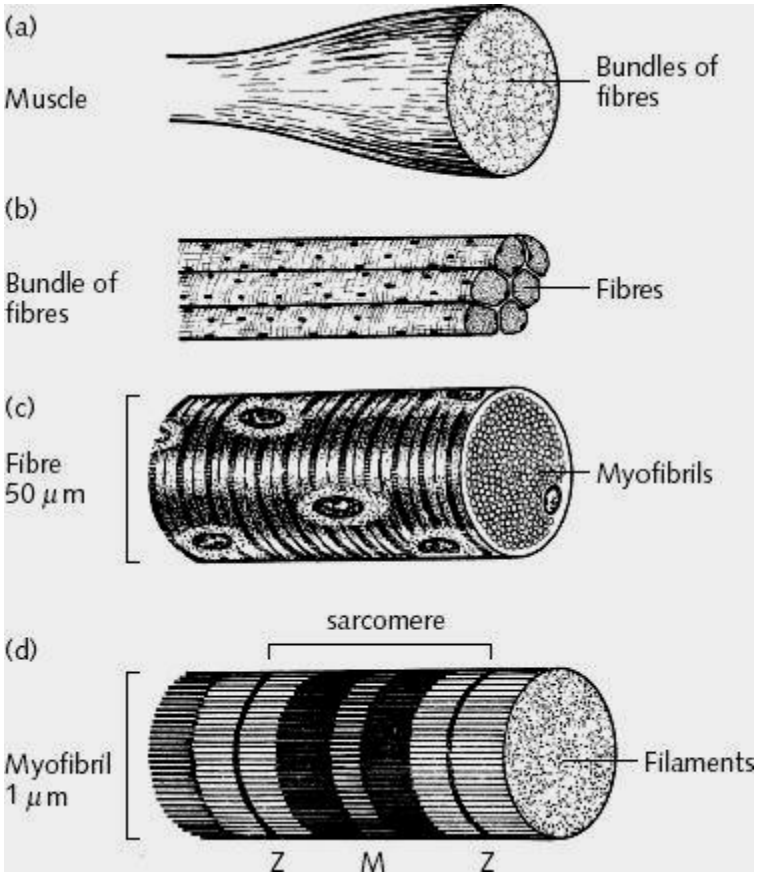

Figure 2. Skeletal muscle at increasing magnification: (a) the whole muscle; (b) bundle of muscle fibres; (c) a single muscle fibre; (d) a single myofibril, composed of myofilaments (Modified from Jennett, 1989).

2.2 Body Composition

Body composition research is primarily focused on the study of how muscle, adipose, and bone tissues are partitioned in the body (Malina et al., 2004). Body composition can be measured using X-rays or anthropometric devices such as measuring tapes and skin calipers (Lukaski, 1987). More advanced methods utilizing Dual-Energy X-ray Absorptiometry (DEXA), bioelectrical impedance, MRI and underwater weighing result in better predictions of an individual's body composition, including BMC, FM, and FFM. One of the primary limitations of these more advanced methods is that they are

more costly and are not as readily available for research purposes. This limits how often and easily these devices can be used and creates a barrier for the inclusion of more accurate tissue mass information into biomechanical models.

2.2.1 Whole Body

Men on average have a total FFM of approximately 60 kg, while women have closer to 43 kg, with minimal differences between those who are sedentary and physically active (Kyle et al., 2001). Sedentary men have approximately 14-15 kg (18-19 %) of FM, and those who are physically active have 12 kg (16 %), while women have 16-17 kg (26-27 %) and 14 kg (24 %), respectively (Kyle et al., 2001).

Women between the ages of 55 and 65 years have on average a total BMC of 2.07 kg, while age-matched men have significantly more (2.96 kg) (Binder and Kohrt, 2000). Similar characteristics are seen with participants between the ages of 18 and 41 years, with a noticeable increase for both women (2.6 kg) and men (3.6 kg) (Norcross and Van Loan, 2004). Men also have greater total LM on average (58.5 kg, 79 % of their body mass) than women (41.0 kg and 68 %) (Perez-Gomez et al., 2008).

2.2.2 Android and Gynoid Fat

The distribution of fat in the body is often categorized as android (upper body) fat or gynoid (lower body) fat distribution. People with these general fat distribution patterns are also commonly referred to as having an apple shape (android) or pear (gynoid) shape (Figure 3). Men tend to accumulate fat in the android pattern, with fat accumulating around the abdomen to a greater extent. Women are more likely to

accumulate fat in the gynoid pattern, which involves more fat deposition in the hips and thighs (Brody, 1999).

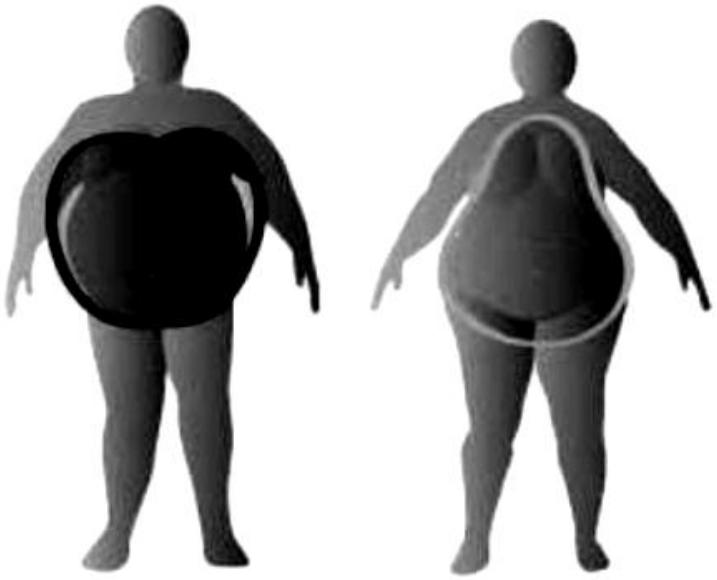

Figure 3. (a) Apple (android) versus (b) pear (gynoid) fat distribution patterns (Modified from Insel et al., 2010).

A study by Ley et al. (1992) measured and compared the body fat distribution differences using DEXA between men and women, and found that the proportion of android fat was significantly higher in men (48.6 % versus 40.3 %) and gynoid fat was significantly greater in women (43.4 % versus 35.4 %). Women also had leg FM that was significantly greater than that of males; differences which remained significant after adjusting for height, age, and body mass index (BMI).

2.2.3 Leg and Foot

Research on leg tissue mass composition differences between the sexes is limited. Mazess et al. (1990) used DEXA to determine the differences in the amounts of thigh and leg FM, LM, and BMC between men and women. Total thigh and leg tissue mass was found to be greater for males (26.3 kg) than females (23.7 kg). At the individual tissue level, males had greater lean tissue and BMC (22.2 kg, and 1.25 kg) than females (15.9 kg and 0.86 kg) in the thigh and leg. Females (7.8 kg) had greater FM in the thigh and leg than males (4.1 kg), on average. Schinkel-Ivy et al. (2012a) also found significant differences in the amount of FM and LM between the sexes in the leg. Males were found to have more LM and less FM on average. Males also had greater amounts of total WM, although this difference was not found to be significant (Figure 4). Differences in LM, WM, and FM all remained when tissue masses in the leg and foot were normalized to total body mass (Schinkel-Ivy et al., 2012b) (Figure 5).

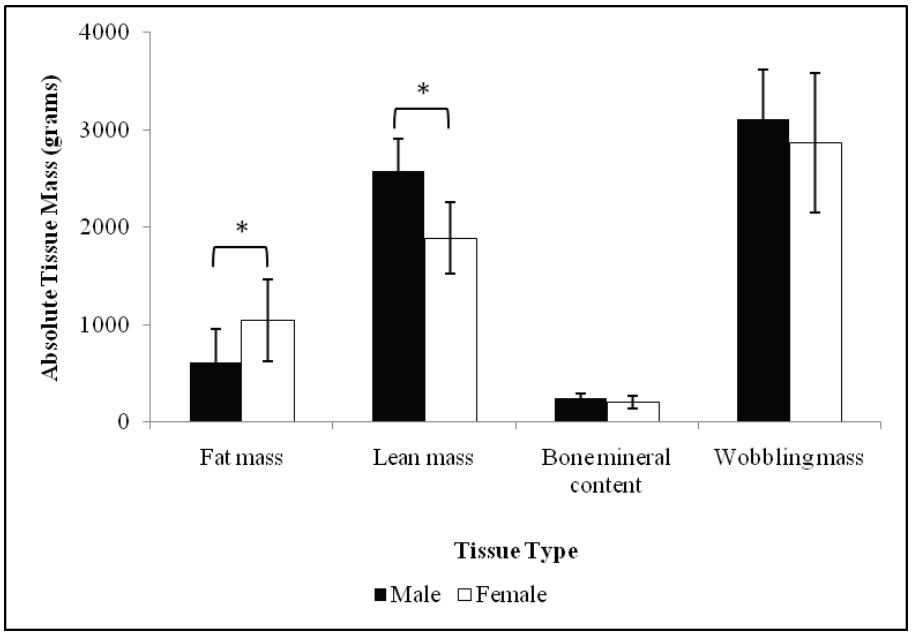

Figure 4. Sex differences in fat mass, lean mass, bone mineral content and wobbling mass in the leg (Modified from Schinkel-Ivy et al., 2012a).

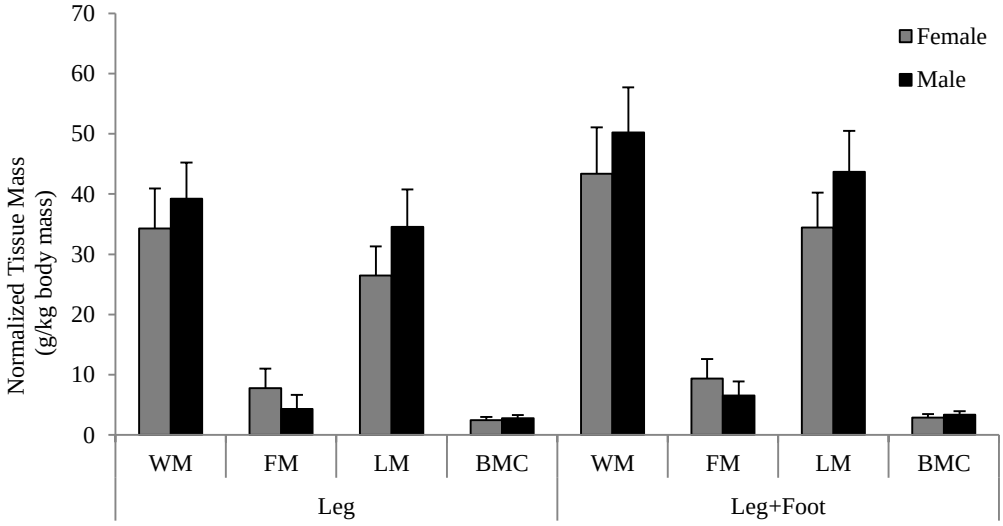

Figure 5. Sex differences in normalized fat mass, lean mass, bone mineral content and wobbling mass in the leg and leg+foot (Modified from Schinkel-Ivy et al., 2012b).

2.2.4 Tissue Mass Prediction Using Regression Equations

Whole body tissue composition can be quantified using a variety of methods, including skin fold thickness and anthropometric measurements, bioelectrical impedance, MRI and underwater weighing (Mattsson and Thomas, 2006), but individual soft (FM, LM, and WM) and rigid (BMC) tissue masses of the body can be determined using DEXA (Binder and Korht, 2000; Norcross and Van Loan, 2004; Perez-Gomez et al., 2008). To address the limitations of DEXA, such as radiation exposure, expense, and its limited access for research, Holmes et al. (2005) developed regression equations that enable soft tissue masses of the lower extremities of living people to be predicted using simple anthropometric measures (segment lengths, circumferences, breadths and skinfolds). In their study, twelve prediction equations were developed, one each for FM, LM, WM and BMC of the thigh, leg and leg + foot segments, using multiple stepwise

regression analysis. Data from a separate sample of participants were used to validate the equations. Excellent between- and within-measurer reliability for these anthropometric measurements have been previously established for trained personnel, with intra-class correlation coefficients of 0.79, 0.86, 0.85, and 0.86 for lengths, circumferences, breadths and skinfolds, respectively (Burkhart et al., 2008). Small errors in the anthropometric measurements resulted in larger errors in FM, LM, WM and BMC estimates with maximum mean between measurement errors of 24.2 %, 22.9 %, 9.2 % and 4.5 %, and within measurement errors of 11.1 %, 10.4 %, and 4.7 % and 9.3 %. The equations resulted in mean errors of 5.3 %, 7.9 %, 11.2 %, and 21.4 % for the predicted FM, LM, WM, and BMC masses for the thigh, leg, and leg + foot segments, respectively, when compared to those obtained from DEXA (Holmes et al., 2005).

2.3 Biomechanical Models

A model can be described as a set of equations that depict physical events, or a particular aspect of the real world (Kroemer and Snook, 1988). Biomechanical models of the human body are used to predict the kinetics and/or kinematics of various body segments and systems (i.e. musculoskeletal) that would be difficult, if not impossible to collect from a living person. The better the human models are able to accurately represent real life, the more accurate the kinetic and kinematic predictions made with the models will be, and the more impact such models will have on areas of research for which they were designed.

Until 20 years ago, body segments incorporated into biomechanical models were considered as stiff, stable elements that did not deform. Consequently, investigators

modeled these segments as rigid bodies (Pain and Challis, 2006). Human body segments consist of muscle, adipose tissue, skin, connective tissue, and bone, and while bone can be considered fairly rigid, the other soft tissues are not (Challis and Pain, 2008). Assuming that body segments are rigid while modeling can lead to large errors when performing either direct or indirect dynamics analyses, especially when there are impulsive forces experienced, such as during impact (Pain and Challis, 2006). The effects of soft tissue movement on force attenuation have been investigated and their importance has been recognized. WM models have been developed to investigate the role of soft tissue in impact loading (Gruber et al., 1998; Pain and Challis, 2004) and to examine how different distributions of rigid and soft tissue affect overall force attenuation (Gittoes et al., 2006) (Figure 6).

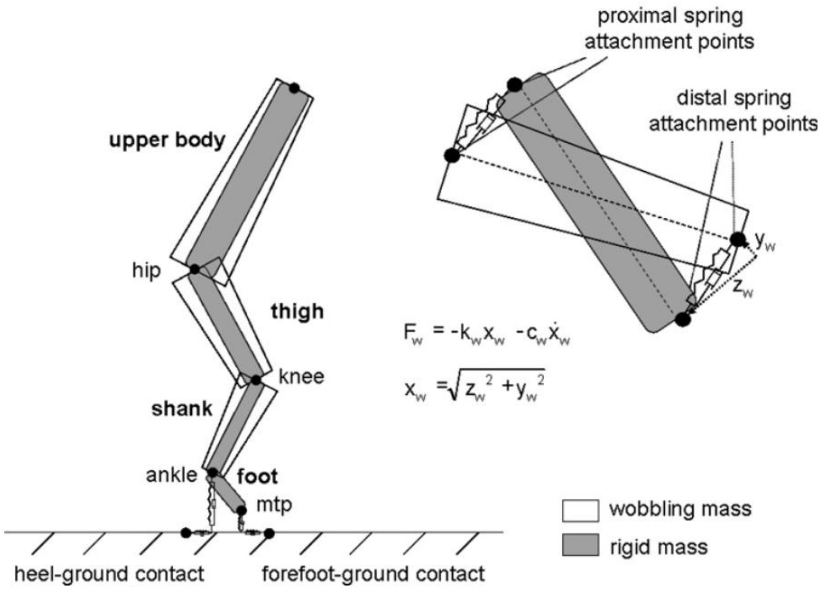

Figure 6. Wobbling mass model, with inner rigid skeleton segments and outer wobbling mass segments (Modified from Gittoes et al., 2006).

Gittoes et al. (2006) found that the inclusion of soft tissue properties into their model contributed up to an 8.6 times BW reduction in peak vertical GRF, and it has been

suggested that soft tissues significantly affect impact force magnitude in the first 100 ms of landing. Pain and Challis (2006) found torques about the ankle, knee and hip joints that were up to 50 % lower when they included soft tissue into their biomechanical model. Due to these findings, further experimental analysis into the role that soft tissues play and the effects that they have on the outputs from biomechanical models, appears warranted.

2.4 Drop Landing Versus Pendulum Technique

The kinematics (e.g. displacement, velocity) and kinetics (e.g. forces, torques) of the lower extremity that result from impact have been studied extensively. Impacts are commonly initiated using various techniques such as running and walking on a treadmill, drop landings, and pendulums.

Drop landings have been performed in the past by participants simply stepping off an elevated surface (Decker et al., 2003; Gittoes et al., 2006; Schmitz et al., 2007; Yeow et al, 2009), or by using a hang bar positioned above a force platform (Kernozek et al., 2005), which is typically mounted flush with the surrounding floor. Landings can be performed on a single foot (Kernozek et al., 2005; Zhang et al., 2000; Zhang et al., 2005), with the other foot landing next to the force platform, or with both feet (Gittoes et al., 2006; Pain and Challis, 2006; Yeow et al., 2009). Using this type of approach, the effects of lower extremity kinematics (Yeow et al, 2009), fatigue (Coventry et al., 2006), soft tissue movement (Pain and Challis, 2006), and sex (Decker et al., 2003) on GRFs, joint torques, tibial accelerations, energy absorption, and shock attenuation have been investigated.

Human pendulums have been used previously to assess a variety of measures associated with lower extremity impact, such as tibial accelerations (Duquette and Andrews, 2010; Flynn et al., 2004; Holmes and Andrews, 2006), wall reaction forces (Fowler et al., 1997; Lafortune and Lake, 1995), and the effects that knee angles (Lafortune et al., 1996a) have on tibial response. Pendulums allow for the reproduction of impact loads similar to those encountered in human locomotion, in a consistent manner between and within participants, while controlling for joint angles and impact velocities (Lafortune and Lake, 1995).

Pendulum designs have ranged from a car seat mounted on a steel frame (Fowler et al., 1997) to a plastic or steel rectangular frame with a canvas bed (Duquette and Andrews, 2010; Lafortune and Lake, 1995) (Figure 7). The seat or bed frames are typically suspended from above by cables or pipes. Bed-like designs usually require participants to lie supine on the device, while the leg under investigation extends over the leading edge of the frame. Participants are released after being pulled back a predetermined distance in order to produce consistent impact velocities and forces. Duquette and Andrews (2010), Flynn et al. (2004), Holmes and Andrews (2006), Lafortune and Lake, 1995 and Schinkel-Ivy et al. (2012a) targeted velocities between 1.0 and 1.15 m/s, and impact forces of 1.8–2.8 times BW, to closely resemble the impact conditions during running (Cavanagh and Lafortune, 1980).

While the pendulum apparatus has varied somewhat between studies, the impact apparatus has traditionally consisted of force platforms vertically mounted to the wall (Fowler et al., 1997), a steel mounting base and concrete slab (Lafortune and Lake, 1995)

(Figure 7), or to a steel grid which is secured to the wall and floor (Duquette and Andrews, 2010; Flynn et al., 2004; Holmes and Andrews, 2006; Schinkel-Ivy et al., 2010).

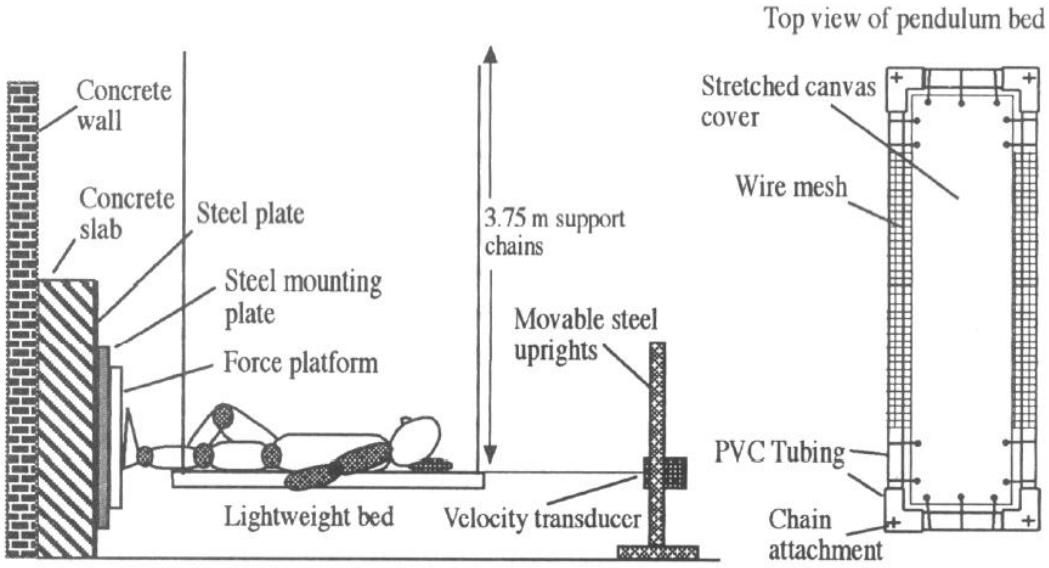

Figure 7. Schematic diagram of a human pendulum apparatus (Modified from Lafortune and Lake, 1995).

Fowler and Lees (1998) compared the kinetic and kinematic characteristics of the lower body that resulted from impacts using a pendulum apparatus and a drop landing technique. They found that, upon initial contact with the ground or wall, there were no significant differences in any of the investigated ankle, knee, and hip angles between the two investigated impact techniques. Therefore, based on the similarities between the two impact techniques, it was concluded that pendulum-based impacts provide a stimulus similar to that of drop jumps.

2.5 Vertical Ground Reaction Forces

The term impact force is used in human locomotion to describe the force produced due to the collision between the foot and the ground, while active forces are generated by movement due to muscular activity (Nigg et al., 1995). GRFs are the forces that the ground exerts back onto the foot following impact (Challis and Pain, 2008), and vertical GRFs are impact forces that are oriented in the vertical direction (Cavanagh and Lafortune, 1980). The magnitude of these forces is an important risk factor for lower extremity injuries (Yeow et al., 2009). To quantify the force between the foot and the ground, force platforms are utilized which can measure forces in six different directions (+/- X, Y, Z) (Nigg et al., 1995). During impact, the magnitude of the GRF is determined from the mass of the body impacting the force platform, and its acceleration. Impact forces during running reach their maximum magnitude within 50 ms of the foot making first contact with the ground (Nigg et al., 1995) and reach an average peak amplitude of approximately 2.2 times BW (Cavanagh and Lafortune, 1980) (Figure 8). A second active force peak occurs around 100 ms after foot contact and reaches an average amplitude of almost 3 times BW (Cavanagh and Lafortune, 1980) (Figure 8).

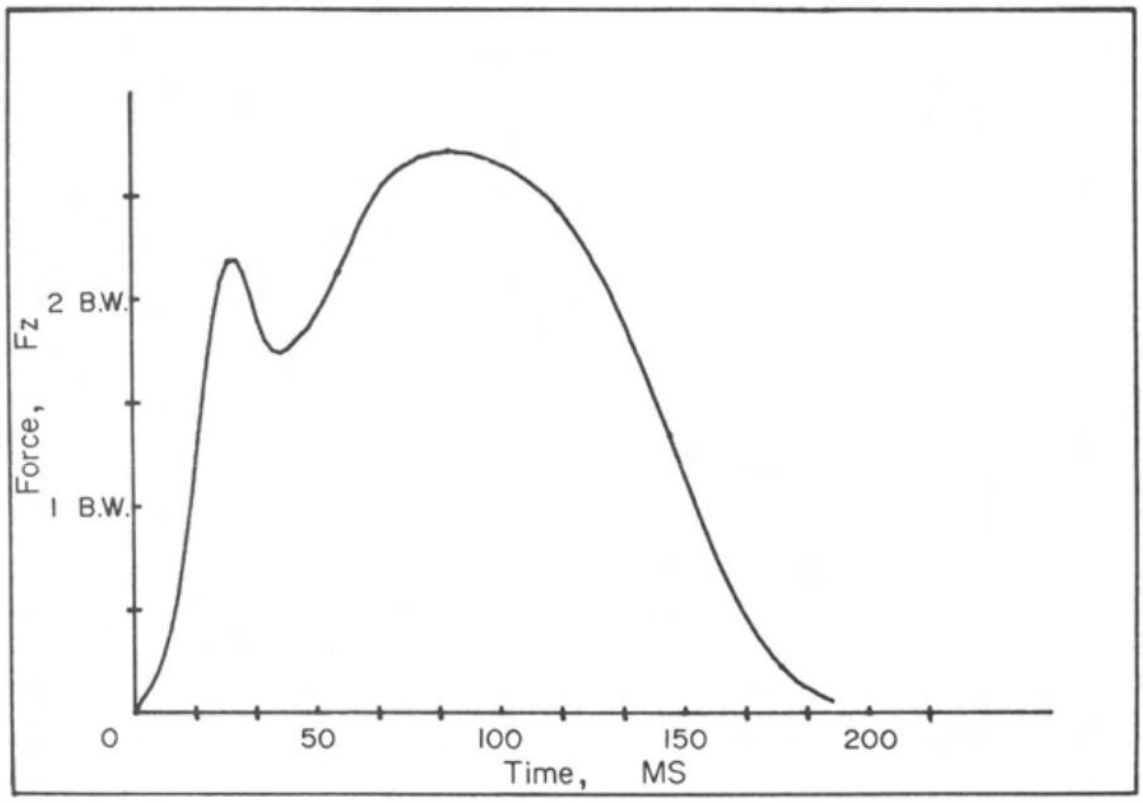

Figure 8. Vertical ground reaction force (Modified from Cavanagh and Lafortune et al., 1980).

Liu and Nigg (2000) investigated the influences of mass and mass distribution between the rigid and WM in the upper and lower body, on impact forces during running. They found that increases in upper body wobbling and rigid masses had minimal effect on impact forces, while increases in these tissue masses in the lower body led to significant increases in the impact force peak. Increases in overall body mass has been shown to result in increases in GRFs measured during walking, with obese individuals (BMI 30-40 kg/m^2; body mass 110.6 kg) having greater absolute GRFs (≈ 1000 N) than normal weight individuals (BMI 18-25 kg/m^2; body mass 67.7 kg) (≈ 600 N) (Browning et al., 2009). When these forces were normalized to body mass (N/kg), the forces were similar between the two groups (Browning et al., 2009). Therefore, the differences in the

measured vertical GRFs between the two groups are almost directly attributable to the increases in BW.

2.6 Shock Wave Attenuation

Forces created from the contact between the foot and the ground are transmitted proximally through the ankle joint, along the tibia, through the knee joint, and eventually all the way to the head (Whittle, 1999). These forces can be seen as waves that are associated with accelerations and decelerations of the body's tissues (Shorten and Winslow, 1992). The term 'shock wave' refers to the propagation of this wave (a stress wave) through the body's tissues. Attenuation is the weakening or reduction in force, intensity, effect, quantity, or value that occurs as the distance from the source increases as a result of absorption, scattering, or spreading in three dimensions (Attenuation, n.d.). Shock wave attenuation is therefore the reduction in the impact force amplitude that occurs as it propagates proximally through the body's tissues. The term 'shock' has been described by Nigg et al. (1995) as a transient condition whereby a system's equilibrium is disrupted by a sudden change in force application.

Shock wave attenuation through the body has been measured and quantified by attaching skin-mounted accelerometers to the anteromedial surface of the distal tibia and the head (Brizuela et al., 1997; Chu and Caldwell, 2004; Coventry et al., 2006; Dufek et al., 2009; Mercer et al., 2003; Mercer et al., 2010; Zhang et al., 2005). Accelerometers are commonly secured with an elastic strap to reduce any unwanted movement between the underlying tissue and the accelerometer (Shorten and Winslow, 1992). The peaks of the acceleration waveforms (PA) at each of these regions have been used to quantify the

amount of shock wave attenuation that is occurring (Duquette and Andrews, 2010; Flynn et al., 2004; Hennig and Lafortune, 1991; McLean, et al., 2011) (Figure 9).

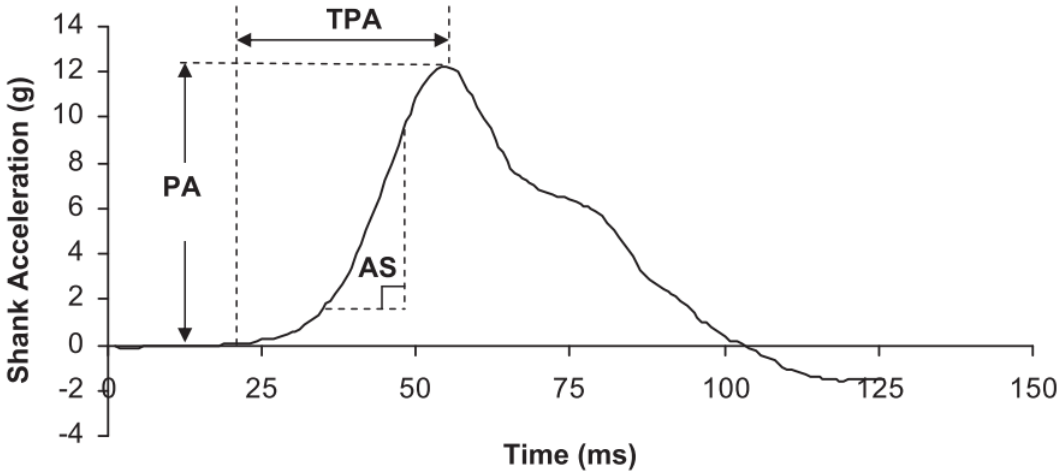

Figure 9. Tibial acceleration waveform highlighting peak tibial acceleration (PA), time to peak tibial acceleration (TA), and tibial acceleration slope (AS) (Modified from Duquette and Andrews, 2010).

Voloshin and Wosk (1982) described shock attenuation (SA) as the quotient of the acceleration of a proximal segment (e.g. head) and a more distal segment (e.g. tibia). The amount of SA that occurs can be determined using Equation 1 (Chu and Caldwell, 2004; Dufek et al., 2009; Zhang et al., 2005).

$$SA = \left[1 - \left(\frac{a_{proximal}}{a_{distal}}\right)\right] X\ 100 \qquad \text{(Eq. 1)}$$

where, $a_{proximal}$ and a_{distal} are the peak accelerations (g) of the proximal and distal segments (e.g. head and tibia), respectively.

Chu and Caldwell (2004) measured participants' PAs at the frontal bone of the head and the anteromedial aspect of the tibia during a treadmill running task. They determined that close to 75 % of the shock wave was attenuated by segments between the

two accelerometers by the time the shock wave reached the head; a result that compared favourably to other studies (Coventry et al., 2006; Dufek et al., 2009).

Impact forces of approximately 3 times BW are produced during contact with the ground during running (Cavanagh and Lafortune, 1980) and 10 times BW following landing from a maximal jump (Ortega et al., 2010). Shock wave attenuation can occur passively through the movement of soft tissue (fat, muscle, skin) relative to bone, or by active mechanisms, such as knee and hip flexion during impact (Mercer et al., 2010) and altering leg muscle activation (Duquette and Andrews, 2010; Flynn et al, 2004; Holmes and Andrews, 2006; Nigg and Liu, 1999).

2.6.1 Passive Structures

Both soft (fat, muscle, cartilage, etc.) and rigid (bone) tissues contribute to passive shock wave attenuation following impacts. The rapid deceleration of the leg caused by impact during running or jumping results in the soft tissues of the leg moving relative to the rigid tissue (bone). This soft tissue movement has been shown to serve a protective role during impact events such as running (Cole et al., 1996) and drop landings (Pain and Challis, 2006; Schinkel-Ivy et al., 2012a, b). The reduction in peak vertical GRFs that results from the soft tissue motion relative to bone translates into reduced joint loads during these tasks (Pain and Challis, 2006). It has been shown that following hand impacts, the impact energy is dissipated considerably by the soft tissues (Pain and Challis, 2002) as the shock wave travels proximally. The heel pad also acts to absorb a large amount of the shock wave by deforming upon ground contact. During a drop

landing test, Kinoshita et al. (1993) reported that there was an average heel pad deformation of 11.3 mm, which accounted for 79 % of the impact energy being absorbed.

The mass of both the soft and rigid tissues in the body has been shown to affect shock wave attenuation through the lower extremity (Schinkel-Ivy et al., 2012a). Increases in FM, LM, WM and BMC led to decreases in the peak acceleration response measured at the proximal tibia medial to the tibial tuberosity, with magnitudes of bone mass and LM having the most significant contribution to the decreases in tibial accelerations (Schinkel-Ivy et al., 2012a).

2.6.2 Active Structures

2.6.2.1 Muscle Activation

Muscle activation is considered one of the primary ways that the attenuation of the shock wave produced following impact can be affected. Changes in lower extremity muscle activity prior to landing may control skeletal movement and affect impact forces during landing (Nigg and Liu, 1999). A failure of the muscles to actively absorb the impact energy may overload the passive structures, and consequently lead to injury (Derrick et al., 1998). As a muscle's activation increases, so does its stiffness. A more compliant, or less stiff lower extremity, would be more effective at attenuating the shock wave following impact (Derrick et al., 2000).

Whole body fatigue limits the musculoskeletal system's ability to protect itself from heel impact-generated shock waves, which may result in greater shock wave acceleration amplitude at the knee (Verbitsky et al., 1998). Whole body fatigue, or cardiovascular fatigue is usually accomplished through a graded exercise test on a

treadmill and has been represented by increases in oxygen consumption (Mercer et al., 2003) or by decreases in the pressure of end tidal carbon dioxide ($PETCO_2$) (Verbitsky et al., 1998). Comparing a whole body fatigued to an unfatigued condition showed a significant increase in the peak acceleration amplitudes recorded at the tibial tuberosity for fatigued runners on a treadmill (Verbitsky et al., 1998). Mercer et al. (2003) had participants go through a graded exercise test on a treadmill and found that when participants were fatigued, there was on average 12 % less shock attenuation occurring between the foot and head.

While the above studies focused on the effects of whole body fatigue, Flynn et al. (2004) studied local muscle fatigue by measuring the amount of muscular activation in the tibialis anterior and gastrocnemius muscles using electromyography (EMG). By also measuring accelerations at the tibial tubercle, they found that the mean overall peak acceleration and acceleration slope decreased significantly following fatigue. They concluded that the leg muscles became less stiff when fatigued, which reduced the overall stiffness of the leg segment and increased the amount of attenuation (i.e. lower peak accelerations) the leg was able to provide.

2.6.2.2 Joint Angles

Previous examinations of the kinematics of the lower extremity joints (hip, knee and ankle) during landing illustrate the importance of these joints in shock wave attenuation, the magnitude of which is dependent on the degree of flexion (Coventry et al., 2006). In a study by Lafortune et al. (1996b), the mean peak acceleration at the head decreased by 45 %, while the peak acceleration at the shank increased by 57 %, as the

initial knee angle (i.e. prior to contact) increased from 0 to 40°. Based on these findings, it appears that larger knee angles expose the shank to more severe shock, while reducing the amount of shock that is transmitted to the head. This results in greater shock wave attenuation through the body. Although the knee angle has been shown to be an important factor to consider when analyzing shock attenuation through the body, the ankle joint during a human pendulum task has also been shown to influence lower extremity accelerations, as increasing ankle dorsiflexion at contact from 1 to 9.2° resulted in a decrease in 20 % of peak tibial acceleration (Duquette and Andrews, 2010).

2.6.2.3 External Factors

External factors such as footwear design, braces and the nature of the contacting surface also have an influence on shock attenuation. Greater ankle support from either a high top shoe or ankle taping reduces the normal range of movement, in particular, ankle plantarflexion. This can reduce the force attenuating ability of the ankle joint and increase the risk of overuse injuries (Brizuela et al., 1997). Adding tape or a brace to the ankle also reduces the amount of time to reach peak impact force, which decreases the force attenuating ability of the lower extremity following impact (Riemann et al., 2002).

Shoes which have softer midsoles are better at attenuating impact forces during landings, thereby helping to reduce impact-related injuries (Zhang et al., 2005). The softness of the contact surface has also been evaluated in terms of the effect it has on impact force attenuation. For example, Lafortune et al. (1996a) covered their force platform with ethylene-vinyl acetate (EVA) foam to represent a soft contact surface (hard = force platform alone). They concluded that changing from a harder to a softer surface

caused a 28 % reduction in the wall reaction force. The harder surface also caused an increase in peak acceleration at both the tibia and the head following impact.

2.6.3 Sex and Shock Attenuation

Differences in passive and active structures between the sexes have been shown to result in differences in total shock attenuation through the body. Dufek et al. (2009) compared the peak accelerations of the leg and head during a treadmill running task for both sexes, showing that males attenuated 71.7 % of the shock wave by the time it reached the head, while females attenuated 83.7 %. This difference may be explained by passive structures, as females typically have greater proportions of adipose tissue (Malina et al., 2004). Peak tibial accelerations following heel impacts also tend to be greater for females (Figure 10), which may be attributable to the greater amount of FM, or the lesser amount of LM, BMC, or WM found in the leg segments of women when compared to men (Schinkel-Ivy et al., 2012a).

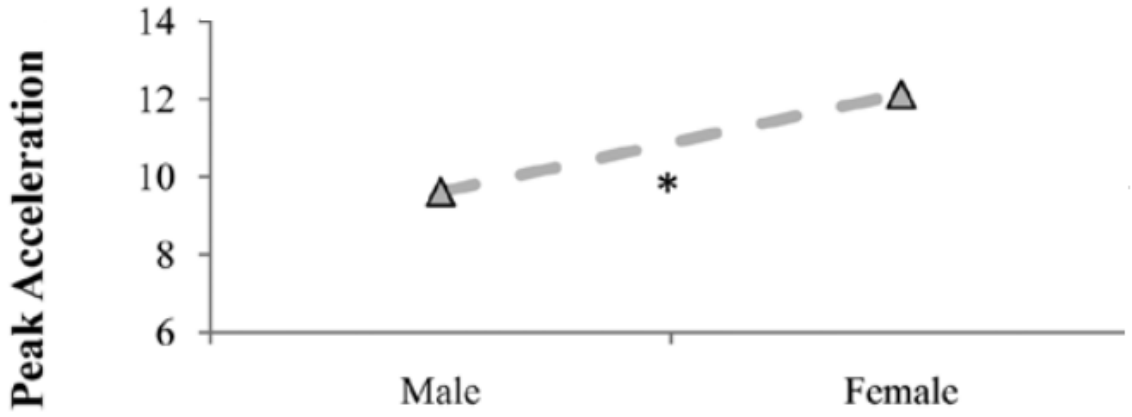

Figure 10. Comparison of male and female peak tibial acceleration (g) (Modified from Schinkel-Ivy et al., 2012a).

Peak head accelerations have been shown to be both similar between the sexes (Dufek et al., 2009) and greater for females (Mercer et al., 2010), while tibial accelerations are consistently greater for females (Dufek et al., 2009; Mercer et al., 2010; Schinkel-Ivy et al., 2012a). The greater tibial accelerations and peak vertical GRFs observed in women may increase demands on the lower extremity tissues and be a factor contributing to women's greater susceptibility to various injuries, such as anterior cruciate ligament (ACL) tears (Arendt et al., 1999), and stress fractures (Jones et al., 2002)

2.7 Energies

There are several mechanisms responsible for minimizing the amount of shock wave acceleration experienced by the body. The body's passive and active structures work together to dissipate the energy of the impact in order to protect the body from injury. Following drop landings, it has been shown that the ankle, knee, and hip joints all play an important role in energy dissipation (Derrick et al., 1998; Devita and Skelly, 1992; Norcross et al., 2010; Yeow et al., 2011a, b; Zhang et al., 2000). Segment soft tissue movement (Pain and Challis, 2002) and heel pad deformation (Aerts et al., 1995; Alcantara et al., 2002; Challis et al., 2008; Chi and Schmitt, 2005) also act to dissipate a fair amount of energy following impact. Using a WM model, Pain and Challis (2001) showed that the heel pad and soft tissues of the shank work together to dissipate the impact energy by 89.9 %, compared to only 45 % for a rigid body model. They also illustrated the importance of the shank soft tissues by demonstrating that peak forces experienced by the heel pad, while connected to a rigid shank, were over 100 % greater than those for a heel pad connected to a shank with a WM component.

Pain and Challis (2002) measured the energy lost following karate strike impacts to a force platform using a technique that assessed the amount of soft tissue deformation that occurred among sets of four skin surface markers. The change in area, defined by the difference in the maximum and minimum areas divided by the mean area of the quadrilaterals (set of four markers), was found to be a total of 11 %. Compression waves resulting from the impacts travelled longitudinally with respect to the muscle fibres and were therefore assumed by Pain and Challis (2002) to be almost completely non-dispersive (Deffieux et al., 2009; Gennisson et al., 2010). Consequently, they estimated the total energy carried by (i.e. energy density) this soft tissue motion using Equation 2 and the inertial parameters of the forearm (as per Pain and Challis, 2002).

$$Ed = ½ \rho \cdot A^2 \cdot \omega^2 \qquad \text{(Eq. 2)}$$

where Ed = energy density (J/m^2), ρ = density of material the wave is propagating through (kg/m^3), A = amplitude of the wave (cm), and ω = angular frequency (rad/s).

By multiplying the calculated energy density (261 J/m^2) by the mean CSA of the forearm soft tissue (0.0043 m^2), Pain and Challis (2002) found the energy carried by the soft tissue wave to be 1.1 J. Comparing this to the mean kinetic energy of the forearm at impact (1.6 J), Pain and Challis (2002) reported that the deformation of the soft tissue accounted for 70 % of the energy lost from the forearm during the karate strike.

2.8 Soft Tissue Motion

Many studies suggest that errors in human motion measurements can arise due to soft tissue movement relative to the underlying bone (Fuller et al., 1997; Gao and Zheng, 2008; Leardini et al., 2005). Errors are largely dependent on the analysis system used

and on individual soft tissue characteristics of participants (Houck et al., 2004). The motion that occurs between soft tissue and bone during movement is commonly viewed as error (or soft tissue artefact – STA) and effort is typically invested by researchers to remove it from their data rather than studying its importance (Peters et al., 2010). However, removing soft tissue motion eliminates an important contributor to shock attenuation during human impacts (Pain and Challis, 2002).

Most of the previous research in this area has only quantified the magnitude of skin displacement relative to the underlying bone during a dynamic task, while both the bone and skin are in motion (Akbarshahi et al., 2010; Houck et al., 2004; Manal et al., 2003; Sangeux et al., 2006; Stagni et al., 2005). For example, comparing the movement of the bone and soft tissue of the proximal tibia during a natural cadence walking task showed an average difference of 7.4, 3.7, and 2.1 mm along the X (medial-lateral), Y (anterior-posterior) and Z (superior-inferior) axes, respectively (Manal et al., 2003). The STA along the medial-lateral, anterior-posterior, and superior-inferior axes during level walking and during a step up task showed significant differences in both the thigh and shank segments (Akbarshahi et al., 2010) (Table 1). Fuller et al. (1997) compared the movement of marker arrays which were mounted on bone pins, with arrays attached directly to the skin. Overall, movement of the skin relative to the underlying bone during a variety of activities reached magnitudes of up to 20 mm.

Table 1. Mean (RMS) error due to STA for each skin marker, and for both the thigh and shank segments for the two tasks. M-L: medio-lateral; A-P: antero-posterior; S-I: superior-inferior (adapted from Akbarshahi et al., 2010).

	Level Walking			Step-up		
	M/L	A/P	S/I	M/L	A/P	S/I
Thigh	9.7 (±0.9)	6.2 (±1.9)	7.6 (±3.1)	10.7 (±5.4)	5.9 (±3.0)	12.6 (±4.7)
Shank	8.4 (±3.3)	6.0 (±1.2)	3.3 (±0.2)	6.9 (±1.9)	4.3 (±0.2)	2.7 (±0.2)

Measuring the movement of soft tissue relative to bone may provide us with a better understanding of its effect on shock attenuation. Pain and Challis (2002) adhered skin markers to the forearm of a single participant and recorded a mean vertical displacement of 17 mm following a karate strike against a solid object. After impact, the markers continued downward due to the inertia of the soft tissue, then rebounded upwardly past their initial starting position, until eventually coming to rest shortly thereafter (Figure 11). Using a similar technique, soft tissues were reported to have a mean displacement of 18 mm in the shank and 32 mm in the thigh (Pain and Challis, 2006).

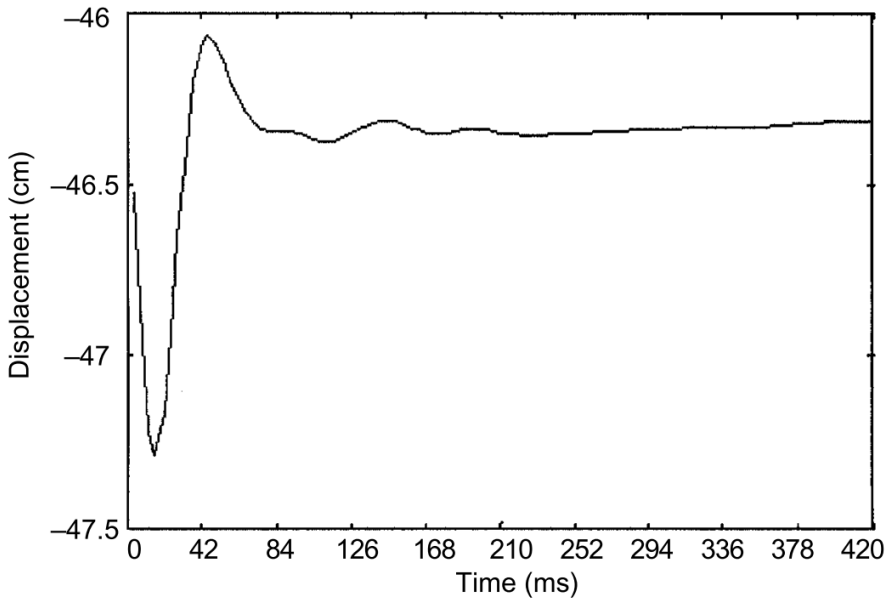

Figure 11. Displacement of a typical marker in the vertical direction after impact (t=0) (Modified from Pain and Challis, 2002).

Different movement analysis techniques have been employed in the past to measure soft tissue motion including fluoroscopy (Kuo et al., 2011, Peters et al., 2010;

Sati et al., 1996; Stagni et al., 2005; Wrbaškić and Dowling, 2007), X-ray (Maslen and Ackland, 1994; Tranberg and Karlsson, 1998), MRI (Sangeux et al., 2006), and 3D stereophotogrammetry (Akbarshahi et al., 2010; Ball, 2011; Bridgman et al., 2010; Cappozzo et al., 2005; Ferber et al., 2002; Fuller et al.,1997; Holden et al., 1997; Houck et al., 2004; Leardini et al., 2005; Manal et al., 2003; Pain and Challis, 2002; Scholz, 1989; Stagni et al., 2005; Telfer et al., 2010). Each of these methods is described below, including some of their associated limitations.

2.8.1 Intracortical Pins and Percutaneous Skeletal Trackers

Intracortical pins and skin markers used in combination have been deemed the gold standard for measuring differences in skeletal and soft tissue motion during human movement analysis (Benoit et al., 2006; Peters et al., 2010). The largest issue with this method is the need to subject participants to a small surgical procedure. Participants are first injected with a local anaesthetic around the areas of pin insertion. Once the anaesthetic takes effect, a manual drill is used to insert intracortical pins through the soft tissue, and into the bone of focus (Reinschmidt et al., 1997). The diameter of the pins range from 2.5 to 3.6 mm, with pin insertion depths up to 20 mm (Holden et al., 1997). The most common areas for insertion are the lateral femoral condyle (Holden et al., 1997), and the lateral tibial condyle (Holden et al., 1997; Houck et al., 2004) for measuring the motion of the hip and knee, respectively. A less common insertion point is in the posterolateral aspect of the calcaneus (Reinschmidt et al., 1997) to measure movement of the ankle. After bone pin insertion, markers, commonly in clusters of three (Reinschmidt et al., 1997) or four (Houck et al., 2004; Lafortune et al., 1992), are placed at the distal end of the pin to track bone movement. These markers provide estimates of

displacement, velocity, and accelerations of the bone to which the marker is attached (Fuller et al., 1997). While it is generally accepted that this technique provides a valid representation of the kinematics of bone during human motion, there are numerous reasons why it would be inappropriate for clinical use, including pain associated with pin insertion and the risk of infection due to skin penetration (Fuller et al., 1997). Another limitation to using bone pins is the possible effect the pins or the anaesthetic may have on walking patterns (Houck et al., 2004), as such invasive methods may either constrain the movement of soft tissue or alter the normal movement patterns of participants (Peters et al., 2010). Due to the invasiveness of such a technique, kinematic analyses that may be important for clinical assessments have to rely largely on the tracking of superficial skin markers (Reinschmidt et al., 1997).

Similar to intracortical pins, the use of a Percutaneous Skeletal Tracker (PST) involves the insertion of numerous pins into underlying bone (Holden et al., 1997; Houck et al., 2004). However, PSTs are different in that the markers are attached directly to the apparatus, which prevents some of the limitations to using intracortical bone pins, including bending (Holden et al., 1997) and loosening (Houck et al., 2004). While PSTs are more rigid, they constrain soft tissue movement and may affect normal movement patterns to a greater extent. For example, Holden et al. (1997) reported that a PST affected walking patterns by adding approximately 9 % to the estimated mass of the shank and 31 % to the principle moments of inertia about the shank X or Y axis for one participant.

2.8.2 Stereophotogrammetry and Skin Markers

Three dimensional motion analysis using stereophotogrammetry and skin markers is most commonly used in human motion analysis (Akbarshahi et al., 2010; Cappozzo et al., 2005). To track skin movement that occurs, it is necessary to mount skin surface markers along the length of the segment using double sided adhesive tape (Fuller et al., 1997; Gao and Zheng, 2008; Houck et al., 2004), or straps (Fuller, et al., 1997; Manal et al., 2003). To track the markers once applied, optoelectronic camera systems can be utilized. There are two basic types of systems: active, which use infrared light emitting diodes (LEDs) (Ball, 2011; Fuller et al., 1997; Houck et al., 2004; Scholz, 1989), and passive, which utilize passive retro-reflective markers (Akbarshahi et al., 2010; Bridgman et al., 2010; Ferber et al., 2002; Holden et al., 1997; Manal et al., 2003; Pain and Challis, 2002; Stagni et al., 2005; Telfer et al., 2010). Both optoelectronic systems require the use of motion position sensors or cameras to track the marker movement, with typical setups using between one and twelve cameras. Single markers allow analysis of the displacement, velocity and acceleration of specific areas, while marker triads allow rotations and translations of the skin surface to be measured (Gao and Zheng, 2008).

The main difference between the two optoelectronic systems is that with passive systems, light is reflected off a spherical marker, and in active systems, the markers themselves emit light (diodes). Another difference is that passive marker systems require much more editing of data following collection (Richards, 1999). While these types of systems appear ideal for looking at soft tissue motion, they are only able to capture images at fairly low frame rates. Frame rate for data capture decreases as the number of total markers used increases. For example, using an Optotrak Certus System (Northern

Digital Inc., Waterloo, Canada) to monitor soft or rigid tissue movement, the sample rate is limited by the total number of markers, calculated as in Equation 3:

$$4600/(N+2)\ \text{Hz} \qquad \text{(Eq. 3)}$$

where N = number of markers.

This is a major limitation for analyses of soft tissue motion resulting from impact due to the impulsive nature of such events. For example, following heel impacts, it is common to investigate the passive impact phase (Challis and Pain, 2008), which occurs within the first 50 ms of landing (Nigg et al., 1995). As many as 28 markers have been used to accurately measure the soft tissue motion in the lower extremity during such a task (Pain and Challis, 2006). Using Equation 3, the maximum sample rate for this set up would be only 153 Hz. Another issue with this type of system is the expense, as multiple cameras may be necessary to properly track highly dynamic or asymmetrical activities (Chu et al., 2010; Dufek et al., 2009; Ford et al., 2007; Gao and Zheng, 2008).

2.8.3 Magnetic Resonance Imaging

Magnetic Resonance Imaging (MRI) technology allows the bones and surrounding soft tissues to be displayed in three dimensions non-invasively (Sangeux et al., 2006). One advantage of MRI is that participants are not subjected to the radiation that is experienced during X-ray based methods, including fluoroscopy (Peters et al., 2010). To track tissue motion using MRI, marker sets are adhered to the area of interest with external fixtures. Adalat capsules, containing water and other inactive ingredients, have been used as skin markers in marker sets because of their low cost and highly visible MRI signal (Sangeux et al., 2006). Problems with this technique are that

movements are restricted to those that can be performed within the tunnel of an MRI machine, and that only static postures can be imaged, having to be pieced together afterwards. Dynamic MRI exists, allowing joints to be measured during continuous movement, but acquiring volumetric image data in real time is problematic because of the trade-off between the signal-to-noise ratio (SNR), and the spatial and temporal resolution of the device (Gilles et al., 2005).

2.8.4 X-ray

X-ray images only allow tracking of skin movement in two dimensions (2D) and in static conditions (Leardini et al., 2005). Therefore, evaluating any sort of dynamic task with this method is impossible (Stagni et al., 2005). A common method to track soft tissue movement using X-ray-based methods involves attaching 2 to 3 mm steel balls to the participants' skin using double sided tape. This allows the soft tissue movement of these areas to be tracked relative to the underlying bone (Maslen and Ackland, 1994; Tranberg and Karlsson, 1998).

With X-rays, the skin is free to move unimpeded by screws or pins, but a small amount of radiation is involved with every trial, which limits the total number of exposures one can safely withstand (Tranberg and Karlsson, 1998). Another limitation of this technique, which is also the case for many other methods, is the need for a trained professional to collect the data. While X-ray machines are more readily available than other methods, the lack of accessibility makes developing simple, reliable methods for analyzing tissue motion and its properties difficult with this approach.

2.8.5 Fluoroscopy

Fluoroscopy, or X-ray fluoroscopy, works very similarly to traditional X-ray, but dynamic movements can be assessed (Kuo et al., 2011, Peters et al., 2010; Sati et al., 1996). However, dynamic assessments using fluoroscopy are limited because of the slower sampling rates (30 frames/second) associated with this approach (Wrbaškić and Dowling, 2007). While fluoroscopy does not restrict skin movement, the very limited field of view only allows for a small area of markers to be tracked at a time (Stagni et al., 2005). After collection, extensive data processing is also required, which makes the general applicability of this type of procedure even more limited (Leardini et al., 2005).

2.9 ProAnalyst® Motion Tracking Reliability

Previous work was performed by Brydges et al. (2012) to assess the reliability of using a software system with automatic feature tracking capabilities. The purpose was to quantify the reliability both between- and within-measurers, with respect to the initial selection of automatic tracking features (e.g., anatomical landmarks) by trained personnel and to assess the effect errors in this initial feature selection had on other outcomes measures such as velocity. Three trained measurers were responsible for digitizing selected columns of markers based on anatomical landmarks, while one measurer repeated the process 6 months later. Measurers successfully selected the same column of markers more than 87 % of the time, while differing by two columns less than 1 % of the time. Overall, there were small differences in the initial position of selected markers during digitization of < 0.8 cm and < 0.5 cm, between and within measurer, respectively. These measurement differences had a minimal effect on the calculated velocities, with

small between (< 3.7 cm/s) and within (< 2.6 cm/s) measurer differences. Good to excellent reliability was shown for all data analyzed, with intra-class correlation coefficients (ICCs) of 0.82 and 0.89 between-measurers and 0.96 and 0.96 within-measurer, for position and velocity measurements, respectively. This study established excellent reliability of soft tissue position and velocity data from manually digitized skin markers following heel-first impacts. One of the primary benefits of a technique utilizing massless markers on the skin for tracking soft tissue motion is that they do not interfere with the natural motion of the underlying tissues, which would occur in many of the previously described techniques which require externally mounted devices (e.g. accelerometers, active markers).

2.10 Tissue Velocities

The velocities of in vivo tissues have not been assessed frequently in the literature. However, maximum breast tissue velocities of 93.1 cm/s and 92 cm/s have been reported by Bridgman et al. (2010) and Scurr et al. (2010) for two-step star jump and running tasks, respectively. Passive retro-reflective markers applied to the breast in both of these studies, were tracked using numerous calibrated infrared cameras. This technique allowed for the measurement of the anterior/posterior, medial/lateral, and vertical displacement of the soft tissue, and demonstrated that breast displacement and velocity are significantly greater in the vertical direction (Bridgman et al., 2010; Scurr et al., 2010).

The motion of in vitro tissue samples has also been analyzed, for example, muscle tissue was found to move with velocities greater than 4 times those measured for adipose

tissue (Bishop et al., 1998). Reported adipose tissue velocities (≈ 75 cm/s) are similar in magnitude to average peak velocities for in vivo breast tissue (≈ 70 cm/s) (Bridgman et al., 2010). The differences in observed velocities between adipose and muscle tissue demonstrates the potential significance that differences in tissue composition between individuals may have on overall tissue velocity. The similarity between the velocities of in vitro fat tissue and in vivo breast tissue is understandable as fat can account for greater than 50 % of the volume of the breasts, with glands accounting for the rest (Vandeweyer and Hertens, 2002).

Brydges et al. (2012) used high speed video to monitor soft tissue movement following a drop landing via motion tracking software to quantify the movement of various markers on the leg and foot. Soft tissue velocities were higher than those previously reported for breast tissue, with peak velocities approaching 140 cm/s. Higher velocities for lower extremity tissue may be attributable to the difference in tissue composition within the body.

CHAPTER III

METHODS

This study was a secondary analysis of previously collected data undertaken at the University of Windsor.

3.1 Participants

Twenty healthy young adults (9 male, 11 female) with a mean (SD) age of 23.7 (2.35) years, mass 71.0 (16.74) kg, and height of 1.72 (0.09) m, who were free of pain and injury in the lower extremity and back over the previous year, consented to participate in this study (Table 2). All methods were approved by the Research Ethics Board of the University of Windsor and informed consent was obtained from all participants. Participants were required to complete a general health questionnaire (Appendix A) to discover any possible issues with the participants' feet, legs or lower back, or any general health conditions which may have excluded them from participation.

Table 2. Mean (SD) age, height and body mass of all participants.

Participants	Age (years)	Height (m)	Body Mass (kg)
Male (n=9)	24.3 (2.96)	1.80 (0.06)	85.9 (12.01)
Female (n=11)	23.4 (1.03)	1.66 (0.05)	58.7 (6.74)

3.2 Apparatus

3.2.1 Pendulum and Impact Apparatus

A human pendulum was used to control initial impact conditions, allowing consistent impacts to be applied to the foot (Lafortune and Lake, 1995) that were similar in magnitude for impact force (1.8-2.8 times BW) and velocity (1.0-1.15 m/s) to those

experienced during running (Cavanagh and Lafortune, 1980; Duquette and Andrews, 2010; Flynn et al., 2004; Holmes and Andrews, 2006; Schinkel-Ivy et al., 2010). The pendulum was constructed using a rectangular steel frame (190.5 cm x 52.5 cm) and canvas bed having a total mass of 13 kg (Duquette and Andrews, 2010; Flynn et al., 2004; Holmes and Andrews, 2006; Schinkel-Ivy et al., 2010). Participants lay supine on the bed of the pendulum, which was suspended from the ceiling using four steel cables. The joint space of the right knee of each participant was aligned with the leading edge of the bed and the leg was held in full extension in order to allow the foot to impact a wall mounted force platform (Figure 12). The left leg was flexed at the knee such that the foot was resting on the pendulum bed. The force platform was rigidly mounted to a steel grid that was secured to the laboratory wall and floor.

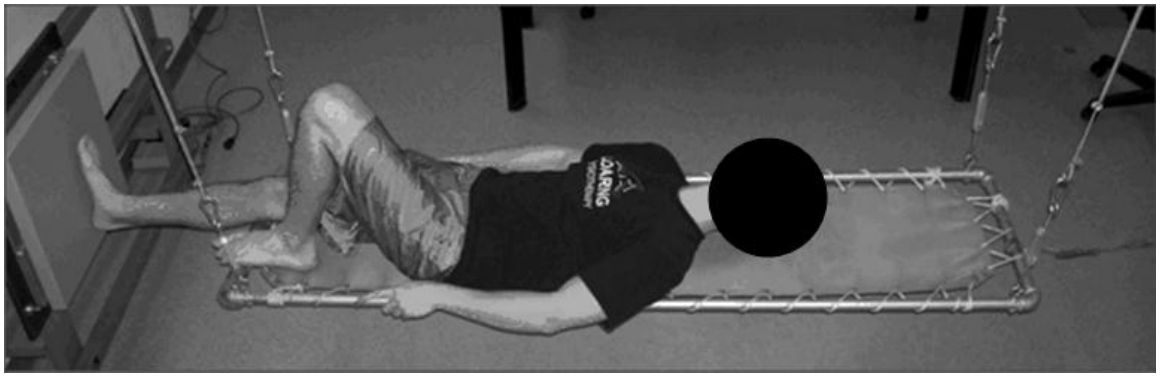

Figure 12. Participant lying supine on the human pendulum apparatus.

3.2.2 Drop Landings

A second set of impacts were applied using a drop landing technique. Participants were instructed to step off a 15 cm high box, landing on their right foot, heel first, onto a floor mounted force platform. A 15 cm drop was used as it typically produced impact

forces similar in magnitude to those targeted previously using the pendulum apparatus (1.8-2.8 times BW).

3.2.3 Markers

A grid pattern of black markers (0.5 cm circumference), with an inter-marker distance of 2 cm, was placed on the shaved right shank of each participant using permanent marker. A flexible plastic stencil (overhead transparency) with holes was wrapped around the shank (participants were in a seated position with the shank fully extended about the knee) with a designated row aligned with the anterior surface of the tibia to ensure that marker placement remained consistent between participants. A second stencil with identical hole arrangement to the first, was used to place markers distal to the medial malleolus, including the heel pad and first metatarsal (Figure 13).

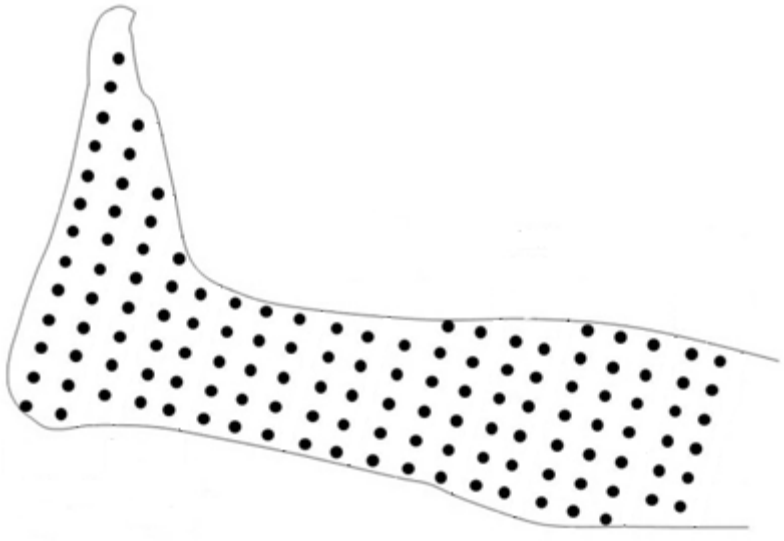

Figure 13. Schematic diagram of marker grid (2x2cm squares of dots) on the foot and shank.

3.2.4 Force Platforms

A force platform (AMTI-OR6-6-1000, A-Tech Instruments Ltd., Scarborough, ON, Canada, natural frequency of 1000 Hz) was rigidly anchored to a 1.8 cm thick steel plate, which was bolted to the impact apparatus (steel grid secured to the laboratory wall and floor) used for the pendulum impacts. A second identical force platform was rigidly secured to the laboratory floor with the top surface flush with the floor tiles. This platform was used for the drop landing trials.

3.2.5 Velocity Transducer

A velocity transducer (Celesco DV30J, Don Mills, ON, Canada) was attached to the trailing end of the pendulum, enabling the simultaneous measurement of pendulum displacement and velocity throughout the duration of the impact.

3.2.6 High Speed Camera

A high speed camera (Fastec Imaging, San Diego CA, Troubleshooter HR; 1000 frames/s, 640 x 480 resolution) was used to capture the medial aspect of the foot and shank (heel pad to knee) in the sagittal plane for each trial during the pendulum and drop landing impacts.

3.3 Procedures

A summary of the procedures followed is provided in Figure 14. Each part of the procedures is described in more detail in a separate section below.

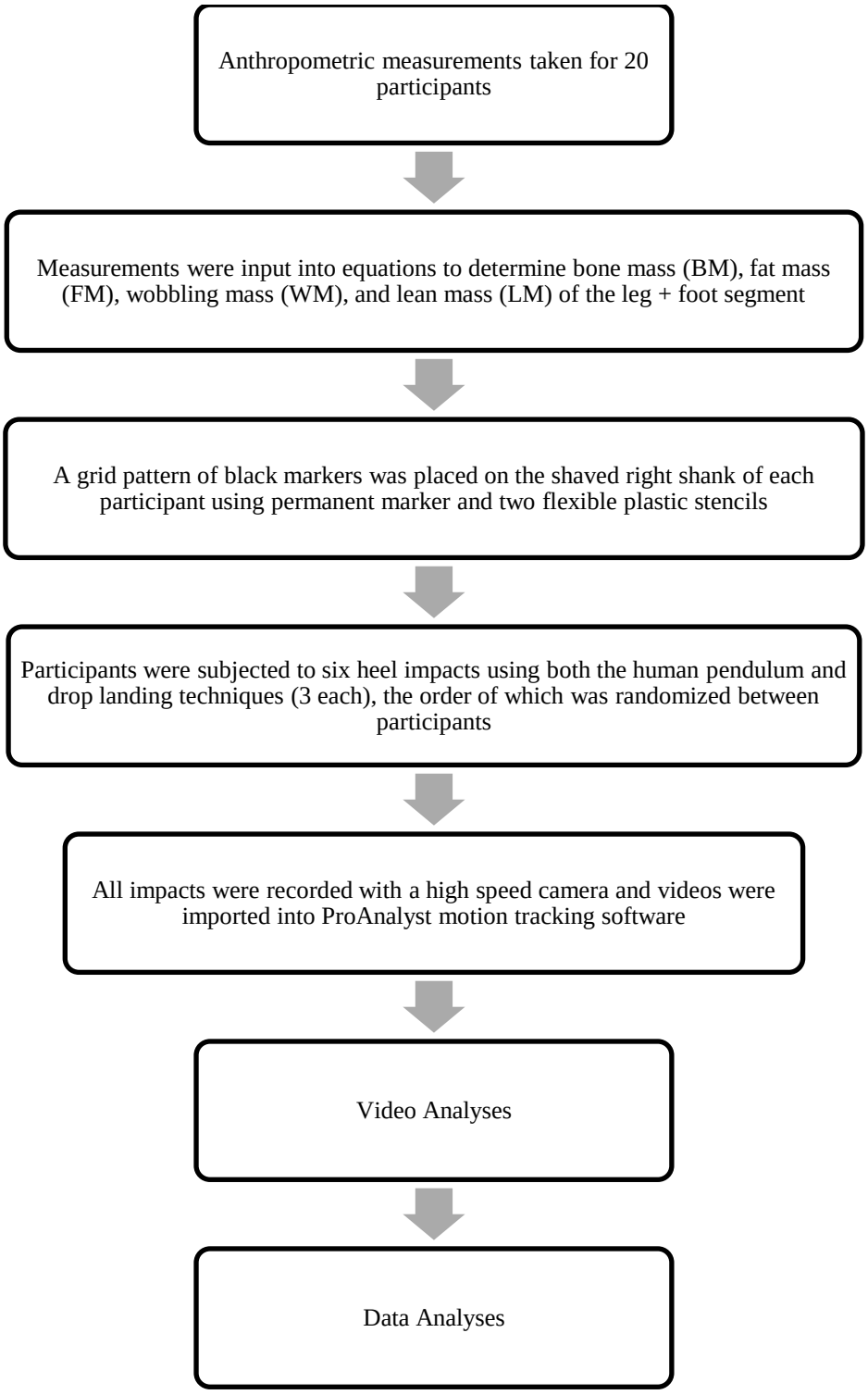

Figure 14. Flowchart of procedures.

3.3.1 Anthropometric Measurements

Participants had both legs measured using standard anthropometric measurement equipment (a soft, flexible measuring tape anthropometer; Lafayette Instrument Company, Lafayette, IN), and skinfold calipers (Slimguide, Creative Health Products; Plymouth, MI C-120). Measurements included six different lengths, six circumferences, eight breadths, and four skinfold thicknesses (Appendix B). Excellent between- and within-measurer reliability for these measurements have been previously established for trained personnel (Burkhart et al., 2008). The anthropometric measurements were input into equations which were developed to determine the BMC, FM, WM, and LM of the leg + foot segment of healthy people between the ages of 17 and 30 years (Holmes et al., 2005) (Appendix C).

3.3.2 Impact Procedures

Following marker placement, participants were impacted using two different techniques. The first set of three impacts was applied using the human pendulum as per Schinkel-Ivy et al. (2012a). Briefly, participants were securely strapped to the pendulum in the supine position with the joint space of the right knee aligned with the leading edge of the pendulum frame. Participants were pulled backed a predetermined distance and were instructed to impact their heel against the force platform after being released. A few trial impacts (2-4) were conducted to determine the proper pull back distance to achieve a velocity of 1.0 m/s - 1.15 m/s and an impact peak force of 1.8 - 2.8 times BW (Cavanagh and Lafortune, 1980; Duquette and Andrews, 2010; Flynn et al., 2004; Holmes and Andrews, 2006; Schinkel-Ivy et al., 2010). A second set of three impacts were applied to the unshod heel of each participant using the drop landing technique. A total of 6

experimental trials were collected for each participant (3 pendulum impacts and 3 drop impacts), the order of which were randomized between participants.

3.3.3 Video Analysis

The videos of each trial were imported into ProAnalyst® motion tracking software (ProAnalyst®; Xcitex, Cambridge, MA). Prior to analysis, the videos were subjected to a calibration process with 6 cm between three markers being used as the calibration unit (Figure 15). The videos were reversed to make black images white and white images black. A 5x5 Laplacian high pass filter was applied to detect marker edges, followed by a despeckle filter to remove speckles beneath a given size (minimum # pixels - 10) and threshold (+/- cutoff - 128) using an eight point connectivity (Figure 16). Analysis of the markers began just prior to heel impact and continued until the leg was stationary. This was done in an attempt to isolate the soft tissue motion caused by the impact. A total of between 150 and 250 frames (milliseconds) were analyzed for each video.

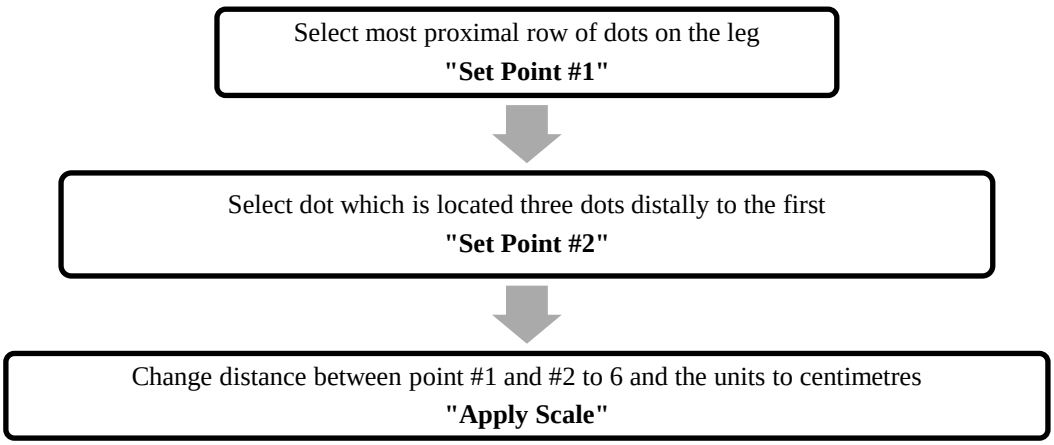

Figure 15. Calibration process performed for all videos.

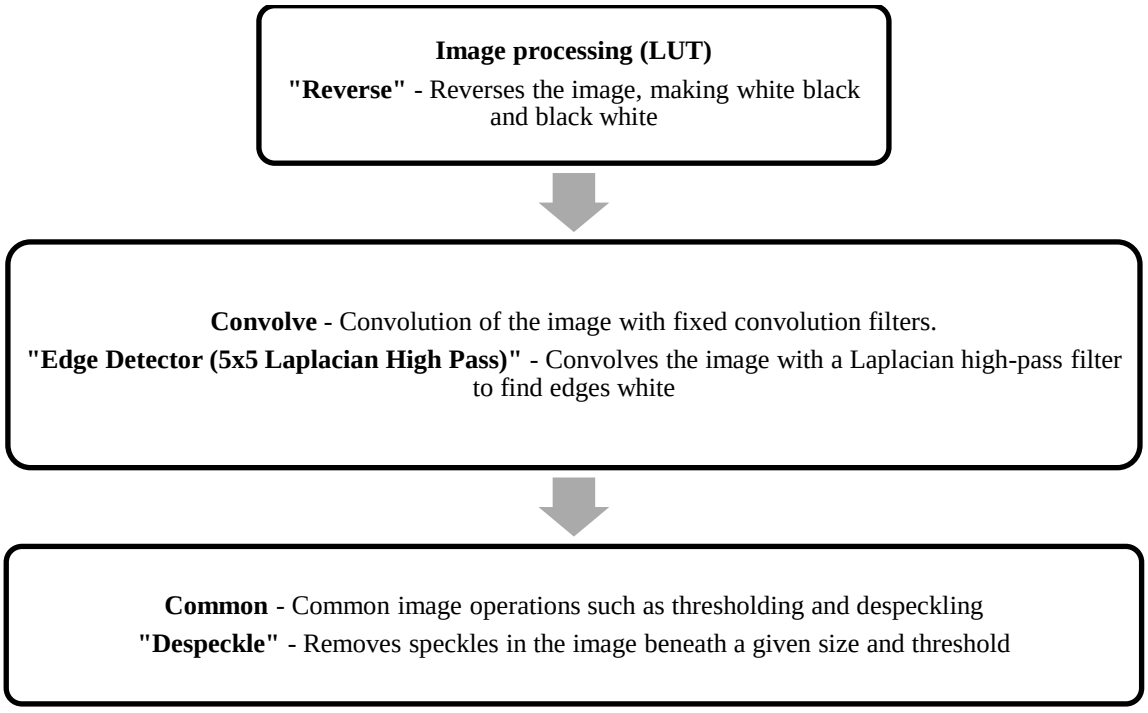

Figure 16. Filters applied to videos within ProAnalyst®.

Three analysts were trained to select two columns of markers from four zones at 0 %, 25 %, 50 % and 75 % of the distance from the medial malleolus to the knee joint centre (Figures 17 and 18). A fifth zone was selected for analysis at the level of the heel pad (Figures 17 and 18). Each analyst randomly evaluated half of the participants' videos. Following marker selection, ProAnalyst® automatically tracked the selected markers (search region multiplier - 250 %; threshold tolerance - 0.75) and outputted the X (perpendicular to the long axis of the tibia, running anterior to posterior) and Y (parallel with the long axis of the tibia) coordinates of each selected marker. The search region multiplier configures how large an area to search as a percentage of the initial region size. Larger values will result in larger search areas, but will take a longer time to complete the search. ProAnalyst® assigns a value between 0 and 1 for all points within

the search region indicating how well they match the template region. All values below the threshold used (0.75) are ignored. For example, a threshold of 1.0 indicates that only perfect matches will be accepted. Lowering this value will help if the tracking algorithm is failing to track a feature.

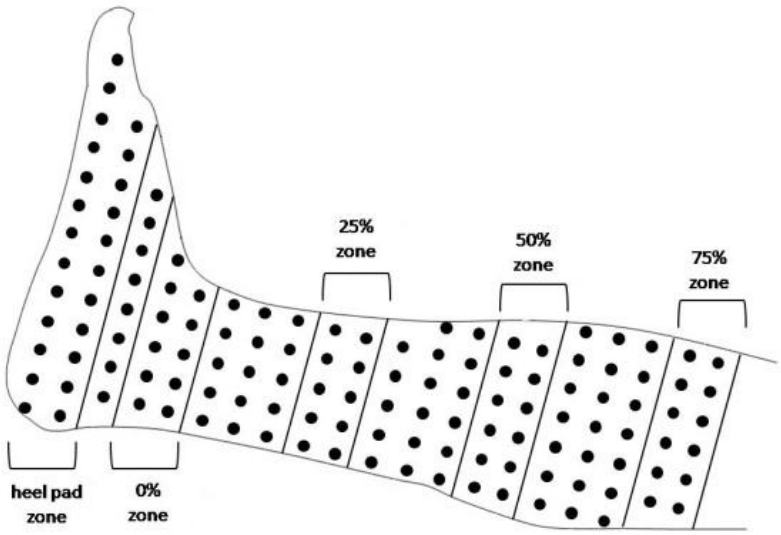

Figure 17. Schematic diagram of marker grid (2x2cm squares of dots) and analysis zones on the foot and shank.

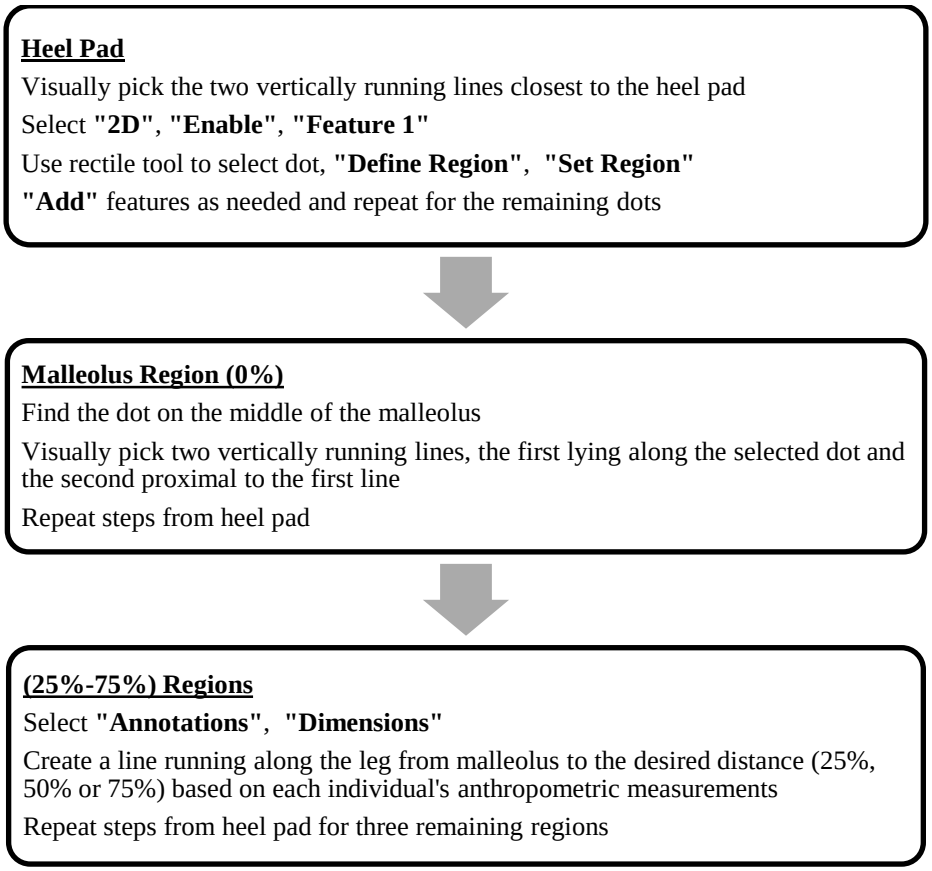

Figure 18. Flow chart of dot (marker) selection procedure performed by the three trained analysts.

3.4 Data Analysis

A total of 8 variables were assessed when observing the soft tissue movement following a human pendulum swing heel impact. These included the displacement and velocity in the proximal, distal, anterior and posterior directions. Each zone was split into anterior and posterior sections by visually dividing the leg in half to create a total of 10 regions (Figure 19). One random marker from each of the ten regions (within the 5 established zones) was used for soft tissue displacement and velocity analysis.

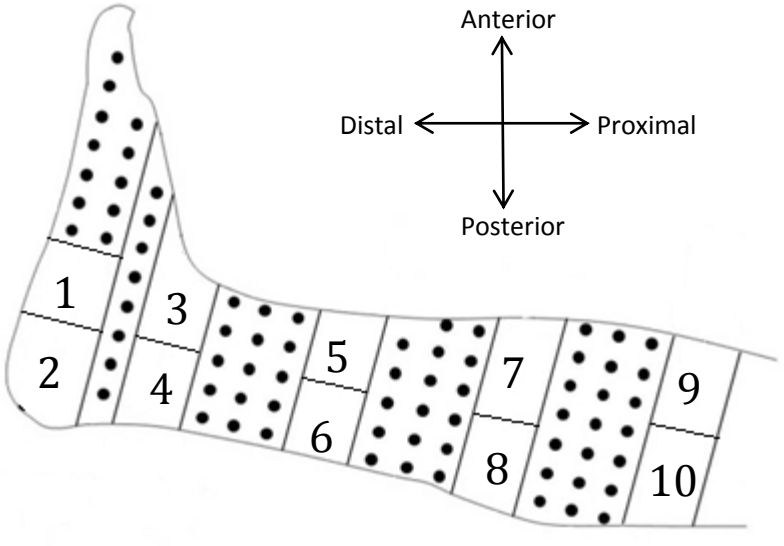

Figure 19. Schematic diagram of marker grid (2x2 cm squares of dots) and the ten regions on the foot and shank.

The displacement data were filtered at a cut-off frequency of 35 Hz with a dual pass, 4th order Butterworth filter. The cut-off frequency was determined by performing a residual analysis, as per Winter (2005). The filtered displacement data of all markers were then imported into a customized LabView (LabVIEW® 2010, National Instruments, Austin TX) program, where the peak displacement in the proximal, distal, anterior and posterior directions was determined. The filtered displacement data were differentiated to determine the peak velocities in all four directions for each soft tissue marker selected from the different regions. The amplitude and frequency of the displacement waveform for each marker were used to quantify the energy density of a non-dispersive wave using Equation 2 (repeated below), as described by Pain and Challis (2002).

$$Ed = \tfrac{1}{2}\,\rho \cdot A^2 \cdot \omega^2 \qquad \text{(Eq. 2)}$$

where Ed = energy density (J/m^2), ρ = density of material the wave is propagating through (kg/m^3), A = amplitude of the wave (cm), and ω = angular frequency (rad/s).

Frequency analysis was performed to determine the mean marker frequency from the power spectrum for each marker using a windowed Fast Fourier Transform (FFT) analysis. The mean marker frequency (Hz) for each region was converted to units of radians/second by using Equation 4 to determine the angular frequency which was utilized in Equation 2.

$$Hz \cdot 2 \cdot \pi = \text{Angular frequency} \quad \text{(Eq. 4)}$$

The densities of adipose tissue or FM (0.9196 g/cm^3: Farvid et al., 2005) and muscle tissue (LM) (1.06 g/cm^3: Seggal et al., 1986) were used to establish the overall density of the soft tissue for each participant, based on the proportion of adipose and muscle mass determined from the prediction equations of Holmes et al. (2005).

To determine the energy carried by the soft tissue wave, the calculated energy density was multiplied by an estimate of the mean cross-sectional area (CSA) of leg soft tissue (Equation 5).

$$E = Ed \times CSA_S \quad \text{(Eq. 5)}$$

where E = energy carried by the soft tissue wave (J), Ed = energy density (J/m^2), and CSA_S = soft tissue cross-sectional area (cm^2).

Since the legs of the participants in this study were not scanned during the original data collection session, direct estimates of the CSA_S (in units of cm^2) were not possible. Therefore, the mean CSA_S for each participant was estimated in several steps,

starting with an analysis of horizontal sections from videos of the Visible Human Project (e.g. Figure 20) for both a male and female (Visible Human Server, n.d.), using ProAnalyst® motion tracking software. From approximately 20 video frames (slices) spanning the entire length of the leg, from the knee joint to the ankle joint, the CSA of the leg (CSA_L) (soft tissue and bone) and CSA of the bone (CSA_B) (bone = fibula and tibia) were determined (in arbitrary units) for four of the five zones (0%, 25 %, 50 %, and 75 %). The ratio of CSA_S to CSA_L (SLR) was then calculated for each zone as in Equation 6.

$$SLR = 1 - BLR \quad \text{(Eq. 6)}$$

where BLR = bone to leg cross-sectional area ratio (i.e. CSA_B/CSA_L); and SLR = soft tissue to leg cross-sectional area ratio (i.e. CSA_S/CSA_L).

The SLR provided an estimate of the relative proportion of the cross-sectional area of the leg comprised by the soft tissues, for both men and women. This ratio was assumed to be consistent in magnitude to the ratio for the sample of living participants studied here.

The product of the SLR (CSA_S/CSA_L), determined from the Visible Human Project cadavers, and estimates of the CSA_L (cm^2) for the study participants, resulted in estimates of the CSA_S (cm^2) for each participant, which were input into Equation 5. The mean CSA_L for each participant was estimated using both the leg circumference measurements taken at the time of data collection and the ProAnalyst software to measure the anterior-posterior breadth for each zone, with the assumption that the cross-sections of the legs of the participants were roughly spherical in shape.

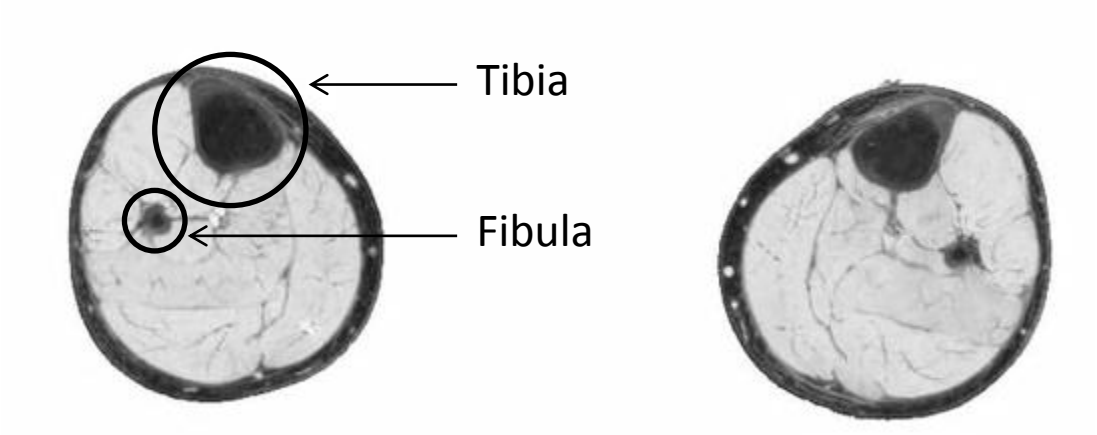

Figure 20. Screenshot of a single frame of the male Visible Human Project, consisting of bone (tibia and fibula) and soft tissue (Modified from Visible Human Server, n.d.).

To determine the percentage of total energy dissipated due to soft tissue movement following heel impacts, the calculated energy carried by the soft tissue (Equation 5) was divided by the mean kinetic energy of the leg at impact (Equation 7), where the mass of the leg was calculated based on the previously described tissue mass prediction equations.

$$KE_L = \tfrac{1}{2}\, m_L \cdot v_L^{\,2} \qquad \text{(Eq. 7)}$$

where KE_L = kinetic energy of the leg (J), m_L = mass of the leg (kg), and v_L = velocity of the leg (m/s).

To quantify the soft tissue deformation occurring throughout the foot and leg segment, the filtered displacement data were used for four markers (2 x 2 square) in each of the five zones (HP, 0 %, 25 %, 50 %, and 75 %) (Figure 21). These data were imported into a customized LabView (LabVIEW® 2010, National Instruments, Austin

TX) program and changes in quadrilateral area, defined by the difference in the maximum and minimum areas divided by the mean area of the quadrilaterals (set of four markers), were calculated.

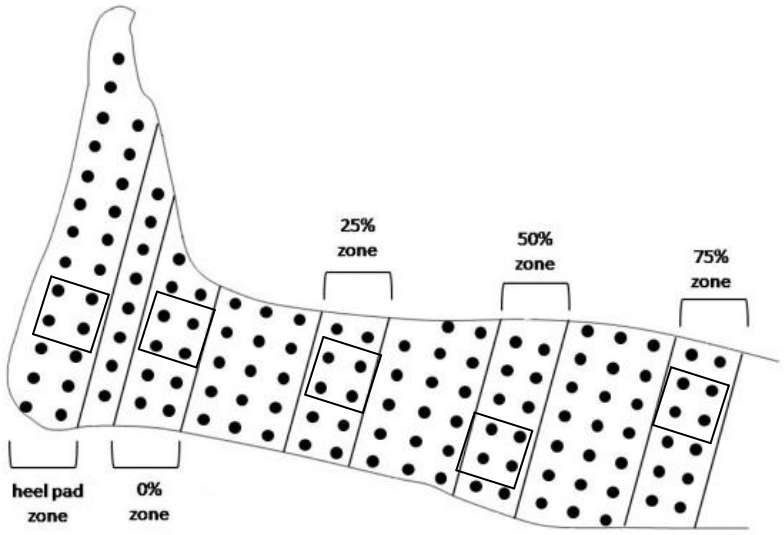

Figure 21. Example of four markers being selected (square box) within each zone for soft tissue deformation calculations.

3.4.1 Statistical Analysis

Purpose 1: quantify the displacement and velocity of, and the amount of energy dissipated by, the soft tissues of the leg following impact;

Mean marker displacements and velocities were obtained by taking the average of the three trials in the proximal, distal, anterior and posterior directions for the marker selected in each region. The mean displacement of markers in each region was used, along with the marker frequency, to determine the energy density. As indicated in the

Results (Section 4.1.3), the method used by Pain and Challis (2002) could not be replicated without causing severe distortion to the displacement signals. Consequently, the energy carried by the soft tissue shock wave, and the energy dissipated by the soft tissue, were not reported in this thesis. Refer to Section 4.1.3 for more details. The amount of tissue deformation was obtained by measuring the change in area, defined by the difference in the maximum and minimum areas divided by the mean area of the quadrilaterals (set of four markers), in each of the five zones (HP, 0 %, 25 %, 50 %, 75 %) of the leg.

Purpose 2: determine if there are differences in soft tissue motion and impact energy dissipation due to sex, trial, impact method utilized (drop landing vs. pendulum) or as a function of the region of the leg measured;

Three-way mixed Analyses of Variance (ANOVA) with between-subject factor: sex (male, female); and within-subject factors: leg region (1-10) and trial (1-3), were performed to examine any mean differences in the dependent measures soft tissue displacement, soft tissue velocity, and the amount of tissue deformation (change in quadrilateral area) due to passive soft tissue movement of the leg. Impact method (drop landing vs. pendulum) was removed from the statistical analyses due to issues with the drop landing video analysis using ProAnalyst® (See more details in Section 4.2.2). Alpha was set at 0.05 for all comparisons and pairwise comparisons were performed on any significant main effects, while simple effects tests were performed on any significant interaction. All statistical tests were performed with SPSS 19 (IBM SPSS statistics, IBM Corporation, Somers NY).

Purpose 3: determine the relationship between the displacement, velocity and energy absorption ability of the soft tissues of the lower extremity and the individual leg tissue masses (FM, LM, WM, BMC).

Pearson correlation analyses were performed to determine the relationship between the magnitudes of individual leg tissue masses (WM, LM, FM, BMC) and the displacement and velocity of the soft tissues in the leg. As noted above (for Purpose 1), energy dissipation was not determined in this thesis. Consequently, the relationship between energy dissipation and leg tissue masses was not performed.

CHAPTER IV

RESULTS

4.1 Purpose 1

Quantify the displacement and velocity of, and the amount of energy dissipated by, the soft tissues of the leg following impact.

4.1.1 Soft Tissue Displacement

The greatest amount of soft tissue displacement occurred in region 10, with distal displacement reaching a mean peak magnitude of 2.14 cm; while the least amount of soft tissue displacement occurred in the proximal direction in region 1 (0.05 cm) (Table 3). Males (2.17 cm) and females (2.11 cm) both had the greatest amount of soft tissue displacement in region 10 for both the proximal and distal directions. In the anterior and posterior directions, males had the greatest movement in region 4 (1.37 cm), while females had the greatest movement in region 10 (1.18 cm).

Table 3. Mean (SD) overall, male and female peak soft tissue displacements (cm) in the proximal, distal, anterior and posterior directions for each of the 10 regions.

	Regions									
Overall	1	2	3	4	5	6	7	8	9	10
Proximal	0.05 (0.10)	0.32 (0.20)	0.06 (0.10)	0.20 (0.14)	0.07 (0.08)	0.11 (0.10)	0.08 (0.10)	0.14 (0.14)	0.06 (0.12)	0.18 (0.20)
Distal	1.97 (0.52)	1.08 (0.24)	1.68 (0.36)	1.23 (0.23)	1.66 (0.16)	1.63 (0.20)	1.72 (0.18)	1.90 (0.23)	1.87 (0.23)	2.14 (0.27)
Anterior	0.58 (0.52)	0.25 (0.25)	1.07 (0.72)	1.01 (0.64)	0.98 (0.55)	1.08 (0.54)	0.77 (0.36)	1.03 (0.43)	0.73 (0.40)	0.98 (0.56)
Posterior	0.16 (0.09)	0.24 (0.09)	0.11 (0.08)	0.11 (0.06)	0.08 (0.06)	0.12 (0.07)	0.13 (0.08)	0.25 (0.15)	0.30 (0.25)	0.50 (0.28)
Male										
Proximal	0.05 (0.13)	0.33 (0.20)	0.05 (0.11)	0.20 (0.18)	0.07 (0.08)	0.10 (0.10)	0.07 (0.08)	0.11 (0.11)	0.05 (0.06)	0.13 (0.12)
Distal	2.29 (0.52)	1.15 (0.28)	1.90 (0.38)	1.28 (0.24)	1.69 (0.19)	1.70 (0.21)	1.76 (0.19)	2.00 (0.28)	1.88 (0.22)	2.17 (0.35)
Anterior	0.86 (0.66)	0.32 (0.34)	1.47 (0.82)	1.37 (0.76)	1.24 (0.62)	1.32 (0.63)	0.84 (0.32)	1.02 (0.44)	0.63 (0.38)	0.74 (0.48)
Posterior	0.17 (0.10)	0.25 (0.08)	0.13 (0.10)	0.11 (0.08)	0.09 (0.07)	0.11 (0.05)	0.11 (0.04)	0.22 (0.11)	0.35 (0.29)	0.52 (0.31)
Female										
Proximal	0.05 (0.08)	0.31 (0.22)	0.07 (0.09)	0.19 (0.12)	0.08 (0.09)	0.12 (0.11)	0.09 (0.12)	0.17 (0.16)	0.08 (0.15)	0.23 (0.24)
Distal	1.71 (0.35)	1.03 (0.20)	1.50 (0.23)	1.18 (0.22)	1.64 (0.13)	1.56 (0.17)	1.68 (0.16)	1.82 (0.14)	1.86 (0.26)	2.11 (0.21)
Anterior	0.35 (0.20)	0.19 (0.14)	0.74 (0.41)	0.72 (0.35)	0.78 (0.41)	0.89 (0.40)	0.72 (0.40)	1.03 (0.45)	0.80 (0.41)	1.12 (0.56)
Posterior	0.15 (0.08)	0.23 (0.10)	0.09 (0.05)	0.11 (0.06)	0.07 (0.05)	0.12 (0.08)	0.14 (0.10)	0.28 (0.17)	0.26 (0.22)	0.48 (0.27)

4.1.2 Soft Tissue Velocity

Mean peak velocities were greatest in the distal direction for all regions overall. The greatest observed peak velocity of 105.6 cm/s occurred in region 10 while the soft tissues moved distally following impact (Table 4). Mean peak velocities were greater in the anterior than posterior direction, with the greatest difference in velocities between the two directions occurring in distal to intermediate regions of the leg (regions 3-6) (Table 4). Similar to the mean overall results, males and females both experienced the greatest soft tissue velocities while the soft tissues moved distally (Table 4). The greatest velocity occurred in region 10 for both males and females (102.7 cm/s and 107.9 cm/s, respectively). The smallest velocities occurred in the posterior direction for both males (17.7 cm/s) and females (17.0 cm/s), with velocities increasing in more proximal regions (Table 4).

Table 4. Mean (SD) overall, male and female peak soft tissue velocity (cm/s) in the proximal, distal, anterior and posterior directions for each of the 10 regions.

	Regions									
Overall	1	2	3	4	5	6	7	8	9	10
Proximal	18.6 (3.2)	21.7 (3.9)	22.7 (7.7)	22.3 (4.9)	31.6 (8.6)	33.2 (9.6)	35.5 (10.6)	49.9 (13.7)	41.5 (15.5)	61.5 (17.7)
Distal	87.2 (12.7)	62.5 (9.5)	78.3 (7.5)	76.3 (8.2)	95.2 (6.9)	94.8 (6.5)	99.3 (6.7)	102.1 (5.6)	101.3 (7.7)	105.6 (6.7)
Anterior	40.4 (21.3)	25.0 (13.9)	64.7 (32.6)	61.2 (29.1)	52.4 (23.5)	64.1 (24.6)	40.6 (14.6)	51.1 (14.4)	35.7 (10.8)	47.4 (16.2)
Posterior	17.3 (4.8)	21.2 (6.7)	23.7 (13.3)	20.6 (10.5)	24.7 (13.4)	30.5 (12.4)	27.9 (11.2)	48.8 (15.0)	33.8 (10.0)	63.2 (21.7)
Male										
Proximal	18.8 (3.4)	21.9 (4.6)	23.1 (9.5)	22.7 (4.3)	28.3 (6.8)	27.7 (5.0)	30.9 (7.6)	41.2 (7.8)	34.1 (7.0)	50.5 (9.3)
Distal	91.7 (13.4)	62.3 (11.8)	80.0 (6.9)	77.0 (8.0)	95.4 (6.3)	95.6 (5.8)	98.7 (5.4)	100.5 (4.4)	100.4 (5.4)	102.7 (5.6)
Anterior	53.1 (22.3)	29.5 (15.2)	82.1 (33.5)	74.9 (34.6)	61.8 (25.3)	72.5 (26.7)	44.5 (10.8)	50.2 (13.4)	31.7 (11.1)	41.7 (13.5)
Posterior	17.7 (3.9)	21.9 (6.6)	28.6 (16.6)	23.7 (13.3)	29.6 (17.4)	33.6 (15.4)	28.1 (8.1)	45.4 (14.4)	34.5 (12.3)	52.8 (17.4)
Female										
Proximal	18.4 (3.1)	21.5 (3.5)	22.4 (6.5)	22.0 (5.5)	34.3 (9.2)	37.7 (10.3)	39.2 (11.5)	57.0 (13.5)	47.0 (18.5)	70.5 (18.0)
Distal	83.6 (11.4)	62.6 (7.9)	77.0 (8.0)	75.8 (8.8)	95.0 (7.6)	94.2 (7.2)	99.8 (7.9)	103.5 (6.3)	102.1 (9.4)	107.9 (6.8)
Anterior	30.0 (14.1)	21.3 (12.3)	50.5 (25.0)	50.0 (18.6)	44.7 (19.8)	57.2 (21.4)	37.4 (17.0)	51.9 (15.7)	39.0 (10.0)	52.2 (17.3)
Posterior	17.0 (5.6)	20.6 (7.0)	19.6 (8.7)	18.1 (7.4)	20.7 (7.9)	28.0 (9.3)	27.8 (13.6)	51.5 (15.6)	33.3 (8.3)	71.7 (21.8)

4.1.3 Energy Dissipation

The investigated displacement signals were only several hundred milliseconds long. Applying a FFT to the signals (< 1 second in length) caused the signals to become extremely distorted, with peaks occurring between 5 and 6 Hz (Figure 22). Although it was possible to calculate the energy density of the soft tissue waves using these values (as per the method outlined by Pain and Challis (2002)), the results were knowingly incorrect using this approach (see description below and Figures 23 and 24). Therefore, the energy dissipation of the soft tissues was not reported in this thesis.

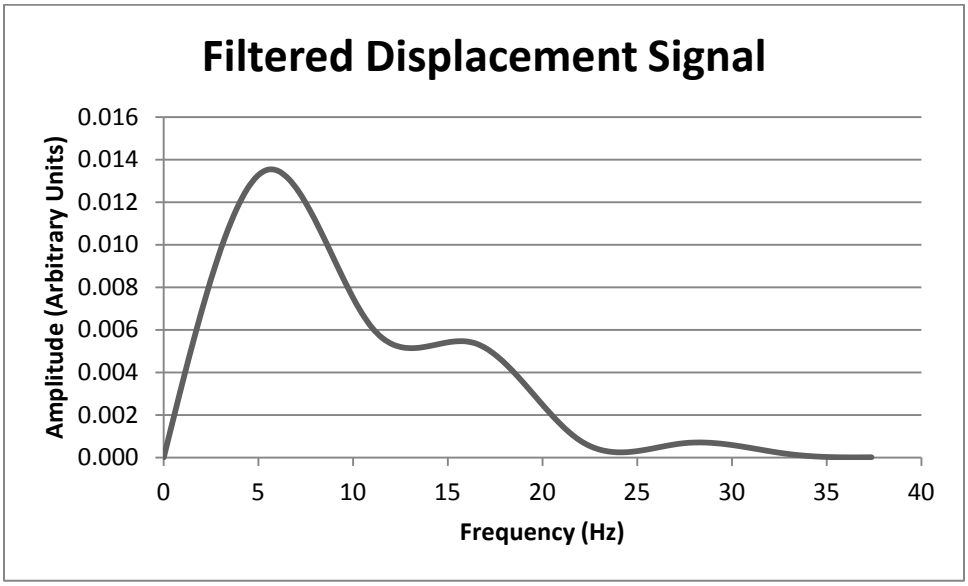

Figure 22. Frequency content (Hz) of a filtered displacement data sample.

The signal distortion that occurred following the FFTs was determined to be the result of the short duration of the signals (i.e. < 1 second). Various techniques were attempted to increase the length of the displacement signals to at least 1 second in duration to facilitate the frequency analysis. For example, each signal was repeated and

grouped together until the signal was greater than 1 second in duration. The repeated signals were also flipped and reversed prior to being grouped together to avoid any sudden steps in the signal caused by start and end points which were different in magnitude from each other. These modified signals were then run through the FFT (Figure 23).

In order to determine if any signal distortion was occurring during the FFT processing, multiple sine waves were generated with known frequencies (1-20 Hz) and run through the analysis software. The FFT procedure returned accurate results for all signals that were at least 1 second long (see example for 3 Hz sine wave in Figure 24). When the signal was shorter than 1 second in duration (see example for 200 ms in Figure 24), the distortion is clear (relative to the known signal frequency content). At signal lengths similar to what was analyzed in this study, the frequency distributions began to resemble those from the original filtered displacement data (peaks around 5.5 Hz (Figure 24).

Other methods of quantifying the frequency content of signals less than 1 second in duration were not found, following widespread searches and consultations. Because the frequency content of the filtered displacement signals was extremely sensitive to signal length, and clear evidence of signal distortion was presented, the method described by Pain and Challis (2002) could not be replicated and is in question.

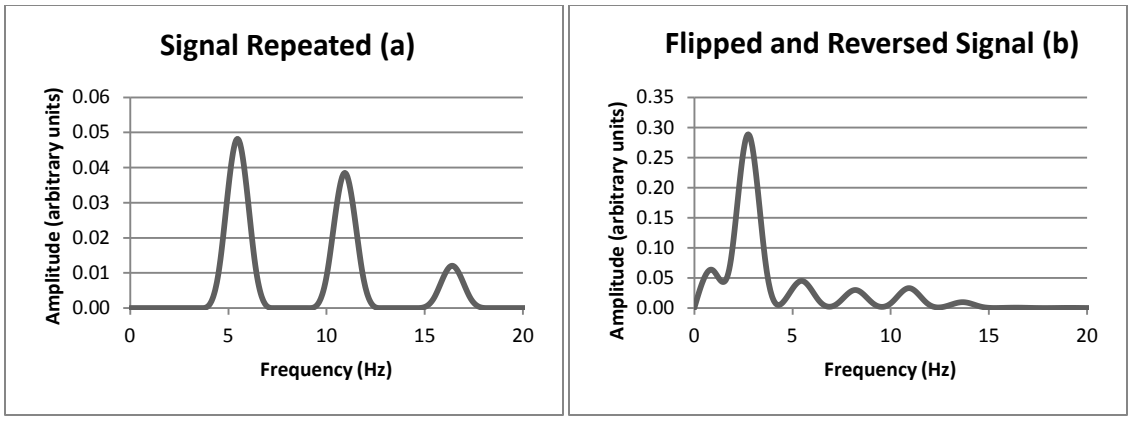

Figure 23. Frequency content (Hz) of a filtered displacement data sample after repeating the signal (a), and flipping and reversing the signal (b).

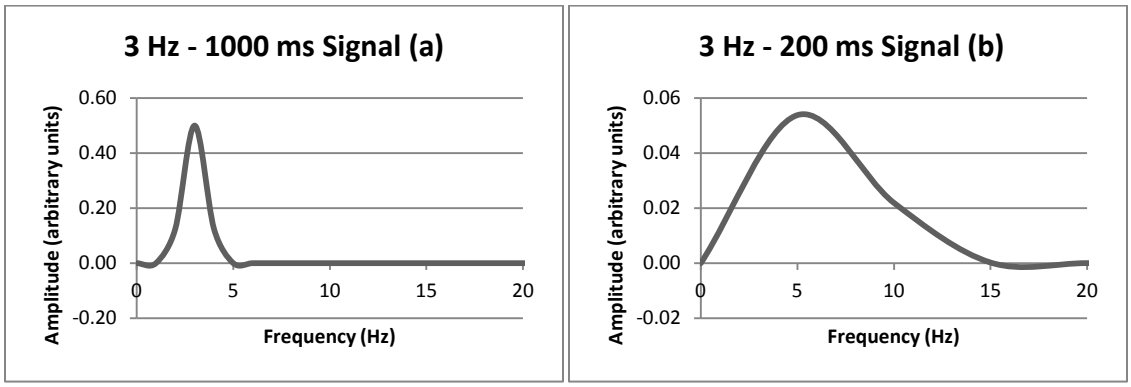

Figure 24. Frequency content (Hz) of a known 3 Hz data sample with 1000 ms (a) and 200 ms (b) of data.

4.1.4 Soft Tissue Deformation

The average change in area of the quadrilaterals (defined by four markers in each region), was 8.63 %. The change in area generally increased across the zones from distal to proximal (Table 5). The greatest change in area was seen in the 75 % zone at 14.15 %, whereas the soft tissue in the 0 % zone deformed to less than half of this at 6.03 % (Table 5). Due to marker dropout, it was not possible to capture a quadrilateral set of markers in each zone for every participant throughout the duration of the impact. Therefore, the

number of participants reported for each zone is less than the total number of participants in the study (Table 5).

Table 5. Maximum, minimum, mean (cm^2), and percent change in area (%) of quadrilaterals, defined by markers in each zone, that occurred following impacts.

	Zones				
	HP (n = 13)	0 % (n = 19)	25 % (n = 14)	50 % (n = 9)	75 % (n = 7)
Max	3.57	3.39	3.60	3.54	3.86
Min	3.34	3.19	3.35	3.25	3.38
Mean	3.47	3.29	3.51	3.44	3.67
Change (%)	6.80	6.03	7.55	8.61	14.15

4.2 Purpose 2

Determine if there are differences in soft tissue motion and impact energy dissipated due to sex, trial, impact method utilized (drop landing vs. pendulum) or as a function of the region of the leg measured.

4.2.1 Impact Energy Dissipated

As indicated previously, the energy density of the soft tissue wave was not calculated. Therefore, no further statistics were performed regarding this variable.

4.2.2 Impact Method

The drop landing technique resulted in considerable angular rotations of the tibia about the ankle in the sagittal plane throughout most of the impact which could not be separated from the motion of the overlying soft tissue in ProAnalyst®. Therefore, only data collected using the pendulum impact technique were reported herein.

4.2.3 Trial

There were no significant main effects of Trial, for any dependent variable. Therefore, the means of the three trials for each condition were used for the following analyses.

4.2.4 Soft Tissue Displacement

A significant main effect of Region was found for proximal [$F(2.317, 41.707) = 13.907$, MSE = 0.121, $p = 0.000$] (Figure 25) and distal [$F(2.856, 51.403) = 59.701$, MSE = 0.332, $p = 0.000$] (Figure 26) displacement. Movement in the proximal direction was significantly greater for region 2 than regions 1, 3, 5, 6, 7 and 9 ($p \leq 0.05$). Soft tissue displacement in the proximal direction was 7 times greater on average for the posterior regions compared to anterior regions (Figure 25). Sample displacement curves for all regions for a single trial are shown in Figure 27.

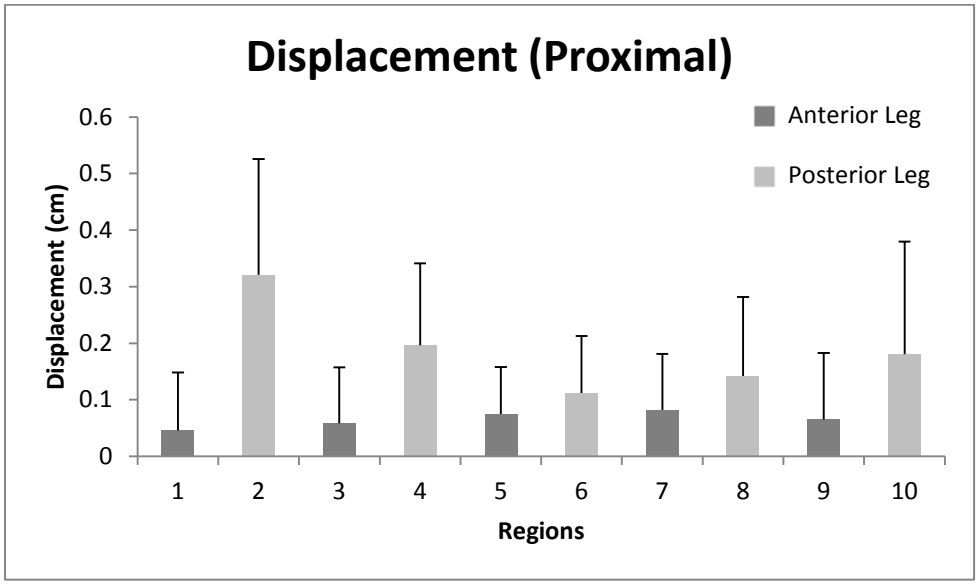

Figure 25. Mean (SD) peak soft tissue displacement in the proximal direction for each region.

The mean tissue displacement distally was 13 times greater than proximally. Mean displacement for region 10 (2.14 cm) was significantly greater than all other regions ($p \leq 0.05$) (Figure 26). There was a gradual increase in distal tissue displacement from more distal to proximal regions. Compared to region 2, there was 54 % more displacement in region 5 and 98 % in region 10.

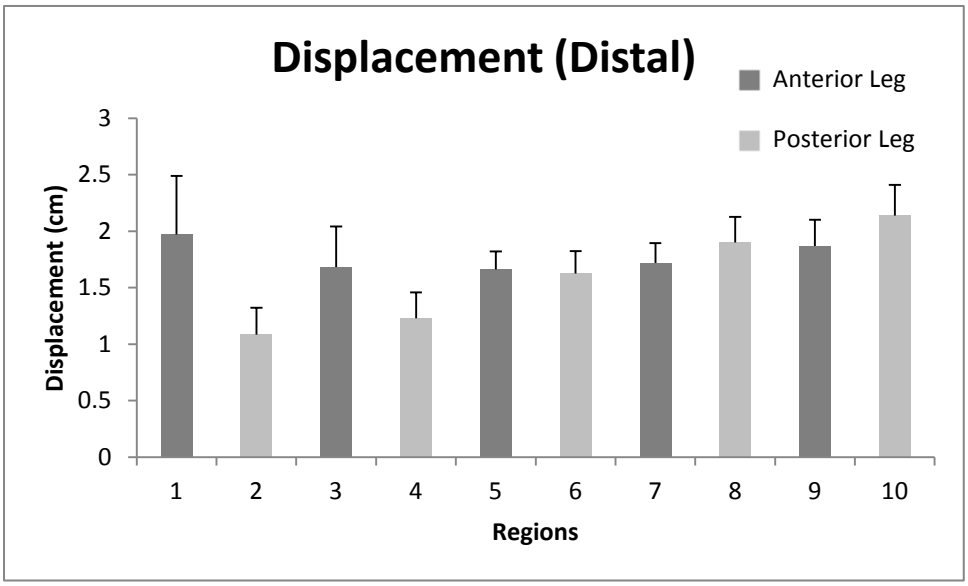

Figure 26. Mean (SD) peak soft tissue displacement in the distal direction for each region.

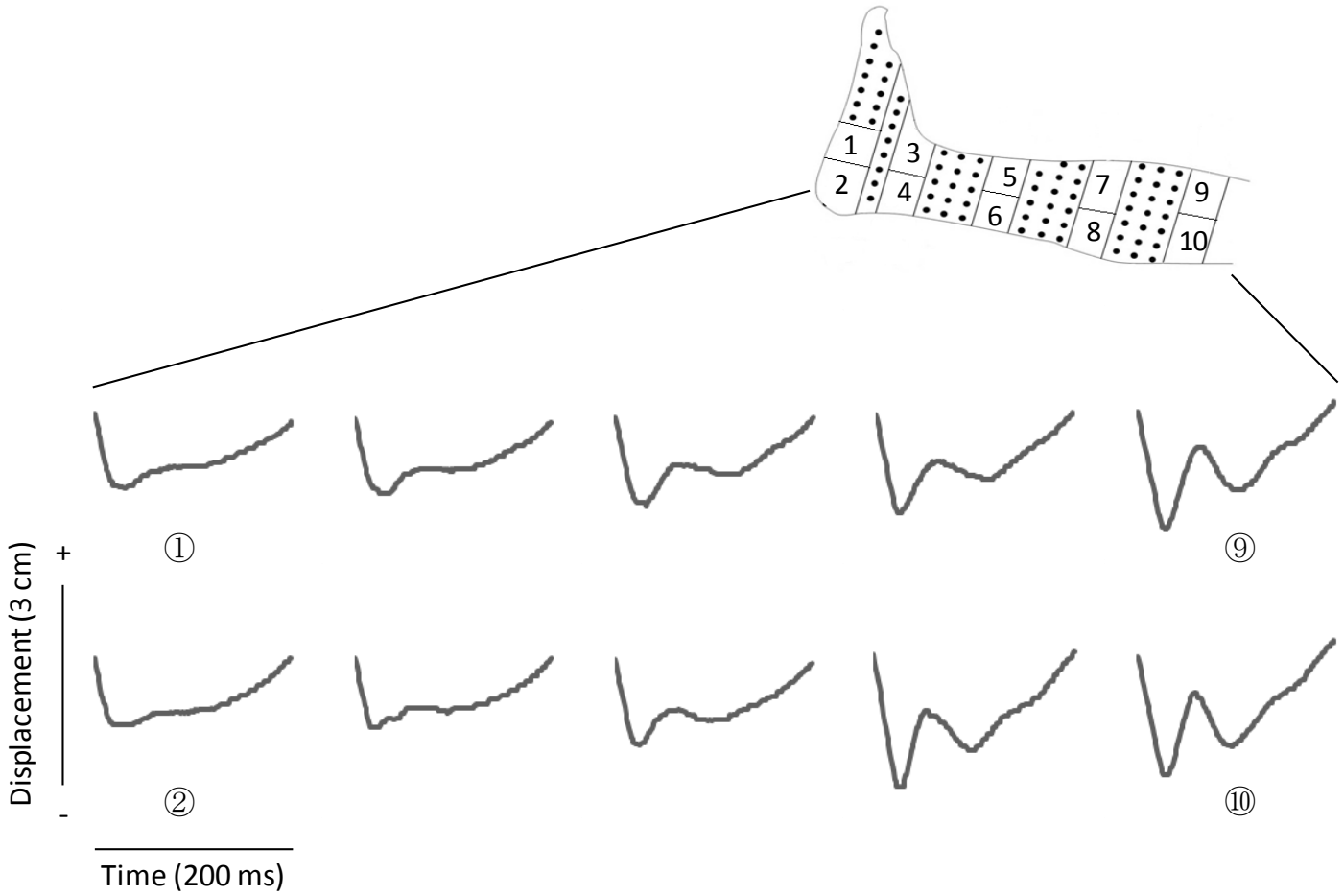

Figure 27. Sample displacement curves (proximo-distal axis) for each region for one trial of one participant. The curves from each region have been aligned in time and displacement in order to show the relative differences in displacement magnitude across the regions.

A significant main effect of Region was found for tissue displacement in the anterior [$F(1.689, 30.407) = 14.104$, MSE = 1.671, $p = 0.000$] (Figure 28) and posterior [$F(1.464, 26.345) = 18.838$, MSE = 0.323, $p = 0.000$] (Figure 29) directions. The greatest mean anterior soft tissue displacement was found in region 6 (1.08 cm), a value that was consistently lower in all more proximal regions (Figure 28). Consistent with other directions of motion, anterior tissue displacement was generally greater in regions on the back of the leg (posterior leg) than on the front (anterior leg). There was significantly less anterior displacement in region 2 compared to regions 4-10 ($p \leq 0.05$).

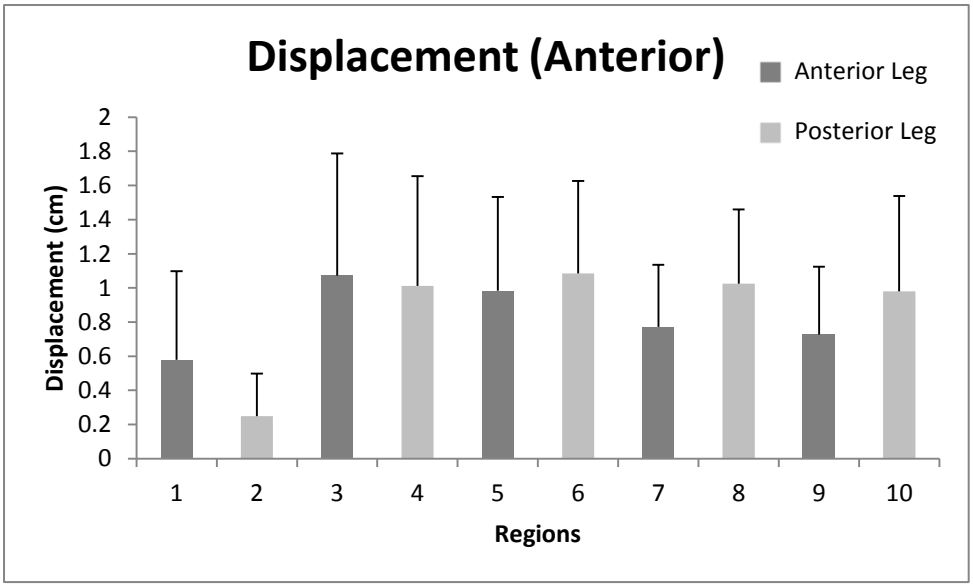

Figure 28. Mean (SD) peak soft tissue displacement in the anterior direction for each region.

Mean posterior displacement significantly increased for each region between region 5 and 10, from a low of 0.08 cm to a high of 0.50 cm (Figure 29). Unlike movement in the proximal and distal directions, the increase in posterior displacement was fairly sharp, starting at region 7. Significant posterior displacement was also found in the heel pad (region 2), which was significantly greater than in more intermediate regions (4, 5, and 6) ($p \leq 0.05$).

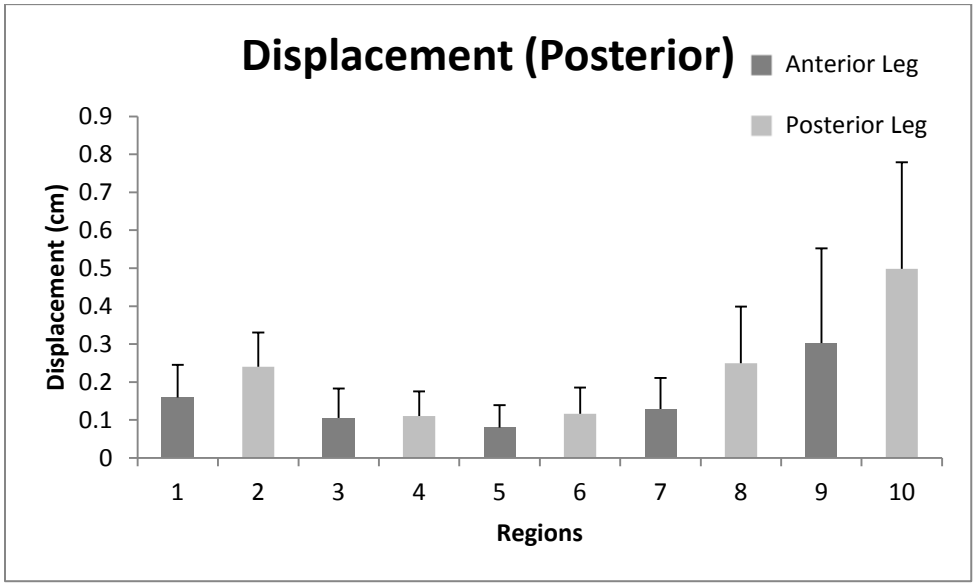

Figure 29. Mean (SD) peak soft tissue displacement in the posterior direction for each region.

4.2.5 Sex, Region and Displacement

There was a significant interaction between Sex and Region on distal soft tissue displacement [$F(2.856, 51.403) = 4.519$, MSE = 0.332, $p = 0.008$] (Figure 30), while this interaction was not significant in the proximal direction [$F(2.317,41.707) = 0.625$, MSE = 0.121, $p = 0.563$]. An analysis of simple effects showed that for females, there was a significant difference between four region comparisons (e.g. region 1 vs. region 2) that were not present for males, while males only had one significantly different region comparison that differed from females ($p \leq 0.05$). Males had significantly more distal displacement for regions 1 [$F(1, 18) = 8.921$, $p = 0.008$] and 3 [$F(1, 18) = 8.579$, $p = 0.009$] than females (Figure 30).

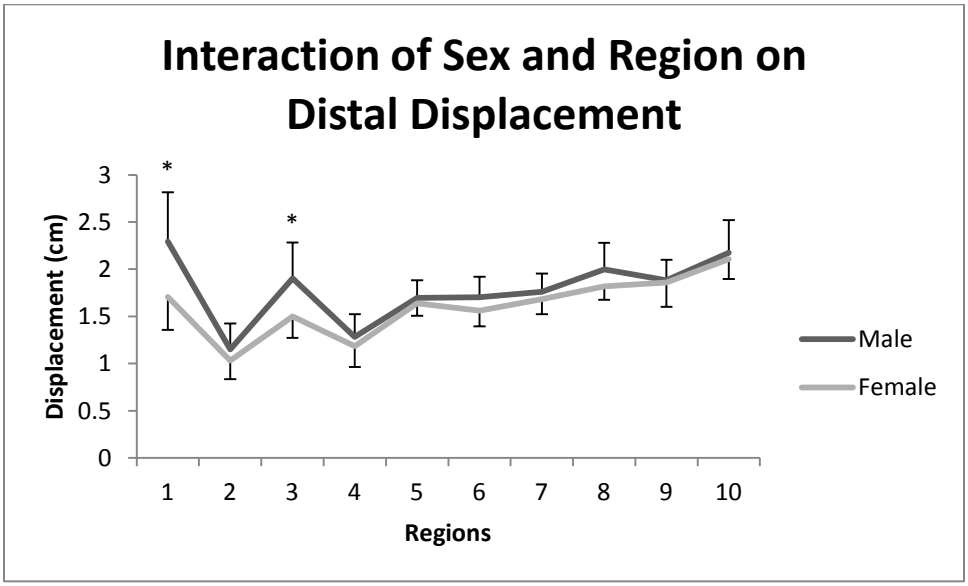

Figure 30. Interaction effect of Sex and Region on distal displacement (* = statistically significant at $p \leq 0.05$).

There was a significant interaction between Sex and Region on displacement in the anterior direction [$F(1.689, 30.407) = 6.669$, MSE = 1.671, $p = 0.006$] (Figure 31), while this interaction was not significant in the posterior direction [$F(1.464,26.345) = 0.497$, MSE = 0.323, $p = 0.557$]. An analysis of simple effects showed that there was a significant difference between 7 different region comparisons for females, but not for males ($p \leq 0.05$). Males had significantly more soft tissue displacement in the anterior direction for regions 1 [$F(1, 18) = 5.806$, $p = 0.027$], 3 [$F(1, 18) = 6.633$, $p = 0.019$] and 4 [$F(1, 18) = 6.438$, $p = 0.021$] than females (Figure 31).

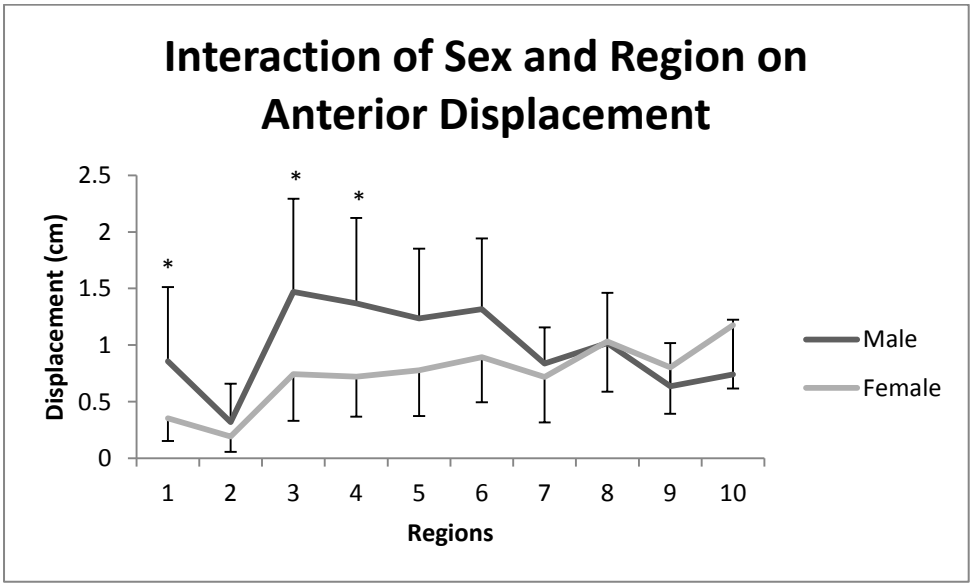

Figure 31. Interaction effect of Sex and Region on anterior displacement (* = statistically significant at $p \leq 0.05$).

4.2.6 Sex

There were no significant main effects of Sex for displacement in the proximal [F(1,18) = 0.283, MSE = 0.009, p = 0.601] distal [F(1,18) = 4.333, MSE = 0.035, p = 0.052], anterior [F(1,18) = 2.097, MSE = 0.134, p = 0.165] or posterior [F(1,18) = 0.136, MSE = 0.005, p = 0.717] directions. There was a significant main effect of Sex on proximal soft tissue velocity [F(1,18) = 7.070, MSE = 244.326, p = 0.016], where females were shown to have approximately 25 % greater velocity than males (Figure 32). There were no significant main effects of Sex for velocity in the distal [F(1,18) = 0.015, MSE = 23.471, p = 0.903], anterior [F(1,18) = 2.478, MSE = 232.424, p = 0.133] or posterior [F(1,18) = 0.046, MSE = 64.187, p = .0832] directions.

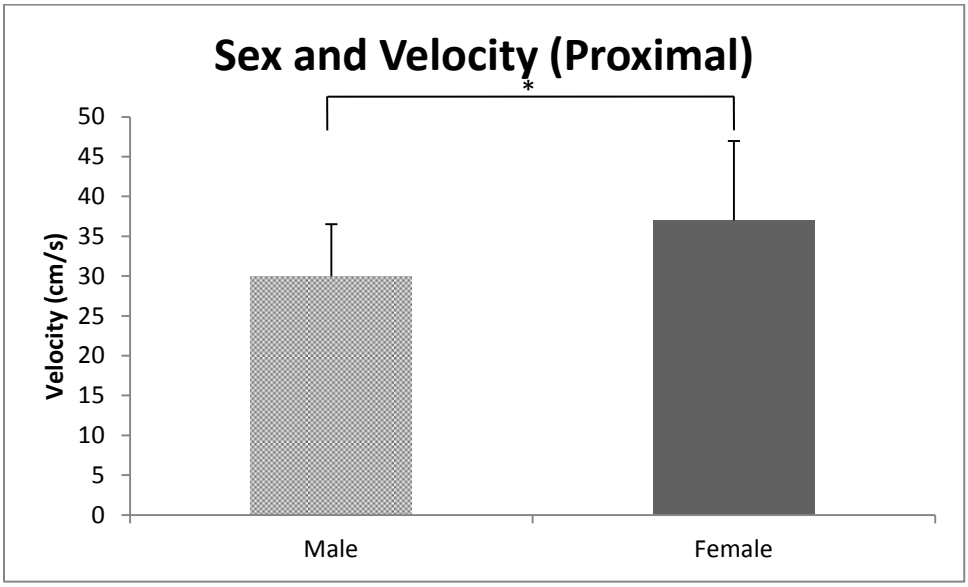

Figure 32. Mean (SD) peak soft tissue velocity in the proximal direction for each Sex (* = statistically significant at p ≤ 0.05).

4.2.7 Soft Tissue Velocity

A significant main effect of Region was found for velocity in the proximal [F(3.542, 63.751) = 57.241, MSE = 478.980, p = 0.000] (Figure 33) and distal [F(3.075, 55.350) = 81.814, MSE = 406.936, p = 0.000] (Figure 34) directions. Velocity in the proximal direction increased steadily from region 1 to region 10, with the largest mean velocities being recorded in regions 8 (49.9 cm/s) and 10 (61.5 cm/s). Velocities in these proximal regions had magnitudes that were more than twice those of regions 1 to 4 (Figure 33). Soft tissue movement in posterior regions (2, 4, 6, 8, 10) were on average 22 % (and up to 48 %) faster than movement in anterior regions (1, 3, 5, 7, 9) within the same zone. Significant differences in mean tissue velocity in the proximal direction were seen in the most proximal zones, with region 8 greater than region 7, and region 10 greater than region 9 ($p \leq 0.05$).

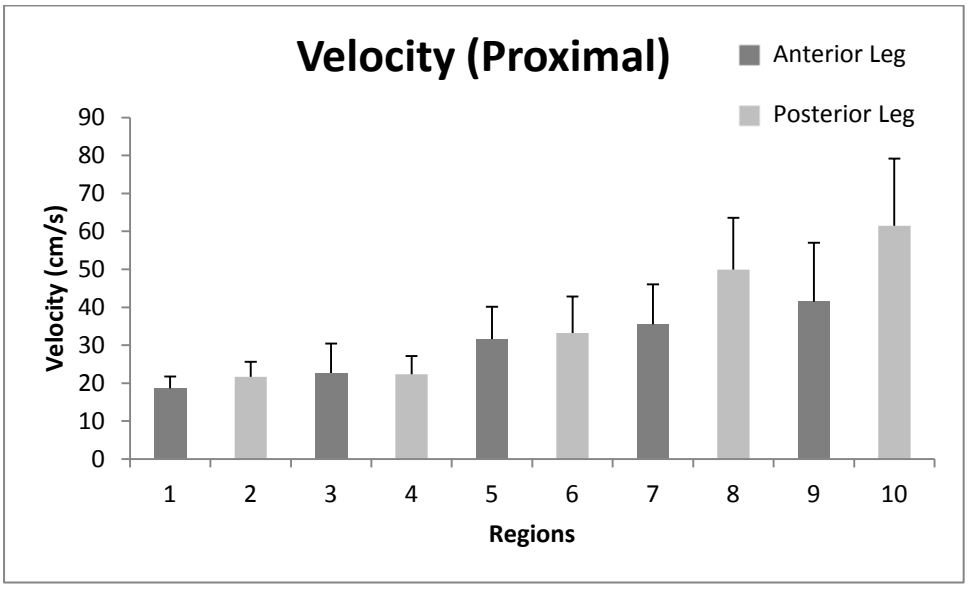

Figure 33. Mean (SD) peak soft tissue velocity in the proximal direction for each region.

The mean tissue velocities moving distally were the greatest in magnitude compared to all other directions, from region 1 (87.2 cm/s) to region 10 (105.6 cm/s) (Figure 34). There was a sharp increase in mean distal soft tissue velocity from 76.3 cm/s to 95.2 cm/s when moving proximally from the 0 % zone (regions 3 and 4) to the 25 % zone (regions 5 and 6), and a more gradual increase of 11 % in the more proximal half of the segment. The velocities of soft tissue movement towards the feet for all regions were significantly greater than region 2 ($p \leq 0.05$).

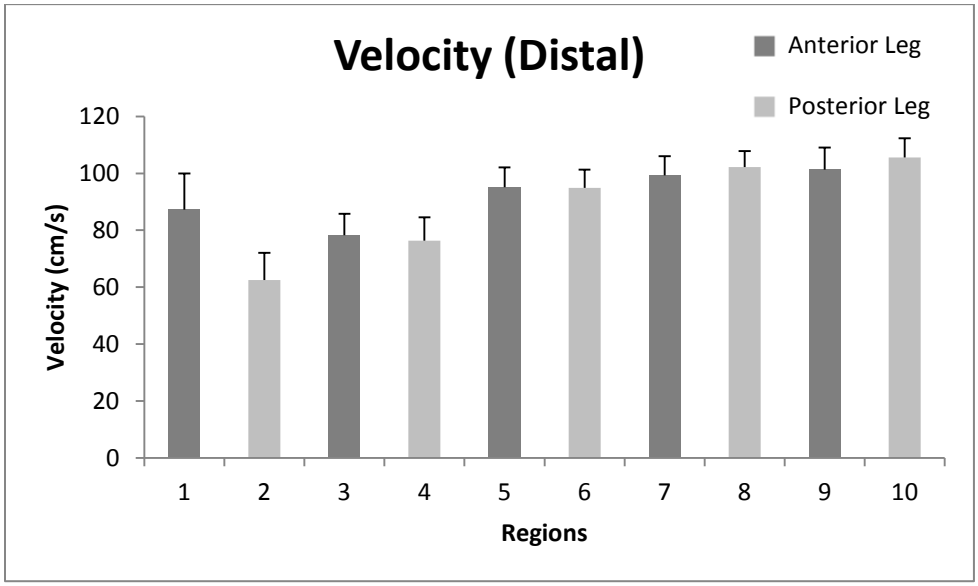

Figure 34. Mean (SD) peak soft tissue velocity in the distal direction for each region.

Significant main effects of Region were also found for velocity in the anterior [F(1.795, 32.308) = 19.706, MSE = 2724.935, p = 0.000] (Figure 35) and posterior [F(3.292, 59.254) = 39.348, MSE = 808.604, p = 0.000] (Figure 36) directions. The mean velocity in the anterior direction was greatest in the 0 % and 25 % zones (Figure 35). Velocity magnitudes steadily decreased from the intermediate (25 % zone) to the more proximal regions (50 % and 75 % zones) to a similar extent for tissue on the back and front of the leg. However, the tissue on the back of the leg in these proximal zones moved with 22 %, 26 %, and 33 % greater velocity, respectively than tissue on the front of the leg ($p \leq 0.05$).

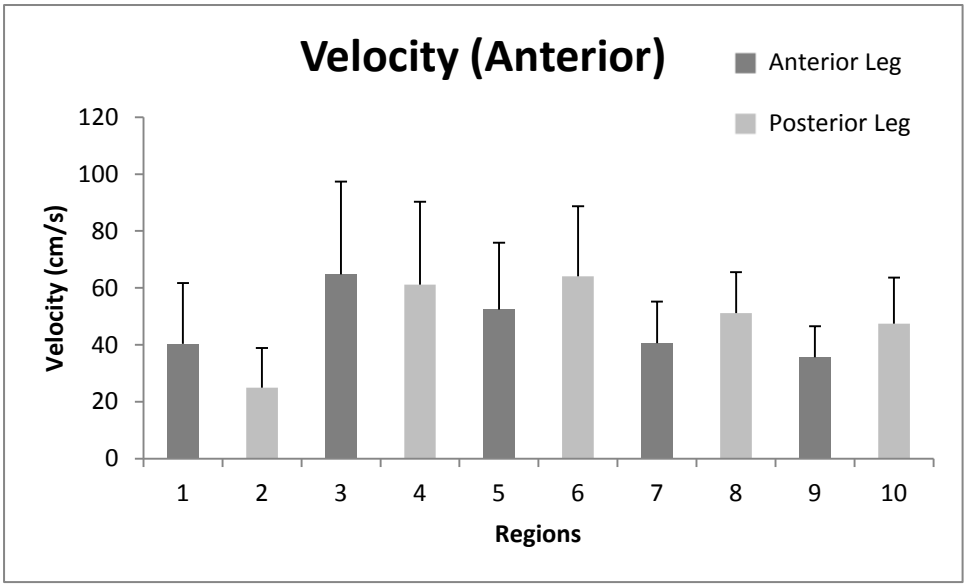

Figure 35. Mean (SD) peak soft tissue velocity in the anterior direction for each region.

The magnitude of posterior velocity increased gradually from region 1 to region 10, with a larger increase seen in posterior regions within the same zone, with the exception of zone 2, as there was greater posterior velocity in region 3 than in region 4 (Figure 36). Similar to proximal and distal movement, the greatest velocity in the posterior direction was found in region 10, which was significantly greater than all other regions ($p \leq 0.05$).

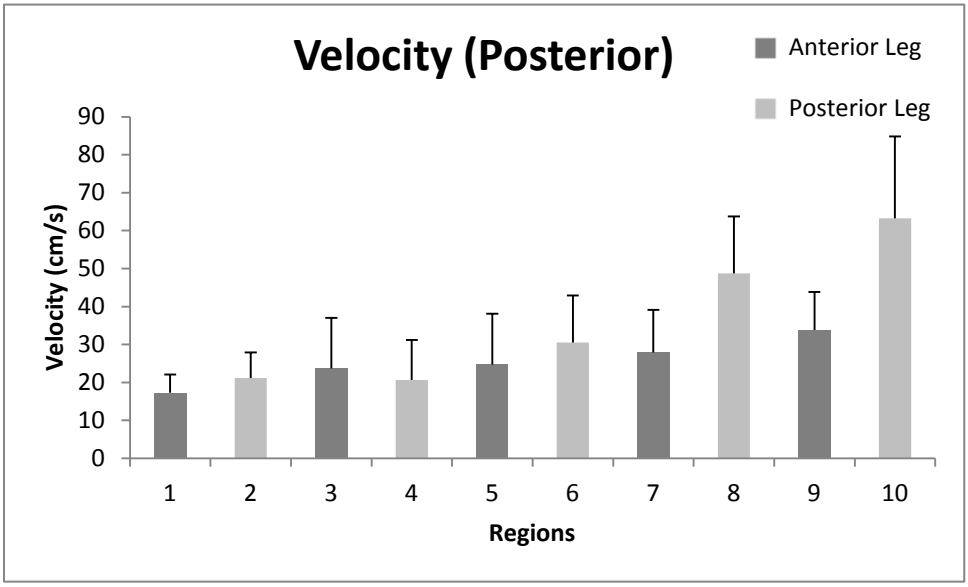

Figure 36. Mean (SD) peak soft tissue velocity in the posterior direction for each region.

A significant interaction existed between Sex and Region on proximal velocity [F(3.542, 63.751) = 4.521, MSE = 478.980, p = 0.04] (Figure 37). Females had significantly more proximal velocity for regions 6 [F(1, 18) = 7.111, p = 0.016], 8 [F(1, 18) = 9.678, p = 0.006] and 10 [F(1, 18) = 9.060, p = 0.008] than males (Figure 37). An analysis of simple effects showed that females were largely responsible for the interaction effect of sex and region on the proximal velocity of the soft tissue as there were significant differences in 19 of the comparisons between regions for females that were not present for males ($p \leq 0.05$). There was not a significant interaction between Sex and Region on distal velocity [F(3.075,55.350) = 1.393, MSE = 406.936, p = 0.254].

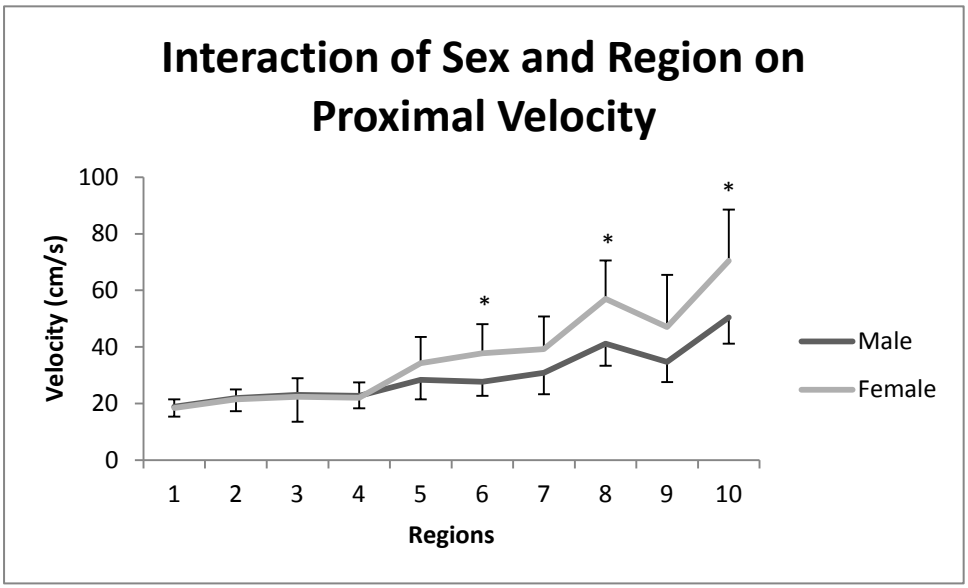

Figure 37. Interaction effect of Sex and Region on proximal velocity (* = statistically significant at $p \leq 0.05$).

There was a significant interaction between Sex and Region on soft tissue velocity in the anterior direction [F(1.795, 32.308) = 5.471, MSE = 2724.935, p = 0.01] (Figure 38). An analysis of simple effects showed that there was a significant difference between ten different region comparisons for females but not for males, while there was only a significant difference between two region comparisons for males that was not present for females ($p \leq 0.05$). Males had significantly more leg soft tissue velocity in the anterior direction for region 1 [F(1, 18) = 8.031, p = 0.011] and 3 [F(1, 18) = 5.858, p = 0.026] than females (Figure 38).

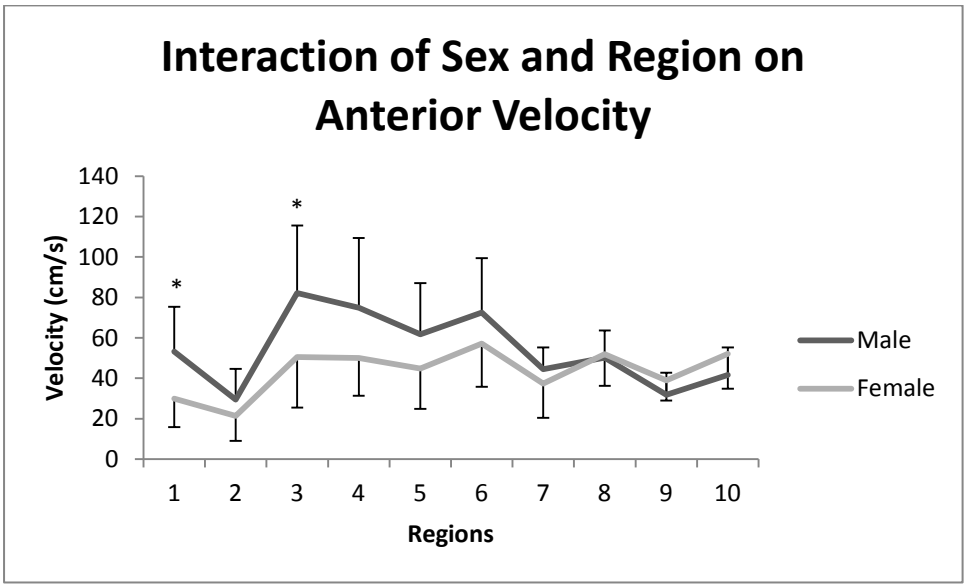

Figure 38. Interaction effect of Sex and Region on anterior velocity (* = statistically significant at $p \leq 0.05$).

Sex and Region had a significant interaction on velocity in the posterior direction [F(3.292, 59.254) = 3.410, MSE = 808.604, p = 0.02] (Figure 39). An analysis of simple effects showed that there were 18 significant differences between regions for females that were not found for males, while only one region comparison was significantly different for males alone ($p \leq 0.05$). Females had significantly greater soft tissue velocity than males in the posterior direction for region 10 [F(1, 18) = 4.419, p = 0.049] (Figure 39).

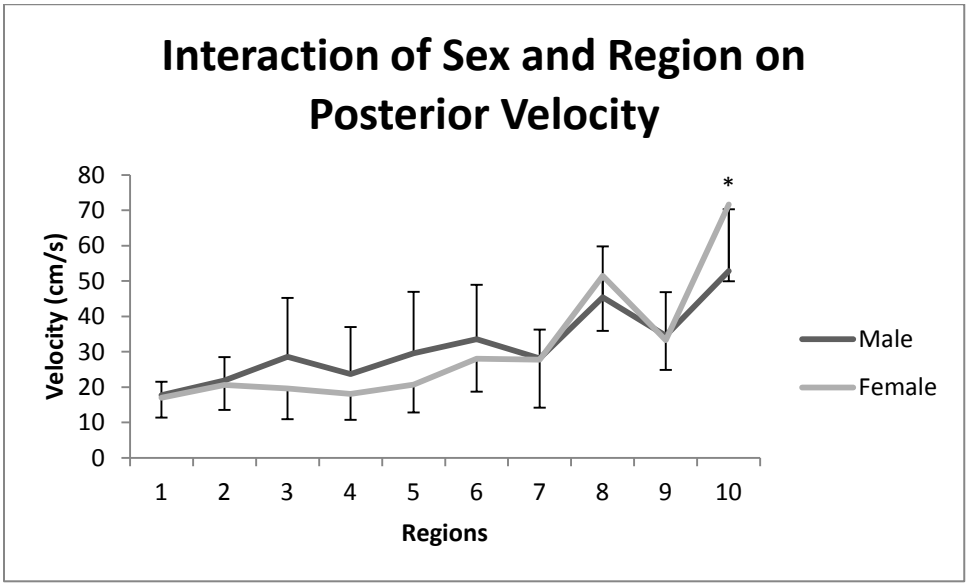

Figure 39. Interaction effect of Sex and Region on posterior velocity (* = statistically significant at $p \leq 0.05$).

4.3 Purpose 3

Determine the relationship between the displacement, velocity and energy absorption ability of the soft tissues of the lower extremity and the individual leg tissue masses (FM, LM, WM, BMC).

4.3.1 Participant Tissue Masses

Female participants were found to have 41 % greater leg FM than males, and males had 38 %, 38 % and 23 % greater LM, BM, and WM, respectively than females (Table 6).

Table 6. Mean (SD) fat mass (g), lean mass (g), bone mass (g) and wobbling mass (g) of all participants.

Participants	Fat Mass (g)	Lean Mass (g)	Bone Mass (g)	Wobbling Mass (g)
Male (n=9)	496.3 (234.3)	2588.6 (364.5)	269.7 (41.6)	3058.9 (223.5)
Female (n=11)	841.2 (313.0)	1592.7 (181.1)	168.0 (24.3)	2346.9 (400.2)

4.3.2 Energy Absorption Ability

As indicated previously, the energy density of the soft tissue wave was not calculated. Therefore, no further statistics were performed regarding this variable.

4.3.3 Displacement-Proximal

For males, there were no significant relationships between the proximal displacement of leg soft tissue and any of the leg soft tissue masses (FM, LM, BMC, and WM) (Table 7). Females had significant positive correlations between both LM and WM and the magnitude of proximal soft tissue displacement in region 2 ($p \leq 0.05$) (Table 8).

Table 7. Pearson correlations (r-values) between male proximal soft tissue displacement in each region (1-10), as well as the entire leg (mean) and specific tissue masses: fat mass (FM), lean mass (LM), bone mineral content (BMC), and wobbling mass (WM) (*=statistically significant at $p \leq 0.05$).

Male	1	2	3	4	5	6	7	8	9	10	Mean
FM (g)	-0.14	-0.56	0.00	0.16	0.11	0.09	0.15	0.01	0.07	-0.06	-0.07
LM(g)	-0.08	0.27	-0.14	-0.09	-0.21	-0.24	-0.19	-0.21	-0.11	-0.12	-0.14
BMC (g)	-0.28	-0.52	-0.19	0.10	-0.02	-0.08	0.07	-0.17	0.1	-0.19	-0.23
WM (g)	-0.34	-0.06	-0.33	0.32	-0.24	-0.22	-0.11	-0.28	-0.16	-0.22	-0.23

Table 8. Pearson correlations (r-values) between female proximal soft tissue displacement in each region (1-10), as well as the entire leg (mean) and specific tissue masses: fat mass (FM), lean mass (LM), bone mineral content (BMC), and wobbling mass (WM) (*=statistically significant at $p \leq 0.05$).

Female	1	2	3	4	5	6	7	8	9	10	Mean
FM (g)	0.17	0.26	0.25	0.12	0.00	-0.15	0.29	-0.05	0.14	0.09	0.15
LM(g)	-0.08	**0.77***	0.03	0.40	-0.36	0.06	-0.29	0.02	-0.09	-0.12	0.14
BMC (g)	0.08	0.54	0.00	0.11	-0.05	-0.02	0.02	0.00	-0.27	-0.12	0.08
WM (g)	0.07	**0.66***	0.16	0.36	-0.16	-0.06	0.12	0.02	0.00	0.03	0.22

4.3.4 Displacement-Distal

Males had significant positive correlations between FM and distal soft tissue displacement in regions 5 and 6, as well as between BMC and distal displacement in regions 5, 6, and 7 ($p \leq 0.05$) (Table 9). Females had significant positive correlations between FM and distal soft tissue displacement in regions 4, 9 and 10, as well as between WM and region 10 ($p \leq 0.05$) (Table 10).

Table 9. Pearson correlations (r-values) between male distal soft tissue displacement in each region (1-10), as well as the entire leg (mean) and specific tissue masses: fat mass (FM), lean mass (LM), bone mineral content (BMC), and wobbling mass (WM) (*=statistically significant at $p \leq 0.05$).

Male	1	2	3	4	5	6	7	8	9	10	Mean
FM (g)	0.35	0.22	0.58	0.34	**0.83***	**0.83***	0.65	0.49	0.55	0.54	0.65
LM(g)	-0.13	-0.12	-0.33	-0.30	-0.46	-0.32	-0.14	-0.02	0.12	-0.01	-0.21
BMC (g)	0.34	0.18	0.52	0.19	**0.71***	**0.77***	**0.67***	0.54	0.65	0.56	0.62
WM (g)	-0.22	0.07	-0.22	-0.31	-0.05	0.09	0.11	-0.01	0.35	0.05	-0.06

Table 10. Pearson correlations (r-values) between female distal soft tissue displacement in each region (1-10), as well as the entire leg (mean) and specific tissue masses: fat mass (FM), lean mass (LM), bone mineral content (BMC), and wobbling mass (WM) (*=statistically significant at $p \leq 0.05$).

Female	1	2	3	4	5	6	7	8	9	10	Mean
FM (g)	-0.60	0.41	-0.07	**0.67***	0.45	0.39	0.46	0.43	**0.69***	**0.71***	0.38
LM(g)	0.26	-0.25	0.11	-0.02	0.36	0.05	0.11	-0.25	0.01	0.20	0.10
BMC (g)	-0.33	0.31	0.02	0.48	0.44	0.33	0.32	0.16	0.36	0.52	0.29
WM (g)	-0.35	0.21	-0.03	0.51	0.51	0.30	0.44	0.21	0.58	**0.70***	0.35

4.3.5 Displacement-Anterior

There were no significant relationships between the anterior displacement of leg soft tissue of males and any of the leg soft tissue masses (FM, LM, BMC, and WM) (Table 11). For females, FM had a significant negative correlation with anterior soft tissue displacement in regions 1, 3, 4, 5, 6, and all regions together ($p \leq 0.05$), while there were also significant negative correlations between BMC and anterior soft tissue displacement in regions 1, 3, 5 and 6, and between WM and regions 1 and 3 ($p \leq 0.05$) (Table 12). Females also had significant positive correlations between LM and anterior soft tissue displacement in regions 9 and 10 ($p \leq 0.05$) (Table 12).

Table 11. Pearson correlations (r-values) between male anterior soft tissue displacement in each region (1-10), as well as the entire leg (mean) and specific tissue masses: fat mass (FM), lean mass (LM), bone mineral content (BMC), and wobbling mass (WM) (*=statistically significant at $p \leq 0.05$).

Male	1	2	3	4	5	6	7	8	9	10	Mean
FM (g)	0.27	0.07	0.35	0.28	0.29	0.23	0.13	-0.08	-0.20	-0.35	0.18
LM(g)	-0.07	-0.09	-0.14	0.02	-0.17	-0.05	-0.12	0.05	0.12	0.12	-0.05
BMC (g)	0.24	0.01	0.33	0.32	0.26	0.25	0.12	-0.07	-0.13	-0.29	0.18
WM (g)	-0.15	-0.26	-0.16	-0.11	-0.25	-0.20	-0.09	-0.19	0.06	-0.11	-0.19

Table 12. Pearson correlations (r-values) between female anterior soft tissue displacement in each region (1-10), as well as the entire leg (mean) and specific tissue masses: fat mass (FM), lean mass (LM), bone mineral content (BMC), and wobbling mass (WM) (*=statistically significant at $p \leq 0.05$).

Female	1	2	3	4	5	6	7	8	9	10	Mean
FM (g)	**-0.67***	-0.32	**-0.75***	**-0.64***	**-0.77***	**-0.71***	-0.58	-0.45	-0.20	-0.15	**-0.65***
LM(g)	-0.18	-0.09	0.01	0.16	0.23	0.30	0.33	0.37	**0.72***	**0.66***	0.40
BMC (g)	**-0.60***	-0.53	**-0.61***	-0.40	**-0.65***	**-0.64***	-0.39	-0.38	0.04	0.06	-0.47
WM (g)	**-0.62***	-0.34	**-0.63***	-0.42	-0.56	-0.50	-0.35	-0.26	0.16	0.15	-0.38

4.3.6 Displacement-Posterior

Males had significant negative correlations between BMC and posterior soft tissue displacement in regions 1, 3, 4 and 5, as well as between WM and region 4 ($p \leq 0.05$) (Table 13). Females had significant positive correlations between FM and posterior soft tissue displacement in regions 3-8, and all regions together ($p \leq 0.05$) (Table 14). Females also had significant positive correlations between LM and posterior displacement in regions 1 and 2, as well as between WM and regions 3 and 4 ($p \leq 0.05$) (Table 14).

Table 13. Pearson correlations (r-values) between male posterior soft tissue displacement in each region (1-10), as well as the entire leg (mean) and specific tissue masses: fat mass (FM), lean mass (LM), bone mineral content (BMC), and wobbling mass (WM) (*=statistically significant at $p \leq 0.05$).

Male	1	2	3	4	5	6	7	8	9	10	Mean
FM (g)	-0.53	-0.07	-0.55	-0.49	-0.50	-0.43	-0.52	-0.38	0.17	0.18	-0.26
LM(g)	-0.09	-0.29	-0.02	-0.24	-0.09	-0.06	0.32	0.46	0.36	0.40	0.35
BMC (g)	**-0.82***	-0.40	**-0.80***	**-0.78***	**-0.75***	-0.66	-0.33	-0.14	0.36	0.34	-0.25
WM (g)	-0.48	-0.60	-0.45	**-0.67***	-0.50	-0.54	0.18	0.09	0.39	0.42	0.01

Table 14. Pearson correlations (r-values) between female posterior soft tissue displacement in each region (1-10), as well as the entire leg (mean) and specific tissue masses: fat mass (FM), lean mass (LM), bone mineral content (BMC), and wobbling mass (WM) (*=statistically significant at $p \leq 0.05$).

Female	1	2	3	4	5	6	7	8	9	10	Mean
FM (g)	-0.04	-0.17	**0.81***	**0.83***	**0.67***	**0.80***	**0.60***	**0.78***	0.34	0.37	**0.68***
LM(g)	**0.66***	**0.81***	0.18	0.36	-0.24	-0.06	-0.19	-0.09	-0.19	-0.27	-0.01
BMC (g)	0.31	0.28	0.54	0.58	0.29	0.40	0.28	0.37	-0.01	-0.01	0.31
WM (g)	0.30	0.24	**0.71***	**0.82***	0.39	0.56	0.47	0.56	0.18	0.15	0.54

4.3.7 Velocity-Proximal

For males, there were no significant relationships between the proximal displacement of leg soft tissue and any of the leg soft tissue masses (FM, LM, BMC, and WM) (Table 15). In regions 3, 4, 8, 9, 10 and all regions together, females had significant positive correlations with FM and soft tissue velocity in the proximal direction ($p \leq 0.05$) (Table 16). There were also significant positive correlations between WM and velocity and region 4 and all regions together ($p \leq 0.05$) (Table 16)

Table 15. Pearson correlations (r-values) between male proximal soft tissue velocity in each region (1-10), as well as the entire leg (mean) and specific tissue masses: fat mass (FM), lean mass (LM), bone mineral content (BMC), and wobbling mass (WM) (*=statistically significant at $p \leq 0.05$).

Male	1	2	3	4	5	6	7	8	9	10	Mean
FM (g)	0.04	0.23	0.15	-0.01	0.15	0.00	0.03	-0.15	0.07	0.30	0.19
LM (g)	-0.35	-0.32	-0.46	-0.57	-0.10	-0.24	-0.11	0.02	0.16	-0.03	-0.36
BMC (g)	-0.15	0.23	0.24	-0.23	0.20	-0.02	0.09	0.04	0.17	0.33	0.27
WM (g)	-0.27	0.21	-0.49	-0.63	0.00	-0.05	0.19	-0.09	0.53	0.01	-0.10

Table 16. Pearson correlations (r-values) between female proximal soft tissue velocity in each region (1-10), as well as the entire leg (mean) and specific tissue masses: fat mass (FM), lean mass (LM), bone mineral content (BMC), and wobbling mass (WM) (*=statistically significant at $p \leq 0.05$).

Female	1	2	3	4	5	6	7	8	9	10	Mean
FM (g)	0.36	-0.02	**0.61***	**0.70***	0.48	0.50	0.57	**0.65***	**0.66***	**0.74***	**0.80***
LM (g)	-0.07	0.52	0.09	0.32	0.39	0.29	0.03	-0.26	-0.12	-0.15	0.03
BMC (g)	0.39	0.02	0.05	0.36	0.42	0.48	0.42	0.21	0.26	0.37	0.43
WM (g)	0.29	0.23	0.40	**0.62***	0.54	0.48	0.54	0.37	0.48	0.54	**0.64***

4.3.8 Velocity-Distal

There were significant positive correlations between magnitudes of FM and the amount of distal soft tissue velocity for regions 5, 6 and 7 for both males and females. Significant positive correlations also occurred for females in regions 4, 8, 9, 10 and all regions together ($p \leq 0.05$). Males had a significant positive correlation between BMC and distal soft tissue velocity in region 6, while a similar relationship existed in region 5 for females ($p \leq 0.05$) (Tables 17 and 18). Females also had significant relationships between WM and distal soft tissue velocity in regions 5, 7, and 9 ($p \leq 0.05$) (Table 18).

Table 17. Pearson correlations (r-values) between male distal soft tissue velocity in each region (1-10), as well as the entire leg (mean) and specific tissue masses: fat mass (FM), lean mass (LM), bone mineral content (BMC), and wobbling mass (WM) (*=statistically significant at $p \leq 0.05$).

Male	1	2	3	4	5	6	7	8	9	10	Mean
FM (g)	-0.07	-0.11	0.41	0.29	**0.87***	**0.88***	**0.73***	0.41	0.57	0.64	0.55
LM (g)	-0.07	-0.38	-0.43	-0.56	-0.57	-0.42	-0.29	-0.15	0.04	-0.34	-0.48
BMC (g)	0.00	-0.38	0.25	-0.01	0.62	**0.75***	0.62	0.37	0.61	0.49	0.35
WM (g)	-0.31	-0.56	-0.30	-0.50	-0.07	0.06	0.13	-0.16	0.39	-0.15	-0.33

Table 18. Pearson correlations (r-values) between female distal soft tissue velocity in each region (1-10), as well as the entire leg (mean) and specific tissue masses: fat mass (FM), lean mass (LM), bone mineral content (BMC), and wobbling mass (WM) (*=statistically significant at $p \leq 0.05$).

Female	1	2	3	4	5	6	7	8	9	10	Mean
FM (g)	-0.49	0.13	-0.01	**0.76***	**0.61***	**0.63***	**0.77***	**0.69***	**0.84***	**0.73***	**0.70***
LM (g)	0.18	0.03	0.13	-0.01	0.32	-0.01	0.01	-0.43	-0.12	-0.09	0.03
BMC (g)	-0.45	-0.01	0.20	0.45	**0.66***	0.50	0.50	0.24	0.40	0.39	0.43
WM (g)	-0.38	0.01	0.03	0.57	**0.67***	0.49	**0.67***	0.37	**0.62***	0.58	0.55

4.3.9 Velocity-Anterior

There were no significant relationships between anterior soft tissue velocity and any of the individual leg tissue masses (FM, LM, BMC, and WM) for males (Table 19). FM was significantly (negatively) correlated with the anterior velocity of soft tissue in the leg in regions 5 and 6 for females ($p \leq 0.05$) (Table 20). BMC also had significant negative relationships with the anterior velocity of leg soft tissue in regions 1, 2, 3, 5, 6, 7 and all regions together for females, while only tissue velocity and LM were significantly (positively) correlated in one region (10) ($p \leq 0.05$) (Table 20).

Table 19. Pearson correlations (r-values) between male anterior soft tissue velocity in each region (1-10), as well as the entire leg (mean) and specific tissue masses: fat mass (FM), lean mass (LM), bone mineral content (BMC), and wobbling mass (WM) (*=statistically significant at $p \leq 0.05$).

Male	1	2	3	4	5	6	7	8	9	10	Mean
FM (g)	0.45	0.11	0.52	0.36	0.54	0.43	0.54	0.08	0.13	-0.36	0.43
LM (g)	-0.09	-0.15	-0.20	-0.04	-0.29	-0.23	-0.20	-0.21	-0.02	0.25	-0.17
BMC (g)	0.48	0.07	0.56	0.47	0.59	0.50	0.63	0.10	0.18	-0.25	0.50
WM (g)	-0.11	-0.34	-0.11	-0.10	-0.20	-0.27	0.06	-0.31	-0.03	0.14	-0.18

Table 20. Pearson correlations (r-values) between female anterior soft tissue velocity in each region (1-10), as well as the entire leg (mean) and specific tissue masses: fat mass (FM), lean mass (LM), bone mineral content (BMC), and wobbling mass (WM) (*=statistically significant at $p \leq 0.05$).

Female	1	2	3	4	5	6	7	8	9	10	Mean
FM (g)	-0.55	-0.43	-0.57	-0.40	**-0.67***	-0.56	**-0.65***	-0.29	-0.23	-0.08	-0.56
LM (g)	-0.01	0.02	0.01	0.26	0.19	0.14	0.31	0.11	0.54	**0.70***	0.26
BMC (g)	**-0.64***	**-0.65***	**-0.66***	-0.45	**-0.71***	**-0.68***	**-0.62***	-0.50	-0.29	0.09	**-0.64***
WM (g)	-0.48	-0.41	-0.53	-0.24	-0.52	-0.47	-0.44	-0.29	-0.05	0.21	-0.41

4.3.10 Velocity-Posterior

There were no significant relationships between the posterior velocity of male and female leg soft tissue and any of the leg soft tissue masses (FM, LM, BMC, and WM) (Tables 21 and 22).

Table 21. Pearson correlations (r-values) between male posterior soft tissue velocity in each region (1-10), as well as the entire leg (mean) and specific tissue masses: fat mass (FM), lean mass (LM), bone mineral content (BMC), and wobbling mass (WM) (*=statistically significant at $p \leq 0.05$).

Male	1	2	3	4	5	6	7	8	9	10	Mean
FM (g)	0.01	0.20	0.40	0.37	0.47	0.40	0.49	-0.24	0.31	-0.10	0.33
LM (g)	-0.13	-0.25	-0.44	-0.45	-0.46	-0.20	-0.10	0.39	0.33	0.32	-0.13
BMC (g)	-0.05	0.06	0.37	0.37	0.36	0.49	0.43	-0.16	0.38	-0.02	0.34
WM (g)	-0.30	-0.31	-0.34	-0.48	-0.36	-0.23	0.18	-0.13	0.33	-0.10	-0.25

Table 22. Pearson correlations (r-values) between female posterior soft tissue velocity in each region (1-10), as well as the entire leg (mean) and specific tissue masses: fat mass (FM), lean mass (LM), bone mineral content (BMC), and wobbling mass (WM) (*=statistically significant at $p \leq 0.05$).

Female	1	2	3	4	5	6	7	8	9	10	Mean
FM (g)	-0.17	-0.14	0.11	0.39	0.03	0.01	-0.08	0.30	0.54	0.12	0.19
LM (g)	0.42	0.49	0.17	0.27	0.05	-0.02	-0.41	0.00	0.09	0.30	0.16
BMC (g)	-0.32	-0.12	-0.31	0.00	-0.38	-0.49	-0.28	0.01	0.24	0.01	-0.20
WM (g)	0.01	0.02	0.07	0.36	-0.03	-0.14	-0.23	0.19	0.47	0.18	0.14

CHAPTER V

DISCUSSION

5.1 Purpose #1

Quantify the displacement and velocity of, and the amount of energy dissipated by, the soft tissues of the leg following impact.

The greatest soft tissue displacements recorded in this study occurred in the distal direction, and increased in magnitude more proximally. From distal (region 2) to proximal (region 10) locations on the leg, mean soft tissue displacements ranged from a minimum of 1.09 cm to a maximum of 2.14 cm. These values compare favourably with past studies on the shank (1.80 cm) following a heel striking task (Pain and Challis, 2006), and the heel pad (1.13 cm) following a drop landing task (Kinoshita et al. 1993).

Peak soft tissue velocities have rarely been reported in the literature, with the exception of those related to breast tissue movement. The velocity of breast tissue movement in the vertical direction has been shown to be 92 cm/s while running (Scurr et al., 2010), and 93.1 cm/s while performing a two star jump (Bridgman et al., 2010). These values are slightly lower in magnitude than the mean peak soft tissue velocity of 105.6 cm/s, which was recorded in this study in the distal direction. The higher velocities for leg soft tissue may be due to differences in tissue composition between the leg and breast. The breast is comprised largely of adipose tissue (Vandeweyer and Hertens, 2002), whereas the leg soft tissue is predominantly a mixture of muscle and adipose tissue.

The soft tissue area deformations ranged between 6.0 % and 14.2 %, with a mean of 8.6 %. These values are similar to those previously reported by Pain and Challis (2002) for the forearm (mean of 11 %). As might be expected by the high degree of malleability of both muscle and adipose tissues (Malina et al., 2004), and the fact that more soft tissue is located proximally in the leg, the greatest amount of tissue deformation in the current study occurred in the most proximal zone (14.2 %). These trends in soft tissue area deformations are consistent with the higher tissue displacements and velocities recorded in more proximal regions.

5.2 Purpose #2

Determine if there are differences in soft tissue motion and impact energy dissipated due to sex, trial, impact method utilized (drop landing vs. pendulum) or as a function of the region of the leg measured.

5.2.1 Leg Region Specific Tissue Movement

Participants' heels were often noted to contact the force platform before the forefoot. This caused visible compression of the heel pad and rotation of the leg about the ankle before forefoot contact. Consequently, the motion of markers in regions around the heel joint cannot be regarded as being entirely a result of soft tissue movement resulting from impact. However, in general, large increases in soft tissue displacement were seen when moving from the 0 % zone (ankle) to the 25 % zone, and from the 25 % to the 50 % zone. Smaller increases were also seen from the 50 % zone to the 75 % zone. This finding is likely largely due to the fact that greater amounts of soft tissue exist in more proximal regions of the leg (Rittweger et al., 2000).

Tissues displaced to a greater extent in posterior regions of the leg than anterior regions within the same zone, which is also believed to be associated with the greater magnitudes of wobbling mass in more posterior regions. For example, the posterior region in the 75 % zone (21.4 mm) showed greater peak soft tissue displacement than the anterior region (18.7 mm). The greatest differences in soft tissue movement between posterior and anterior regions were seen with proximal soft tissue displacement; all zones ranged between a 1.5 (25 % zone) and a 7 times (heel pad) increase from the anterior to the posterior portion of the zone in soft tissue displacement in this direction. This is consistent with how the superficial posterior compartment muscles of the leg (soleus and gastrocnemius), which account for the majority of the girth of the leg (Tortora, 1995), are organized. In comparison, considerably smaller amounts of soft tissue are located on the front of the leg. This relative difference in soft tissue mass between the front and back of the legs explains why there was consistently less soft tissue displacement in anterior regions of the leg, in all directions.

Proximal soft tissue displacement was greatest in region 2 (heel pad) and appears to have been caused by heel pad compression as the leg was decelerated by the force platform. For regions 3-10, proximal tissue displacement was noted to occur after the soft tissue rebounded following its inferior movement caused by heel impact. As the heel pad is a major contributor to shock wave attenuation (Aerts et al., 1995; Alcantara et al., 2002; Challis et al., 2008; Chi and Schmitt, 2005; Ker at al., 1989 Kinoshita et al., 1993), it is not surprising that there was less proximal soft tissue displacement in more proximal zones (25 %, 50 %, and 75 %) in the current study.

Whereas movement towards the head appears to be largely influenced by the location of the soft tissues relative to the impact point (i.e. what zone), the initial displacement of soft tissues towards the feet caused by impact appears to be more dependent on the absolute amount of soft tissue present within the regions. Greater distal soft tissue displacement (2.14 cm) in proximal regions (9 and 10) compared to distal regions (3 and 4) (1.23 cm) highlights the influence of soft tissue magnitude on tissue displacement. This trend is also seen in the posterior direction and is likely a result of smaller amounts of soft tissue in this area. Posterior soft tissue displacement may also have been limited by the horizontal orientation of the pendulum at impact. In this position, the soft tissue on the posterior aspect of the leg is pulled by the force of gravity away from the tibia, towards the ground. This would likely have an influence on the tissues' response to impact, compared to what would normally be seen following a heel strike on the ground during vertically oriented activities such as walking and running.

The velocities of the soft tissue showed very similar trends to the displacements, with the greatest velocities occurring in the most proximal regions of the leg. While the greatest mean peak velocity was in region 10 (105.6 cm/s) during movement of the tissue towards the feet after impact, velocities from regions 5 to 9 were only 10 % lower in this direction on average. While velocities in the proximal and posterior directions were also greater in more proximal regions, the mean velocities of soft tissue travelling in the anterior direction showed a different trend. The highest values in this direction were recorded in the middle sections (0 % and 25 % zones) of the leg, and trailed off in magnitude both distally and proximally. These smaller velocities in the distal regions are similar to the results found for all other directions, while the decrease in anterior velocity

in the proximal regions is unique in comparison. This may also be a result of the horizontal orientation of the pendulum at impact. Prior to impact, the regions with greater amounts of soft tissue (proximal regions) would likely experience greater displacement while the leg is in a stationary position. Due to the proximo-distal orientation of the muscles within the leg, it is expected that the majority of their movement would occur in this direction, limiting their contribution to both anterior and posterior movement of the soft tissue package. Additionally, the muscles' origins and insertions are located within these regions, which could potentially limit the maximum amount of anterior movement, as the tissue would not be pulled as far posteriorly away from the attachment point prior to impact compared to regions in the middle of the leg, due to the horizontal orientation of the leg. Differences in tissue composition between various regions within the leg may also help to explain these results. For example, the magnitude of wobbling mass is believed to be responsible for greater posterior region soft tissue velocity (regions 2, 4, 6, 8, and 10) when compared to anterior regions (regions 1, 3, 5, 7, and 9) within the same zone.

The effect that regional differences in soft tissue motion of the leg have on the kinetics associated with impact should be quantified in order to facilitate future wobbling mass modeling efforts. Although a number of wobbling mass models have been developed and used in biomechanics research to demonstrate the effects of not including the relative motions of soft and rigid tissue elements (Gittoes et al., 2006; Gruber et al., 1998; Pain and Challis, 2006), the shape, orientation and motion of the soft tissues relative to bone have been simplified, which reduces the biofidelity and response of the model. For example, many wobbling mass models include wobbling mass segments

which are coupled to the side of the rigid segments (Gittoes et al., 2006; Gruber et al., 1998), while models which involve an inner rigid mass surrounded by an outer wobbling mass would likely provide more realistic results when trying to represent the human body (Pain and Challis, 2004; Pain and Challis, 2006). With respect to the shape of wobbling mass elements, they have been modelled as symmetrical shapes that do not differ along the proximo-distal axis (Gruber et al., 1998; Pain and Challis, 2004; Pain and Challis, 2006). Cylindrical objects with a greater circumference proximally than distally provide a better representation of how the wobbling mass is distributed within the lower extremity (Gittoes et al., 2006). However, all wobbling mass models to date do not account for the different motion patterns that were evident between the regions and in the different directions outlined in the current study.

5.2.2 Sex and Tissue Movement

Females generally showed greater mean peak soft tissue displacements in the proximal and distal directions, while moving proximally in the leg from region 1 to region 10. However, some small variations were noted as a function of whether the tissue was positioned on the anterior or posterior aspect of the leg. Comparatively, males tended to have greater soft tissue displacement in the anterior and posterior directions than females within sections nearer to the middle of the leg (25 % and 50 % zones), with values decreasing proximally.

Despite these differences in how the leg soft tissues of males and females responded following impact, only one significant sex main effect was observed. The speed of the shock wave, as witnessed through the movement of the soft tissues, was

greater on average for females as it travelled towards the knee joint. This could possibly be attributed to the fact that men's heel pads tend to be thicker (Prichasuk, 1994) and absorb more impact energy than women's (Alcantara et al., 2002). Thicker heel pads in males may also help to explain why tibial accelerations in females have been reported to be greater than those for males (Schinkel-Ivy et al., 2012a). The greater tibial accelerations per gram of LM, WM, and BMC for females (Schinkel-Ivy et al., 2012a) may increase the susceptibility of women to various injuries, such as anterior cruciate ligament (ACL) tears (Arendt et al., 1999), and stress fractures (Jones et al., 2002).

A very interesting trend emerged when comparing the displacement and velocity measurements of males and females. While it was hypothesized that males would have greater tissue displacement and velocity in general, because males on average have greater amounts of wobbling mass in the legs than females (Mazess et al. 1990), this only held true in the current study for more distal leg regions. For most of the dependent measures evaluated, females tended to have greater peak displacements and velocities than males as the analyses progressed more proximally. Females were also found to be largely responsible for the significant interaction effects involving sex, given that they had many more significant region comparisons than males. Sex differences in how the soft tissues move may be explained in part by differences in how the soft tissue masses are distributed within the leg segment between the sexes. In addition, females in this study had 41% more fat mass in their legs, on average, than males. Therefore, it is suggested that the differences in tissue distribution between the sexes (Brody, 1999; Mazess et al., 1990; Prichasuk, 1994) may be significant enough to result in the noticeably different motion characteristics reported herein. Further study of this

phenomenon needs to be undertaken for a broader range of tasks and in three dimensions to be able to determine if the findings from this initial investigation are task- and direction-specific.

5.3 Purpose #3

Determine the relationship between the displacement, velocity and energy absorption ability of the soft tissues of the lower extremity and the individual leg tissue masses (FM, LM, WM, BMC).

5.3.1 Tissue Masses and Movement

Overall, the relationships between the magnitudes of FM, LM, BMC, and WM and soft tissue displacement in the proximo-distal direction were similar between males and females, while movement in the antero-posterior direction showed significant differences. For example, movement of soft tissue in the posterior direction often had opposite relationships with individual tissue masses between the sexes. The differences between the soft tissue displacement for males and females in the antero-posterior direction provide evidence that the tissue masses alone cannot explain the variation witnessed between males and females. These findings highlight that tissue composition has an effect on the kinematics of soft tissue motion following impact, with males and females responding differently in several directions. This, along with the apparent differences in the response of each tissue type in different regions of the leg clearly indicates the importance of taking this information into consideration when developing future wobbling mass models.

The speed of shock wave propagation along the longitudinal axis of long bones has been measured to be approximately 3200 m/s in vitro (Chu et al., 1986; Pelker and Saha, 1983). However, the speed of propagation through the body in vivo is abated by movement of the soft tissues of the leg relative to the underlying bone (Dufek et al., 2009). Shock propagation through soft tissue is much slower than through bone, with values for the soft tissue of the upper extremity reportedly being approximately one percent (37 m/s) of the speed through bone (Pain and Challis, 2002).

The mass of both soft and rigid tissues in the body has been shown to affect shock wave attenuation through the lower extremity. Specifically, greater magnitudes of FM, LM, WM, or BMC were associated with decreases in the peak acceleration response measured at the proximal tibia (Schinkel-Ivy et al., 2012a), with BMC and LM having the stronger relationships. It was hypothesized in the current study that velocity of the soft tissue in the proximal direction would be consistent with previously reported acceleration responses at the proximal tibia. However, this was not found to be the case for males as they did not have any significant correlations between any of the tissue masses and proximal tissue velocity. For females, it was found that greater magnitudes of FM were positively associated with proximal soft tissue velocities in 9 of the 10 regions. Distal soft tissue velocity was significantly greater, with larger magnitudes of FM for several regions for both males and females. Females also had several regions that had significant positive relationships between WM and distal soft tissue velocity. This is understandable, as the amount of FM was found to play a significant role in the magnitude of the distal velocity for both sexes, and since females had significantly more

FM in their legs on average than males, a greater percent of the total WM would be comprised of FM.

The results of the current study also indicate that there were differences between males and females for soft tissue velocity in the anterior direction. Although the correlations between anterior soft tissue velocity and individual tissue masses did not reach significance for any of the leg regions for males, the general trends were often opposite to those shown for females. For example, males had positive relationships between BMC and anterior velocity in 9 of 10 regions ($r = 0.07$ to 0.63), while females had negative relationships in 9 of 10 regions ($r = -0.29$ to -0.71). When considered in their entirety, the velocity results of the current study lend support to the conclusions made for tissue displacement. Overall, it appears that a meaningful link exists between the magnitudes of specific tissue masses of the leg and the kinematics of the soft tissue package of the leg. While it appears that FM is the only tissue type that shows a consistent relationship for both sexes in any direction, there are no general conclusions that can be drawn related to the magnitudes of individual tissue masses and soft tissue motion, based on these results. Given the exploratory nature of the current study, and that there are no previous studies in the literature that have investigated soft tissue displacement or velocity that have taken into account differences in tissue composition between participants, further research in this important area seems warranted.

Leg tissue masses in this study were estimated based on a set of previously developed prediction equations (Holmes et al., 2005). The equations require anthropometric measurements such as skin fold thickness, limb girth, circumference and length measurements as inputs. While the accuracy of skin fold thickness equations for

the assessment of body fat percentage has been shown to be poor at the individual level when compared to DEXA (Rodriguez et al., 2005), the equations used here were validated using tissue masses collected from DEXA, which were replicated with minimal errors (Holmes et al., 2005). There are always errors when anthropometric measurements are taken. However, the reliability of the measurements needed in the current study have been shown previously to be good to excellent both between and within measurers (Burkhart et al., 2008). The equations were developed using 68 healthy young adults (26 M, 42 F) with a mean age, mass, and height of 21.9 ± 2.6 years, 65.4 ± 10.6 kg, and 1.69 ± 0.09 m, respectively. These measures for the current study sample were very similar in magnitude to those reported by Holmes et al. (2005). Therefore, due to the excellent reliability of the measurements taken, and the closeness of the general physical and age profiles of the two participant samples, it is believed that the errors involved with taking the anthropometric measurements in the current study are not a significant limitation of this work. Despite this, it must be noted here that the Holmes et al. (2005) equations provide estimates of tissue masses for the entire leg segment, not tissue masses as a function of leg region. To be able to determine regional differences in tissue mass, additional prediction equations would need to be generated from DEXA scans by using custom regions of interest in the scan software. This is an important consideration when trying to interpret the results of the current study.

One of the goals of this study was to compare the motion of the leg soft tissue following two different impact techniques. Many studies in the past have investigated heel impacts following drop landings (Decker et al., 2003; Gittoes et al., 2006; Schmitz et al., 2007; Yeow et al, 2009), and several have utilized a human pendulum approach

similar to what was used here (Duquette and Andrews, 2010; Flynn et al., 2004; Fowler et al., 1997; Holmes and Andrews, 2006; Lafortune and Lake, 1995; Lafortune et al., 1996a). Only one study was found that showed a comparison between the two techniques, and what was compared was limited to assessments of the angle of the lower extremity joints (Fowler and Lees, 1998). In the human pendulum, the primary alignment of participants' impact legs is in the horizontal plane, whereas impacts resulting from foot contact during gait or running occur predominantly in a vertical orientation. As indicated previously, the horizontal orientation of the leg in this study is likely a main reason for the measured response of the tissue when comparing the motion in the proximo-distal and anterior-posterior directions. In the video records of the drop landing technique it was observed for most of the participants that the proximal portion of the leg continued to translate anteriorly for some time, as it rotated about the ankle joint once heel contact was initiated. The drop landing task required participants to step forward off a raised platform, which caused their body weight to shift anteriorly. In anticipation of the impact on the stiff force platform, and in order to reduce the potential discomfort experienced, participants flexed their knees to help in impact absorption. This action resulted in the segmental motion described above; motion that was not able to be separated out from the motion of the overlying soft tissue using the approach described. Because the soft tissue motion could not be isolated from the motion of the segment during this period, the data from the drop landing technique was not analyzed further.

Shock transmission through the leg has been shown to be affected by leg muscle activation level and ankle joint angle (Duquette and Andrews, 2010; Flynn et al., 2004). Although the position of the participants on the pendulum and the knee angle of the

impact leg were controlled in the current study, the level of muscle activation and ankle posture were not. Previous research has shown that varying degrees of muscle activation exist 50 ms prior to impact, which is thought to be a preparatory mechanism for the expected impact force (Boyer and Nigg, 2004; Burkhart and Andrews, 2013; DeGoede and Ashton-Miller, 2002). These preparatory muscle activations would increase joint and muscle stiffness (Burkhart and Andrews, 2010; Flynn et al., 2004; Holmes and Andrews, 2006) and affect soft tissue vibrations (Nigg, 1997; Nigg and Liu, 1999). As a result, it is likely that the relationships found between the passive soft tissue masses of the leg and their motion are lower than they would be if the activation state of the muscle was also taken into consideration. However, it should be noted that the purpose of this study was to document the natural soft tissue motion that occurred following impact. In order to control muscle activation level, the level has to be known, which would require EMG electrodes to be placed on the soft tissue in question. The natural motion of the soft tissue might therefore be compromised, thereby limiting the conclusions that could be drawn.

Although the high speed videos captured were of reasonable quality, the single camera limited the analyses to two dimensions. This limited the view to the medial aspect of the foot and shank (heel pad to knee) in the sagittal plane. Similarly, the ProAnalyst® motion tracking software was only capable of measuring and outputting data in two dimensions, the X (perpendicular to the long axis of the tibia, running anterior to posterior) and Y (parallel with the long axis of the tibia). Therefore, any soft tissue motion in the medio-lateral direction could not be monitored using this system. Given the lack of evidence to draw on from the literature in this area, the importance of the soft

tissue motion in medio-lateral direction cannot be assessed, relative to the motion in the other two directions (anterior-posterior, proximal-distal), in terms of how it might contribute to attenuating impact induced shock. Given the limitations of using a single camera to quantify three dimensional tissue motion, future evaluations utilizing multiple high speed cameras are critical for advancing our understanding of the complex motions documented in the current study between the different tissues of the leg.

This study is the first to quantify the displacement and velocity of the soft tissues in various regions of the leg following controlled heel impacts. Additionally, data regarding the relationships between soft tissue movement and tissue composition are unique contributions to the literature in this area. It is hoped that these data will drive future biomechanical modeling efforts which are focused on improving our estimates of impact kinematics and kinetics. One of the purposes of the study was to determine the amount of impact energy that can be dissipated by soft tissue movement following an impact event. While the method that was chosen to determine the energy dissipated by the soft tissue of the leg (reported in Pain and Challis, 2002) was found to distort the displacement results, there is a lot to be learned from attempting this analysis. For example, future work should focus on determining and evaluating an appropriate method for converting time-varying signals which are less than 1 second in duration into the frequency domain, without introducing signal distortions similar to those that were experienced using a FFT. Solving this problem would facilitate the calculations of energy dissipation previously proposed.

CHAPTER VI

FUTURE DIRECTIONS

6.1 Muscle Activation and Joint Angles

The results of this study suggest that the displacement and velocity of leg soft tissue following heel impacts are, to some extent, a function of the tissue's composition. However, the measures evaluated in this thesis did not account for changes in muscle activation, or changes in ankle joint angles prior to impacts. It has been shown that joint kinematic strategies (Duquette and Andrews, 2000; Lafortune et al., 1996b) and levels of muscle activation (Flynn et al., 2004) can alter the transmission of impact shock waves. Therefore, in order to properly assess the impact of the passive soft tissue, these other factors need to be controlled. In terms of muscle activation levels, this would be particularly difficult, given that muscle activity is normally measured using electromyography, which involves the fixation of electrodes (and usually wires) to the soft tissue. Fixation of external devices to the skin would likely impact the natural motion of the soft tissue negatively. Fine wire electromyography, which involves inserting very fine wires into the bellies of muscles, might reduce soft tissue motion interference, but is invasive and requires additional expertise and specialized equipment. Alternate approaches to controlling muscle activation levels, without the need to fix external monitoring equipment to the soft tissue, should be considered.

6.2 Drop Landings

Human pendulums allow impacts to be applied consistently in a laboratory setting, but the horizontal orientation of these devices likely contributes to differences in tissue response patterns compared to those that would be experienced during normal gait or running. Drop landings better simulate the vertical orientation of the leg in these activities. Drop landing and pendulum techniques have been compared in the past, and although no differences in lower extremity joint angles resulting from the two techniques were found (Fowler and Lees, 1998), it is not known if soft tissue movement and shock wave attenuation specifically are affected differently by the two approaches. Issues with the automatic tracking of the motion of the soft tissues, relative to segmental motion, in the drop landings proposed in this study, resulted in an inability to compare these responses with those from the pendulum. More sophisticated camera systems and processing software would address this issue. In addition, with higher frame rates, it would be possible to monitor the responses of both the tibia and the soft tissue during the same impact events.

6.3 Three-Dimensional Motion Capture

The camera and software utilized in this study only allowed for the collection of soft tissue movement in two dimensions. Soft tissue motions have been recorded in all three planes (Akbarshahi et al., 2010; Manal et al., 2003; Reinchmidt et al., 1997), and therefore cannot be ignored if a full understanding of the effects that soft tissue motion has on the propagation of impact forces is to be achieved. Similar high speed camera systems exist that utilize multiple cameras to provide three-dimensional representations

of the area of interest. This would provide a more realistic response of the leg following impact, and contribute to the development of more realistic biomechanical models that could significantly improve assessments of soft tissue elements and the kinetic contributions they make to impact shock attenuation through the body (Pain and Challis, 2006).

6.4 Surface Markers

The markers used in this study were very similar in shape, size and arrangement (geometric relationship with respect to one another). The ProAnalyst® motion tracking software assigns each pixel a specific value, giving each marker a fingerprint which the program can recognize. While it was not very common for the program to mistake one marker for another, these types of errors could be minimized in future work by using different makers sizes, shapes and geometries (e.g., like what would be achieved using a speckling pattern with spray paint). It would also be beneficial to utilize the "frames to search after loss" feature provided in the software. This allows the investigator to set (within the program) how many frames to search for a particular marker once the marker has been lost. In the current investigation, when a marker was lost for a single frame, it did not return. Setting this feature at a very low number, even 1 or 2 frames, would allow more markers to be retained throughout the duration of the entire impact. In the current study, only one marker was needed for each region to determine the displacement and velocity, therefore marker drop out did not affect these results. However, four markers were required to calculate the change in area of a set of markers within each region. Marker dropout did reduce the number of participants with complete data somewhat in each region (Table 5); an issue that should be able to be remedied in the future with

improvements to marker detection within the ProAnalyst® motion tracking software used in this thesis.

6.5 Biomechanical Models

Previous biomechanical models which incorporate soft tissue elements have provided valuable evidence in support of their inclusion in such models, to more realistically evaluate the kinetics of impact events. However, the models have not accounted for the differential motions which do exist in the soft tissues, as a function of the location and type of tissue mass within the leg segment (Gruber et al., 1998; Pain and Challis, 2006). Based on the results from the current study, it is apparent that the masses and locations of specific tissues of the leg influence the displacement and velocity of the overall soft tissue package. Not only do tissue masses play a significant role in the kinematics of the soft tissue in the leg, but it has been shown that they do so differently for males and females. The development of biomechanical models may be simplified by using lumped tissue mass elements without varying responses, but this ignores important characteristics of actual wobbling mass tissue that have been reported herein, and which may contribute to our understanding of how our leg tissues respond, and protect us from injury, following impacts. More sophisticated models should be developed that more accurately mimic the varying responses of the leg soft tissues for both males and females.

6.6 Energy Density Calculation

The peak frequency of the displacement waveforms could not be determined in the current study without distorting the signals. Therefore, the amount of energy

dissipated by the soft tissue could not be calculated, as per the method prescribed by Pain and Challis (2002). However, using the proposed method resulted in signal distortions because the length of the signals being evaluated were less than 1 second in duration; a requirement of using traditional Fourier-based approaches for determining the frequency spectrum of a signal. Alternate approaches for transforming short duration time domain signals into the frequency domain need to be researched and evaluated.

Other approaches could also be used in future work to quantify the amount of energy dissipated as a result of impact. This could be accomplished by estimating the change in kinetic energy of the individual tissue mass components, or of the foot and leg segments (as a system) before and after the foot strikes the contact surface.

CHAPTER VII

CONCLUSIONS

The results of this study can be summarized as follows:

- This study was the first to quantify displacements and velocities of leg soft tissue following heel impacts using high speed video analyzed with Pro Analyst® software.
- Leg soft tissue was found to exhibit the greatest displacement and velocity while travelling distally, towards the feet after impact.
- Regions of the leg with greater amounts of total wobbling mass (proximal leg, posterior region) experienced greater displacement and velocity than distal and anterior regions, respectively.
- Soft tissue responses to heel impacts were different between the males and females studied. This is likely due to sex-specific differences in leg tissue composition and distribution.
- The lack of significant trial effects in any of the data presented supports the good to excellent reliability of the analysis techniques previously reported (Brydges et al., 2012).
- The magnitude of tissue masses (FM, LM, BMC and WM) have a significant influence on the magnitude of soft tissue displacement and velocity seen in the leg following impact. FM had the most significant relationship with soft tissue displacement and velocity.

- The results presented in this thesis provide important information about how shock propagates through and is attenuated by the body. This information will advance our understanding of how impact-related injuries occur and lead to the development of more biofidelic biomechanical models which can be used for more accurate injury risk assessments.
- The approach reported by Pain and Challis (2002) to determine the energy density of a non-dispersive wave could not be replicated in this study without introducing significant distortions (error) into the signals. Consequently, the energy dissipation due to intra-segmental soft tissue motion was not quantified as proposed.
- Soft tissue motion resulting from the drop impacts could not be isolated from the motion of the leg segment which occurred during impact. Therefore, the soft tissue responses while horizontally (pendulum) and vertically (drop) oriented, could not be compared.

REFERENCES

Aerts, P., Ker, R. F., De Clercq, D., Ilsley, D. W., Alexander, R. McN. (1995). The mechanical properties of the human heel pad: A paradox resolved. Journal of Biomechanics, 28(11), 1299-1308.

Akbarshahi, M., Schache, A., Fernandez, J., Baker, R., Banks, S., Pandy, M. (2010). Non-invasive assessment of soft-tissue artifact and its effect on knee joint kinematics during functional activity. Journal of Biomechanics, 43, 1292-1301.

Alcantara, E. E., Forner, A. A., Ferrus, E. E., Garcia, A. C., Ramiro, J. J. (2002). Influence of age, gender, and obesity on the mechanical properties of the heel pad under walking impact conditions. Journal of Applied Biomechanics, 18(4), 345-356.

Aref, M. (n.d.). Bones: bone structure. Veterinary Online. Retrieved from http://veterinary-online.blogspot.ca/2012/11/veterinary-online-bones.html

Arendt, E. A, Agel, J., Dick, R. (1999). Anterior cruciate ligament injury patterns among collegiate men and women. Journal of Athletic Training, 34(2), 86-92.

Attenuation (n.d.). The Free On-line Dictionary of Computing. Retrieved from http://dictionary.reference.com/browse/attenuation

Ball, K. A. (2011). Kinematic comparison of the preferred and non-preferred foot punt kick. Journal of Sports Sciences, 29(14), 1545-1552.

Benoit, D. L., Ramsey, D. K., Lamontagne, M., Xu, L., Wretenberg, P., Renstrom, P. (2006). Effect of skin movement artifact on knee kinematics during gait and cutting motions measured in vivo. Gait and Posture, 24(2), 152-164.

Binder, E. F., Kohrt, W. M. (2000). Relationships between body composition and bone mineral content and density in older women and men. Clinical Exercise Physiology, 2(2), 84-91.

Bishop, J., Poole, G., Leitch, M., Plewes, D. B. (1998). Magnetic resonance imaging of shear wave propagation in excised tissue. Journal of Magnetic Resonance Imaging, 8(6), 1257-1265.

Boyer, K. A., Nigg, B. M. (2004). Muscle activity in the leg is tuned in response to impact force characteristics. Journal of Biomechanics, 37, 1583-1588.

Bridgman, C., Scurr, J., White, J., Hedger, W., Galbraith, H. (2010). Three-dimensional kinematics of the breast during a two-step star jump. Journal of Applied Biomechanics, 26(4), 465-472.

Brizuela, G. G., Llana, S. S., Ferrandis, R. R., Garcia-Belenguer, A. C. (1997). The influence of basketball shoes with increased ankle support on shock attenuation and performance in running and jumping. Journal of Sports Sciences, 15(5), 505-515.

Brody, T. (1999). Nutritional Biochemistry, 2nd Edition. Academic Press, 385-386.

Browning, R. C., McGowan, C. P., Kram, R. (2009). Obesity does not increase external mechanical work per kilogram body mass during walking. Journal of Biomechanics, 42(14), 2273-2278.

Brydges, E. A., Burkhart, T. A., Altenhof, W. J., Andrews, D. M. (2012). Reliability of leg soft tissue marker motion following manual digitization. Proceedings of the Canadian Society of Biomechanics, Burnaby, British Columbia, Canada.

Burkhart, T. A., Arthurs, K. L., Andrews, D. M. (2008). Reliability of upper and lower extremity anthropometric measurements and the effect on tissue mass predictions. Journal of Biomechanics, 41(7), 1604-1610.

Burkhart, T. A., Andrews, D. M. (2010). Activation level of extensor carpi ulnaris affects wrist elbow acceleration responses following simulated forward falls. Journal of Electromyography and Kinesiology, 20, 1203-1210.

Burkhart, T. A., Andrews, D. M. (2013, in press). Kinematics, kinetics and muscle activation patterns of the upper extremity during simulated forward falls. Journal of Electromyography and Kinesiology.

Cappozzo, A., Della Croce, U., Leardini, A., Chiari, L. (2005). Human movement analysis using stereophotogrammetry: Part 1: theoretical background. Gait and Posture, 21(2), 186-196.

Carter, D. R. (1978). Anisotropic analysis of strain rosette information from cortical bone. Journal of Biomechanics, 11, 199-202.

Cavanagh, P. R., Lafortune, M. A. (1980). Ground reaction forces in distance running. Journal of Biomechanics, 13, 397-406.

Challis, J. H., Murdoch, C., Winter, S. L. (2008). Mechanical properties of the human heel pad: a comparison between populations. Journal of Applied Biomechanics, 24(4), 377-381.

Challis J. H., Pain, M. T. G. (2008). Soft tissue motion influences skeletal loads during impacts. Exercise and Sport Sciences Reviews, 36, 71-75.

Chi, K., Schmitt, D. (2005). Mechanical energy and effective foot mass during impact loading of walking and running. Journal of Biomechanics, 38(7), 1387-1395.

Chu, J. J., Caldwell, G. E. (2004). Stiffness and damping response associated with shock attenuation in downhill running. Journal of Applied Biomechanics, 20(3), 291-308.

Chu, V., Fong, D., Chan, Y., Yung, P., Fung, K., Chan, K. (2010). Differentiation of ankle sprain motion and common sporting motion by ankle inversion velocity. Journal of Biomechanics, 43(10), 2035-2038.

Chu, M. L., Yazdani-Ardakani, S., Gradisar, I. A., Askew, M. J. (1986). An in vitro simulation study of impulsive force transmission along the lower skeletal extremity. Journal of Biomechanics, 19(12), 979-987.

Cole, G., Nigg, B., van den Bogert, A., Gerritsen, K. (1996). Lower extremity joint loading during impact in running. Clinical Biomechanics, 11, 181-193.

Coventry, E., O'Connor, K. M., Hart, B. A., Earl, J. E., Ebersole, K. T. (2006). The effect of lower extremity fatigue on shock attenuation during single-leg landing. Clinical Biomechanics, 21(10), 1090-1097.

Crossley, K., Bennel, K. L., Wrigley, T., Oakes, B. W. (1999). Ground reaction forces, bone characteristics, and tibial stress fractures in male runners. Medicine and Science in Sports and Exercise, 31(8), 1088-1093.

Decker, M. J., Torry, M. R., Wyland, D. J., Sterett, W. I., Steadman, J. R. (2003). Gender differences in lower extremity kinematics, kinetics and energy absorption during landing. Clinical Biomechanics, 18(7), 662-669.

Deffieux, T., Montaldo, G., Tanter, M., Fink, M. (2009). Shear wave spectroscopy for in vivo quantification of human soft tissues visco-elasticity. IEEE Transactions on Medical Imaging, 28(3), 313-322.

DeGoede, K. M., Ashton-Miller, J. A. (2002). Fall arrest strategy affects peak hand impact force in a forward fall. Journal of Biomechanics, 35, 843-848.

Derrick, T. R., Hamill, J. J., Caldwell, G. E. (1998). Energy absorption of impacts during running at various stride lengths. Medicine and Science in Sports and Exercise, 30(1), 128-135.

Derrick, T. R., Caldwell, G. E., Hamill, J. (2000). Modeling the stiffness characteristics of the human body while running with various stride lengths. Journal of Applied Biomechanics, 16, 36-51.

Devita, P. P., Skelly, W. A. (1992). Effect of landing stiffness on joint kinetics and energetics in the lower extremity. Medicine and Science in Sports and Exercise, 24(1), 108-115.

Dufek, J. S., Mercer, J. A., Griffin, J. R. (2009). The effects of speed and surface compliance on shock attenuation characteristics for male and female runners. Journal of Applied Biomechanics, 25(3), 219-228.

Duquette, A. M., Andrews, D. M. (2010). Tibialis anterior muscle fatigue leads to changes in tibial axial acceleration after impact when ankle dorsiflexion angles are visually controlled. Human Movement Science, 29(4), 567-577.

Farvid, M. S., Ng, T. W. K., Chan, D. C., Barrett, P. H. R., Watts, G. F. (2005). Association of adiponectin and resistin with adipose tissue compartments, insulin resistance and dyslipidaemia. Diabetes, Obesity and Metabolism, 7, 406-413.

Ferber, R., McClay Davis, I., Williams, D. S., Laughton, C. (2002). A comparison of within- and between-day reliability of discrete 3D lower extremity variables in runners. Journal of Orthopaedic Research, 20, 1139-1145.

Flynn, J. M., Holmes, J. D., Andrews, D. M. (2004). The effect of localized leg muscle fatigue on tibial impact acceleration. Clinical Biomechanics, 19(7), 726-732.

Ford, K. R., Myer, G. D., Hewett, T. E. (2007). Reliability of landing 3D motion analysis: implications for longitudinal analyses. Medicine and Science in Sports and Exercise, 39(11), 2021-2028.

Fowler, N., Lees, A., Reilly, T. (1997). Changes in stature following plyometric drop-jump and pendulum exercises. Ergonomics, 40(12), 1279-1286.

Fowler, N. E., Lees, A. A. (1998). A comparison of the kinetic and kinematic characteristics of plyometric drop-jump and pendulum exercises. Journal of Applied Biomechanics, 14(3), 260-275.

Fuller, J., Liu, L., Murphy, M., Mann, R. (1997). A comparison of lower-extremity skeletal kinematics measured using skin- and pin-mounted markers. Human Movement Science, 16, 219-242.

Gao, B., Zheng, N. (2008). Investigation of soft tissue movement during level walking: translations and rotations of skin markers. Journal of Biomechanics, 41, 3189-3195.

Gennisson, J.-L., Deffieux, T., Macé, E., Montaldo, G., Fink, M., Tanter, M. (2010). Viscoelastic and anisotropic mechanical properties of in vivo muscle tissue assessed by supersonic shear imaging. Ultrasound in Medicine and Biology, 36(5), 789-801.

Giladi, C., Milgrom, A., Stein, M., Kashtan, H., Margulies, J., Rand, N., Chisin, R., Steinberg, R., Aharonson, Z., Kedem, R., Frankel, V. H. (1987). Stress fractures and tibial bone width. Journal of Bone and Joint Surgery, 69-B, 326-329.

Gilles, B., Perrin, R., Magnenat-Thalmann, N., Vallee, J.-P. (2005). Bone motion analysis from dynamic MRI: acquisition and tracking. Academic Radiology, 12(10), 1285-1292.

Gittoes, M. R., Brewin, M. A., Kerwin, D. G. (2006). Soft tissue contributions to impact forces simulated using a four-segment wobbling mass model of forefoot-heel landings. Human Movement Science, 25(6), 775-787.

Gruber, K., Denoth, J., Stuessi, E., Ruder, H. (1987). The wobbling mass model. In B. Jonsson, editor, Biomechanics X-B, volume 6B of International Series on Biomechanics. Human Kinetics Publishers, Champaign, Illinois, 1095-1105.

Gruber, K., Ruder, H., Denoth, J., Schneider, K. (1998). A comparative study of impact dynamics: wobbling mass model versus rigid body models. Journal of Biomechanics, 31(5), 439-444.

Hennig, E. M., Lafortune, M. A. (1991). Relationships between ground reaction force and tibial bone acceleration parameters. International Journal of Sport Biomechanics, 7(3), 303-309.

Holden, J. P., Orsini, J. A., Siegel, K. L., Kepple, T. M., Gerber, L. H., Stanhope, S. J. (1997). Surface movement errors in shank kinematics and knee kinetics during gait. Gait and Posture, 5 (3), 217-227.

Holmes, J. D., Andrews, D. M. (2006). The effect of leg muscle activation state and localized muscle fatigue on tibial response during impact. Journal of Applied Biomechanics, 22, 275-284.

Holmes, J. D., Andrews, D. M., Durkin, J. L., Dowling, J. J. (2005). Predicting in vivo soft tissue masses of the lower extremity using segment anthropometric measures and DXA. Journal of Applied Biomechanics, 21(4), 371-382.

Houck, J., Yack, H., Cuddeford, T. (2004). Validity and comparisons of tibiofemoral orientations and displacement using a femoral tracking device during early to mid stance of walking. Gait and Posture, 19(1), 76.

Insel, P., Ross, D., McMahon, K., Bernstein, M. (2010). Nutrition, 4th Edition. Jones & Bartlett Learning. Burlington, MA.

Jennett, S. (1989). Human physiology. Churchill Livingstone, Edinburgh.

Jones, B. H., Thacker, S. B., Gilchrist, J., Kimsey, Jr. C. D., Sosin, D. M. (2002). Prevention of lower extremity stress fractures in athletes and soldiers: a systematic review. Epidemiologic Reviews, 24(2), 228-247.

Ker, R. F., Bennett, M. B., Alexander, R. M., Kester, R. C. (1989). Foot strike and the properties of the human heel pad. Proceedings of the Institution of Mechanical Engineering. Part H, Journal of Engineering in Medicine, 203(4), 191-196.

Kernozek, T. W., Torry, M. R., Hoof, H. V. A. N., Cowley, H., Tanner, S. (2005). Gender differences in frontal and sagittal plane biomechanics during drop landings. Medicine and Science in Sports and Exercise, 37(6), 1003-1012.

Kinoshita, H., Ogawa, T., Kuzuhara, K., Ikuta, K. (1993). In vivo examination of the dynamic properties of the human heel pad. International Journal of Sports Medicine, 14(6), 312-319.

Komi, P. V., Karlsson, J. J. (1978). Skeletal muscle fibre types, enzymes activities and physical performance in young males and females. Acta Physiologica Scandinavica, 103(2), 210-218.

Kroemer, K. H. E., Snook, S. H. (1988). Ergonomic models of anthropometry, human biomechanics, and operator-equipment interfaces. National Academy Press, Washington, D.C, 19-33.

Kuo, M.-Y., Tsai, T.-Y., Lin, C.-C., Lu, T.-W., Hsu, H.-C., Shen, W.-C. (2011). Influence of soft tissue artifacts on the calculated kinematics and kinetics of total knee replacements during sit-to-stand. Gait and Posture, 33, 379-384.

Kyle, U. G., Gremion, G. G., Genton, L. L., Slosman, D. O., Golay, A. A., Pichard, C. C. (2001). Physical activity and fat-free and fat mass by bioelectrical impedance in 3853 adults. Medicine and Science in Sports and Exercise, 33(4), 576-584.

Lafortune, M. A., Cavanagh, P. R., Sommer, H. I., Kalenak, A. A. (1992). Three-dimensional kinematics of the human knee during walking. Biomechanics, 25(4), 347-357.

Lafortune, M. A., Hennig, E. M., Lake, M. J. (1996a). Dominant role of interface over knee angle for cushioning impact loading and regulating initial leg stiffness. Journal of Biomechanics, 29, 1523-1529.

Lafortune, M., Lake, M. (1995). Human pendulum approach to simulate and quantify locomotor impact loading. Journal of Biomechanics, 28(9), 1111-1114.

Lafortune, M., Lake, M., Hennig, E. (1996b). Differential shock transmission response of the human body to impact severity and lower limb posture. Journal of Biomechanics, 29(12), 1531-1537.

Leardini, A., Chiari, L., Croce, U., Cappozzo, A. (2005). Human movement analysis using stereophotogrammetry: Part 3. Soft tissue artifact assessment and compensation. Gait and Posture, 21(2), 212-225.

Ley, C. J., Lees, B., Stevenson, J. C. (1992). Sex- and menopause-associated changes in body-fat distribution. American Journal of Clinical Nutrition, 55, 950-954.

Liu, W., Nigg, B. M. (2000). A mechanical model to determine the influence of masses and mass distribution on the impact force during running. Journal of Biomechanics, 33, 219-224.

Lukaski, H. C. (1987). Methods for the assessment of human body composition: traditional and new. The American Journal of Clinical Nutrition, 46, 537-556.

Malina, R. M., Bouchard, C., Bar-Or, O. (2004). Growth, Maturation, and Physical Activity (2nd Ed). Human Kinetics, Champaign, Ill.

Manal, K. K., McClay Davis, I. I., Galinat, B. B., Stanhope, S. S. (2003). The accuracy of estimating proximal tibial translation during natural cadence walking: bone vs. skin mounted targets. Clinical Biomechanics, 18(2), 126-131.

Maslen B. A., Ackland T. R. (1994). Radiographic study of skin displacement errors in the foot and ankle during standing. Clinical Biomechanics, 9(5), 291-296.

Mattsson, S., Thomas, B. J. (2006). Development of methods for body composition studies. Physics in Medicine and Biology, 51(13), 203-228.

Mazess, R. B., Barden, H. S., Bisek, J. P., Hanson, J. (1990). Dual-energy x-ray absorptiometry for total-body and regional bone-mineral and soft-tissue composition. American Society for Clinical Nutrition, 51, 1106-1112.

McLean, S. G., Palmer, M. L., Lucey, S. M., Lucarelli, D. G., Oh, Y. K., Ashton-Miller, J. A., Wojtys, E. M. (2011). The relationship between anterior tibial acceleration, tibial slope, and ACL strain during a simulated jump landing task. Journal of Bone and Joint Surgery, American Volume, 93-A(14), 1310-1317.

Mercer, J. A., Bates, B. T., Dufek, J. S., Hreljac, A. A. (2003). Characteristics of shock attenuation during fatigued running. Journal of Sports Sciences, 21(11), 911-919.

Mercer, J. A., Dutek, J. S., Mangus, B. C., Rubley, M. D., Bhanot, K., Aldridge, J. M. (2010). A description of shock attenuation for children running. Journal of Athletic Training, 45(3), 259-264.

Milner, C. E., Ferber, R., Pollard, C. D., Hamill, J., Davis, I. S. (2006). Biomechanical factors associated with tibial stress fracture in female runners. Medicine and Science in Sports and Exercise, 38(2), 323-328.

Nigg, B. M. (1997). Impact forces in running. Current Opinion in Orthopedics, 8(6), 34-47.

Nigg, B. M., Cole, G. K., Bruggemann G-P. (1995). Impact forces during heel-toe running. Journal of Applied Biomechanics, 11(4), 407-432.

Nigg, B. M., Liu, W. (1999). The effect of stiffness and damping on simulated impact force peaks during running. Journal of Biomechanics, 32, 849-856.

Norcross, J. J., Van Loan, M. D. (2004). Validation of fan beam dual energy x ray absorptiometry for body composition assessment in adults aged 18-45 years. British Journal of Sports Medicine, 38(4), 472-476.

Norcross, M. F., Blackburn, J., Goerger, B. M., Padua, D. A. (2010). The association between lower extremity energy absorption and biomechanical factors related to anterior cruciate ligament injury. Clinical Biomechanics, 25(10), 1031-1036.

Nordin, M. Frankel, V. H. (2001). Basic biomechanics of the musculoskeletal system (3rd ed.). Lippincott Williams & Wilkins, 26-55.

Ortega, D., Rodríguez Bíes, E. C., Berral de la Rosa, F. J. (2010). Analysis of the vertical ground reaction forces and temporal factors in the landing phase of a countermovement jump. Journal of Sports Science and Medicine, 9(2), 282-287.

Ozdemir, H., Soyuncu, Y., Ozhorhen, M., Dabak, K. (2004). Effects of changes in heel fat pad thickness and elasticity on heel pain. Journal of the American Podiatric Medical Association, 94(1), 47–52.

Pain, M. G., Challis, J. H. (2001). The role of the heel pad and shank soft tissue during impacts: a further resolution of a paradox. Journal of Biomechanics, 34, 327-333.

Pain, M. G., Challis, J. H. (2002). Soft tissue motion during impacts: their potential contributions to energy dissipation. Journal of Applied Biomechanics, 18, 231-242.

Pain, M. G., Challis, J. H. (2004). Wobbling mass influence on impact ground reaction forces: a simulation model sensitivity analysis. Journal of Applied Biomechanics, 20(3), 309-316.

Pain, M. G., Challis, J. H. (2006). The influence of soft tissue movement on ground reaction forces, joint torques and joint reaction forces in drop landings. Journal of Biomechanics, 39(1), 119-124.

Pelker, R. P., Saha, S. (1983). Stress wave propagation in bone. Journal of Biomechanics, 16(7), 481-489.

Perez-Gomez, J., Rodriguez, G. V., Ara, I., Olmedillas, H., Chavarren, J., González-Henriquez, J. J., Dorado, C., Calbet, J. A. (2008). Role of muscle mass on sprint performance: gender differences? European Journal of Applied Physiology, 102(6), 685-694.

Peters, A., Galna, B., Sangeux, M., Morris, M., Baker, R. (2010). Quantification of soft tissue artifact in lower limb human motion analysis: a systematic review. Gait and Posture, 31(1), 1-8.

Prichasuk, S. (1994). The heel pad in plantar heel pain. The Journal of Bone and Joint Surgery, 76(B), 140-142.

Radin, E. L., Orr, R. B., Kelman, J. L., Paul, I. L., Rose, R. M. (1982). Effect of prolonged walking on concrete on the knees of sheep. Journal of Biomechanics, 15(7), 487-492.

Radin, E. L., Parker, H. G., Pugh, J. W., Steinberg, R. S., Paul, I. L., Rose, R. M. (1973). Response of joints to impact loading — III: relationship between trabecular microfractures and cartilage degeneration. Journal of Biomechanics, 6(1), 51-54.

Reinschmidt, C., van den Bogert, A. J., Lundberg, A., Nigg, B. M., Murphy, N., Stacoff, A., Stano, A. (1997). Tibiofemoral and tibiocalcaneal motion during walking: external vs. skeletal markers. Gait and Posture, 6, 98-109.

Richards, J. G. (1999). The measurement of human motion: a comparison of commercially available systems. Human Movement Science, 18, 589-602.

Riemann, B. L., Schmitz, R. J., Gale, M. M., McCaw, S. T. (2002). Effect of ankle taping and bracing on vertical ground reaction forces during drop landings before and after treadmill jogging. Journal of Orthopaedic and Sports Physical Therapy, 32(12), 628-635.

Rittweger, J., Beller, G., Ehrig, J., Jung, C., Koch, U., Ramolla, J., Schmidt, F., Newitt, D., Majumdar, S., Schiessl, H., Felsenberg, D. (2000). Bone-muscle strength indices for the human lower leg. Bone, 27 (2), 319-326.

Rodriquez, G., Moreno, L. A., Blay, M. G., Blay, V. A., Fleta, J., Sarria, A., Bueno, M. (2005). Body fat measurements in adolescents: comparison of skinfold thickness equations with dual-energy X-ray absorptiometry. European Journal of Clinical Nutrition, 59, 1158-1166.

Sangeux, M. M., Marin, F. F., Charleux, F. F., Dürselen, L. L., Ho Ba Tho, M. C. (2006). Quantification of the 3D relative movement of external marker sets vs. bones based on magnetic resonance imaging. Clinical Biomechanics, 21(9), 984-991.

Sati, M., de Guise, J., Larouche, S., Drouin, G. (1996). Quantitative assessment of skin-bone movement at the knee. The Knee, 3, 121-138.

Schinkel-Ivy, A., Burkhart, T. A., Andrews, D. M. (2010). The influence of tissue masses on lower extremity injuries and reported pain in varsity soccer players. Conference Proceedings of the Annual Meeting of the American Society of Biomechanics (34), Providence, RI, 331-332.

Schinkel-Ivy, A., Burkhart, T. A., Andrews D. M. (2012a). Leg tissue mass composition affects tibial acceleration response following impact. Journal of Applied Biomechanics, 28, 29-40.

Schinkel-Ivy, A., Burkhart, T. A., Andrews D. M. (2012b, submitted). Differences in distal lower extremity tissue masses and mass ratios in athletes of sports involving repetitive impacts. Journal of Sports Sciences.

Schmitz, R. J., Kulas, A. S., Perrin, D. H., Riemann, B., Shultz, S. J. (2007). Sex differences in lower extremity biomechanics during single leg landings. Clinical Biomechanics, 22(6), 681-688.

Scholz, J. P. (1989). Reliability and validity of the WATSMART three-dimensional optoelectronic motion analysis system. Physical Therapy, 69(8), 679-689.

Scurr, J. C., White, J. L., Hedger, W. (2010). The effect of breast support on the kinematics of the breast during the running gait cycle. Journal of Sports Sciences, 28(10), 1103-1109.

Shorten, M. R., Winslow, D. S. (1992). Spectral analysis of impact shock during running. International Journal of Sport Biomechanics, 8, 288-304.

Stagni, R., Fantozzi, S., Cappello, A., Leardini, A. (2005). Quantification of soft tissue artefact in motion analysis by combining 3D fluoroscopy and stereophotogrammetry: a study on two subjects. Clinical Biomechanics, 20(3), 320-329.

Telfer, S. S., Morlan, G. G., Hyslop, E. E., Semple, R. R., Rafferty, D. D., Woodburn, J. J. (2010). A novel device for improving marker placement accuracy. Gait and Posture, 32(4), 536-539.

Tong, J., Lim, C. S., Goh, O. L. (2003). Technique to study the biomechanical properties of the human calcaneal heel pad. The Foot, 13(2), 83-91.

Tortora, G. J. (1995). Principles of human anatomy (7th ed.). Wiley, New York, 102-115; 205-227.

Tranberg, R., Karlsson, D. (1998). The relative skin movement of the foot: a 2-D roentgen photogrammetry study. Clinical Biomechanics, 13(1), 71-76.

Vandeweyer, E., Hertens, D. (2002). Quantification of glands and fat in breast tissue: an experimental determination. Annals of Anatomy, 184, 181-184.

Verbitsky, O. O., Mizrahi, J. J., Voloshin, A. A., Treiger, J. J., Isakov, E. E. (1998). Shock transmission and fatigue in human running. Journal of Applied Biomechanics, 14(3), 300-311.

Visible Human Server. (n.d.). Computer Science Department, Peripheral Systems Lab, École Polytechnique. Retrieved from http://visiblehuman.epfl.ch/samples.php.

Voloshin, A., Wosk, J. (1982). An in vivo study of low back pain and shock absorption in the human locomotor system. Journal of Biomechanics, 15, 21-27.

Wearing, S. C., Smeathers, J. E., Yates, B., Urry, S. R., Dubois, P. (2009). Bulk compressive properties of the heel fat pad during walking: a pilot investigation in plantar heel pain. Clinical Biomechanics, 24(4), 397-402.

Whittle, M. W. (1999). Generation and attenuation of transient impulsive forces beneath the foot: a review. Gait and Posture, 10, 264-275.

Winter, D.A., 2005. Biomechanics and motor control of human movement. John Wiley and Sons Inc., Hoboken, New Jersey.

Wood, P. A. (2006). How fat works. Harvard University Press, Massachusetts.

Wrbaškić, N. N., Dowling, J. J. (2007). An investigation into the deformable characteristics of the human foot using fluoroscopic imaging. Clinical Biomechanics, 22(2), 230-238.

Yeow, C. H., Lee, P. V. S., Goh, J. C. H. (2009). Effect of landing height on frontal plane kinematics, kinetics and energy dissipation at lower extremity joints. Journal of Biomechanics, 42, 1967-1973.

Yeow, C. H., Lee, P. V. S., Goh, J. C. H. (2011a). An investigation of lower extremity energy dissipation strategies during single-leg and double-leg landing based on sagittal and frontal plane biomechanics. Human Movement Science, 30(3), 624-635.

Yeow, C. H., Lee, P. V. S., Goh, J. C. H. (2011b). Non-linear flexion relationships of the knee with the hip and ankle, and their relative postures during landing. The Knee, 18, 323-328.

Yu, B., Garrett, W. E. (2007). Mechanisms of non-contact ACL injuries. British Journal of Sports Medicine, 41(1 Suppl), 47-51.

Zhang, S. N., Bates, B. T., Dufek, J. S. (2000). Contributions of lower extremity joints to energy dissipation during landings. Medicine and Science in Sports and Exercise, 32(4), 812-819.

Zhang, S., Clowers, K., Kohstall, C., Yeon-Joo, Y. (2005). Effects of various midsole densities of basketball shoes on impact attenuation during landing activities. Journal of Applied Biomechanics, 21(1), 3-17.

APPENDIX A

GENERAL HEALTH QUESTIONNAIRE (GHQ)

Please answer the following questions.

1. Have you had any prior surgeries to your feet, legs or back?

   [ ] YES [ ] NO

2. Do you suffer from constant soreness in your feet, legs, or lower back?

   [ ] YES [ ] NO

3. Have you had any recent trauma (sprain, strain, major bruising, stitches, etc.) to your feet, legs or lower back?

   [ ] YES [ ] NO

4. Do you suffer from arthritis or any congenital abnormalities concerning your feet, legs, or lower back?

   [ ] YES [ ] NO

5. Do you have any current health conditions that may exclude you from this study (i.e. high blood pressure, pregnancy)?

   [ ] YES [ ] NO

6. Do you have sensitive skin or any skin condition that may cause you to have an allergic reaction to a grid of washable marker being applied to you lower leg?

   [ ] YES [ ] NO

Please note that this questionnaire will be kept confidential. If you answered 'YES' to any of these questions, or if you do not wish to disclose this information, it is your right to not answer or withdraw from the study.

APPENDIX B

DESCRIPTION OF LOWER EXTREMITY ANTHROPOMETRIC MEASUREMENTS (Adapted from Burkhart et al., 2008)

Measurements	Segment	Description and landmarks
Lengths	Thigh (L)	Distance between the superior iliac crest and the lateral aspect of the tibial plateau
	Thigh (M)	Distance between the anterior level of the pubic symphysis and the medial aspect of the tibial plateau
	Thigh (prox, mid)	Distance between the anterior level of the pubic symphysis and the medial aspect of the femur midway between the superior iliac crest and the tibial plateau
	Leg (L)	Distance between the lateral aspect of the tibial plateau and the inferior base of the lateral malleoli
	Leg (M)	Distance between the medial aspect of the tibial plateau and the inferior base of the medial malleoli
	Leg (prox, mid)	Distance between the medial aspect of the tibial plateau and the medial aspect of the tibia midway between the tibial plateau and the malleoli
Circumferences	Thigh (prox)	Distance around the femur and overlying tissue just inferior to the gluteal fold
	Thigh (mid)	Distance around the femur and overlying tissues midway between the superior iliac crest and the tibial plateau
	Knee	Distance around the outmost projections of the tibia
	Leg (mid)	Distance around the calf midway between the tibial plateau and the malleoli
	Ankle	Distance around the tibia and fibula, just superior to the malleoli
	Malleoli	Distance around the most lateral projections of the tibia and fibula
Breadths	Thigh (prox)	Distance across the femur and just inferior to the gluteal fold
	Thigh (mid, M/L)	Distance across the femur and overlying tissue at the level of maximum circumference midway between the superior iliac crest and the tibial plateau
	Thigh (mid, A/P)	Distance across the femur at the level of maximum circumference midway between the superior iliac crest and the tibial plateau
	Knee	Distance between the outmost projections of the tibia at the level of the tibial plateau
	Leg (mid, M/L)	Distance across the tibia and fibula at the level of maximum calf circumference
	Leg (mid, A/P)	Distance across the tibia and fibula at the level of maximum calf circumference
	Ankle	Distance between the lateral aspects of the tibia and fibula just superior to the malleoli
	Malleoli	Distance between the most lateral projections of the tibia and fibula
Skinfolds (cm)	Thigh (mid, A)	Vertical fold on the anterior aspect of the thigh at the level of maximum circumference midway between the superior iliac crest and the tibial plateau
	Thigh (mid, P)	Vertical fold on the posterior aspect of the thigh at the level of maximum circumference midway between the gluteal fold and the popliteal fossa with the subject lying prone
	Calf (mid, M)	Vertical fold on the medial aspect of the calf at the level of maximum circumference with the subject's weight placed on the opposite leg
	Calf (mid, P)	Vertical fold on the posterior aspect of the calf at the level of maximum circumference with the subject lying prone

A = anterior; P = posterior; M = medial; L = lateral; mid = between the anterior and posterior or medial and lateral aspects of a segment; prox = from the proximal end of the segment.

APPENDIX C

LOWER EXTREMITY TISSUE MASS PREDICTION EQUATIONS
(Adapted from Holmes et al., 2005)

Mass Type and Location
Bone Mineral Content Mass (BMC)
Y^1 (thigh) = -444.453 + 18.302(x1) + 275.317(x2) -1.691(x3) + 3.545(x4) -1.835(x5) + 7.467(x6)
Y^1 (leg) = -85.480 + 0.106(x1) + 3.131(x7) + 4.155(x8)
Y^1 (leg + foot) = -173.663 -1.557(x1) + 3.172(x7) + 4.384(x8) -1.387(x9) + 12.253(x10)
Fat Mass (FM)
Y^1 (thigh) = -5796.784 -622.703(x1) + 83.600(x5) + 120.034(x11) -110.279(x12) + 191.186(x13) + 1301.701(x2)
Y^1 (leg) = -927.818 -140.279(x1) + 44.757(x9) + 29.592(x14)
Y^1 (leg + foot) = -1052.842 -96.337(x1) + 42.894(x9)
Lean Mass (LM)
Y^1 (thigh) = -2826.795 + 718.147(x1) + 105.746(x15) -49.727(x5) + 79.150(x12) -54.939(x11) + 39.851(x4) + 123.452(x6)
Y^1 (leg) = -3951.886 + 141.182(x1) + 105.746(x15) -33.229(x9) + 762.337(x2) + 176.228(x10) + 160.907(x16) + 23.170(x17)
Y^1 (leg + foot) = -4869.757 + 153.568(x1) + 93.871(x18) -34.036(x9) + 231.241(x10) + 35.434(x17) + 920.251(x2)
Wobbling Mass (WM)
Y^1 (thigh) = -7523.117 + 11.443(x1) + 76.158(x7) + 238.204(x13) + 34.663(x5) + 57.511(x4) + 42.087(x11)
Y^1 (leg) = -5263.474 -4.012(x1) + 37.256(x18) + 9.287(x9) + 11.045(x17) + 38.141(x19) + 230.608(x15) + 915.125(x2) + 42.199(x14)
Y^1 (leg + foot) = -6612.428 + 14.676(x1) + 1563.505(x2) + 73.223(x14) + 250.583(x15) + 78.034(x18)

x1 = gender (0 for F, 1 for M); x2 = height (m); x3 = prox. mid-thigh length (cm); x4 = lat. thigh length (cm); x5 = ant. mid-thigh skinfold (mm); x6 = med/lat mid-thigh breadth (cm); x7 = participant mass (kg); x8 = prox. mid-calf length (cm); x9 = med. mid-calf skinfold (mm); x10 = med/lat mid-calf breadth (cm); x11 = prox. thigh circumference (cm); x12 = mid-thigh circumference (cm); x13 = ant/post mid-calf breadth (cm); x16 = malleoli breadth (cm); x17 = lateral leg length (cm); x18 = malleoli circumference (cm); and x19 = ankle circumference (cm).

VITA AUCTORIS

NAME:	Evan Andrew Brydges
PLACE OF BIRTH:	Windsor, Ontario, Canada
YEAR OF BIRTH:	1987
EDUCATION:	
2001 - 2006	Essex District High School Essex, Ontario, Canada
2006 - 2010	University of Windsor, Windsor, Ontario, Canada Bachelor of Human Kinetics, Honours Movement Science
2010 - 2013	University of Windsor, Windsor, Ontario, Canada Master of Human Kinetics